HYDROSTATICALLY LOADED STRUCTURES

The Structural Mechanics, Analysis and Design of Powered Submersibles

WILLIAM A. NASH

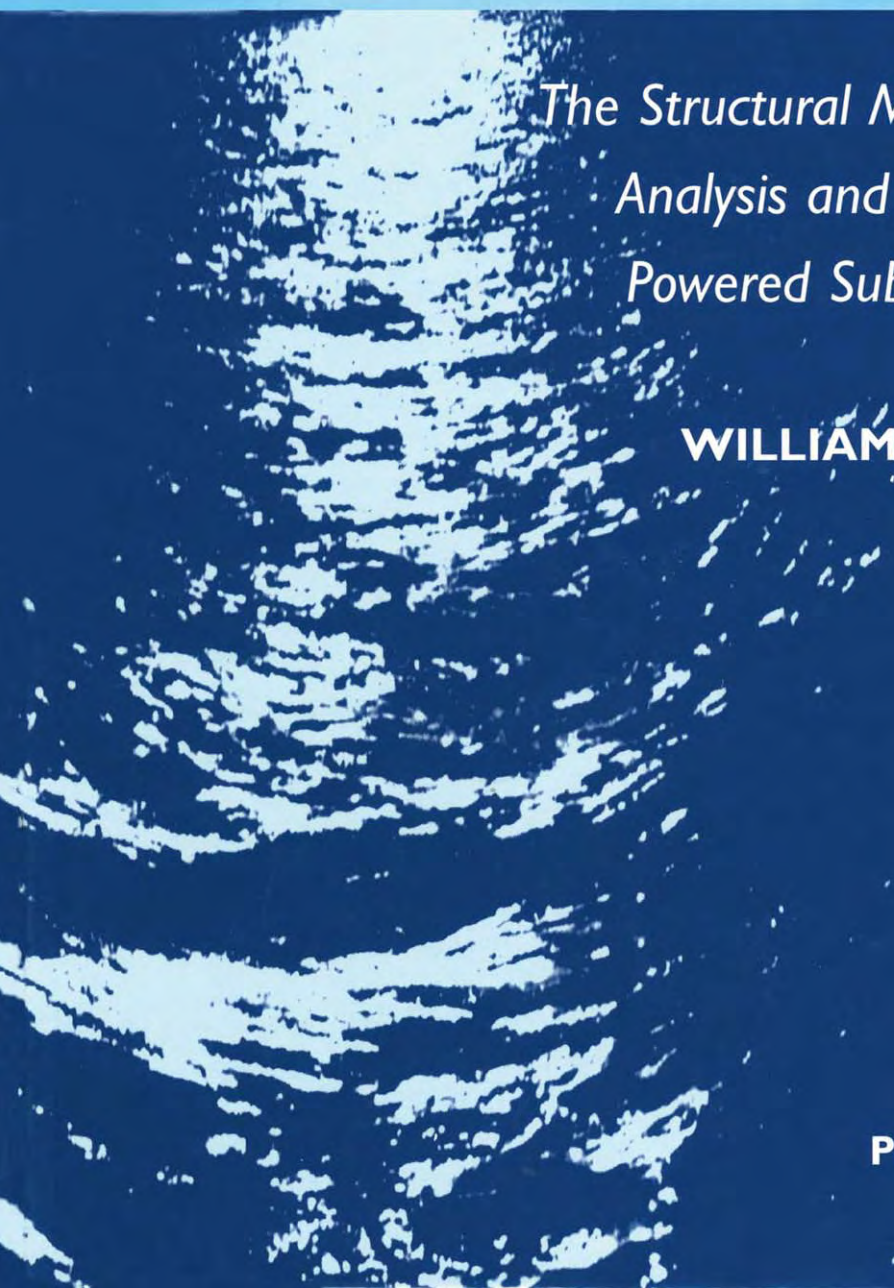

PERGAMON

HYDROSTATICALLY LOADED STRUCTURES

The Structural Mechanics, Analysis and Design of Powered Submersibles

Elsevier/Pergamon Titles of Related Interest

Books

CHRYSSOSTOMIDIS
Behaviour of Offshore Structures (BOSS '94)

NOOR & DWOYER
Computational Structural Mechanics and Fluid Dynamics

PANASYUK *et al.*
Advances in Fracture Resistance and Structural Integrity (ICF8)

SALAMA *et al.*
Advances in Fracture Research (ICF7)

Journals (free specimen copy gladly sent on request)

Applied Ocean Research
Engineering Failure Analysis
Engineering Structures
International Journal of Non-linear Mechanics
International Journal of Solids and Structures
Marine and Petroleum Geology
Marine Structures
Ocean Engineering
Oceanographic Literature Review

HYDROSTATICALLY LOADED STRUCTURES

The Structural Mechanics, Analysis and Design of Powered Submersibles

WILLIAM A. NASH, Ph.D.

Professor of Civil Engineering,
University of Massachusetts, Amherst, MA, USA

PERGAMON

U.K. Elsevier Science Ltd, The Boulevard, Langford Lane, Kidlington, Oxford, OX5 1GB, England

U.S.A. Elsevier Science, Inc., 660 White Plains Road, Tarrytown, New York 10591-5153, U.S.A.

JAPAN Elsevier Science Japan, Tsunashima Building Annex, 3-20-12 Yushima, Bunkyoku, Tokyo 113, Japan

---

First edition 1995

Library of Congress Cataloging in Publication Data
Nash, William A.
Hydrostatically loaded structures: the structural mechanics, analysis, and design of powered submersibles / William A. Nash.
p. cm.
Includes bibliographical references and indexes.
1. Submersibles--Design and construction. 2. Shells (Engineering).
I. Title.
VM453.N29 1995 623.8'27--dc20 95-24794

British Library Cataloging in Publication Data
A catalogue record for this book is available from the British Library

ISBN 0 08 037876 5

DISCLAIMER

Whilst every effort is made by the Author and the Publishers to ensure that no inaccurate or misleading data, opinion or statement appears in this publication, they wish to make it clear that neither they, their employees, officers and agents accept any responsibility or liability whatsoever for the consequences of any such inaccurate or misleading data, opinion or statement. This disclaimer applies equally to designs which are based on the theories presented in this publication.

Printed and bound in Great Britain by BPC Wheatons Ltd, Exeter

Dedicated to

Julia Emma McKay

Elizabeth Andersen McKay

William Arthur Nash

Abigail Franklin Nash

This Page Intentionally Left Blank

Contents

PREFACE

Hydrostatically Loaded Structures introduces the reader to the structural mechanics, analysis, and design of submersibles intended for exploration of the ocean and lake depths. Such trips could well be for location of mineral resources, inspection of submerged portions of off-shore towers for oil drilling platforms, inspection of ocean bottom pipelines, carrying tourists on underwater adventures, carrying commercial cargo, and other uses yet to be found.

Design of the hydrostatically loaded vehicles involved presents many problems not encountered in design of land-based systems. Not only are localized normal pressures very large, but most of the structural systems are extremely sensitive to initial geometric imperfections. Relative small departures from the nominal geometry become very important. For example, small departures from true circularity of a cylindrical or spherical pressure hull greatly diminishes its capability to descend to great depths. Residual stresses often decrease the load carrying capability of the system. Confirmation of any mathematical analysis of structural behavior must be obtained by comprehensive experimental programs.

The author's interest in structural behavior of submersible systems extends over a number of decades. The present book is the outgrowth of a graduate level course that he has given a number of times over the years. To effectively utilize this book, the reader must necessarily have taken a first course in Strength of Materials, and preferably, a second course in that area, or, alternately, a course in Theory of Elasticity. Each chapter ends with numerous references. together with a bibliography listing (and often briefly summarizing) other publications. These two listings are of equal importance but space does not permit incorporating all items in the bibliography into the detailed text. Nor does space permit discussions of shell dynamics, an obviously important topic.

Much of the book was written while the author was a visiting professor at the Technical University of Darmstadt, Germany. Thanks must go to the Alexander von Humboldt Foundation of Bonn for making that stay possible, and to the faculty in Darmstadt for its hospitality.

The author is particularly indebted to Mrs. Pamela Stephan for careful preparation of the computer-generated figures, text formatting, and layout. Thanks also go to Mrs. Kristina Schmid for much of the typing of the text. Lastly, the author is deeply indebted to his wife, Verna B. Nash, for her patience and encouragement during the preparation of the manuscript.

William A. Nash
Amherst, Massachusetts
April, 1995

This Page Intentionally Left Blank

CHAPTER 1

A BRIEF HISTORY OF SUBMERSIBLES

Records from antiquity indicate that Alexander the Great developed a rudimentary type of submersible consisting of a wood case having transparent windows with the system being treated with resin and wax to keep water out. Several versions of this undocumented claim are to be found in ancient records. Much later Leonardo da Vinci (1452–1519) claimed to have developed a submersible but never gave any of the details usually associated with his other inventions [1.1], [1.2].

The next development is due to Cornelius Drebble of England who demonstrated for King James a twelve-man enclosed boat operating under the Thames River. The boat had a wooden top and the men operated oars from inside the vessel. The next documented development is due to David Bushnell which involved an egg-shaped wooden vessel having a propeller turned by hand cranks within the submerged system. It was demonstrated in Maine in about 1790. In 1765 Robert Fulton, of Lancaster, Pennsylvania, developed for the French government the *Nautilus,* a twelve-man submersible powered by hand cranks. He demonstrated its capabilities in Brest, France, in 1802 but was unable to generate any funding for future developments [1.3].

Man's quest to achieve mobility beneath the surface of the sea for both scientific as well as military purposes has led to design and construction of a number of systems capable of going to ever-increasing depths. During the past three decades a host of undersea systems has been developed for deep ocean exploration, e.g., petroleum, minerals, food sources, etc. Here we will document many of these submersible systems. Most are self-propelled but a few of unusual interest but lacking propulsion will also be mentioned. Engineering plans are currently being drawn up by several major nations to utilize newly-designed submersibles as material carriers (mainly petroleum) under the polar ice-cap. The former Soviet Union is also planning to convert surplus military submarines for such utilization [1.4].

Most existing deep submergence systems have pressure hulls of deceptively simple configuration, e.g., a ring-stiffened cylindrical shell, stiffened as well as unstiffened spherical shells, stiffened conical shells, and unstiffened as well as ring-stiffened prolate spheroids. Significant structural additions to these primary load-carrying members are to be found in transverse bulkheads which not only provide additional strength but serve to compartment the vehicle in the event of flooding; reinforcing rings around entry hatches and other penetrations of the pressure hull; and reinforcing

rings in the junction between, say, a cylindrical hull and its conical and/or spherical end closures. Pressure hull configurations are usually selected to meet requirements pertinent to structural efficiency, suitability of internal space to carry payloads, and for hydrodynamic efficiency.

In general these pressure hull configurations are characterized by much smaller radius/thickness ratios than are associated with aerospace applications. In deep submergence systems this ratio is usually less than 50, whereas for flight vehicles ratios of 200 to 500 are common. Even though the hydrospace systems are thus relatively thicker, they are, fortunately, still sufficiently thin that structural analyses based upon the assumption of "thin shell" theory are usually valid. Even so, development of rational strength criteria whose predictions agree with existing experimental evidence has occupied the attention of many research engineers and involved extensive laboratory and even prototype testing. Since the analyst must always make assumptions and idealizations concerning any proposed configuration, it is not to be expected that simple results will be found that will precisely predict structural behavior of the pressure hull. Instead, one must often be content with reasonable upper and lower bounds on load-carrying capacity of the system. Although the introduction of assumptions and idealizations is of course necessary in any other facet of structural analysis and design, e.g., airborne vehicles, high-rise buildings, bridges, ground vehicles, etc., there are at least two significant features of pressure hull design that greatly affect load-carrying capabilities that are essentially absent or negligible in other structural considerations. These are: (a) the presence of initial geometrical imperfections in the form of deviations from, say, a perfect cylindrical shape of a pressure hull, and (b) the presence of significant magnitude initial stresses due to formation of flat plating into some single or double curved configuration for the pressure hull. Item (a) is of importance because the pressure hull is subjected to external pressure which induces a compressive loading into the shell structure. The compressive forces essentially tend to exaggerate the initial geometric imperfections thereby giving rise to localized bending effects which are deleterious to structural integrity. Item (b) is significant since the initial stresses must be added to stresses arising from pressure loading and this combined effect may precipitate premature yielding of the pressure hull. These two features, so difficult to account for prior to construction, serve to differentiate the structural mechanics of deep submersible systems from structural problems associated with other areas of engineering.

Representative Deep Submersibles Developed Since 1951

KUROSHIO. Built in Japan in 1951 by the Nippon K. K. (Japan Steel and Tube Corporation) for tethered explorations up to 656 feet (200 m) mostly related to the fishing industry [1.5].

SEVERYANKA. Built in the Soviet Union, about 1958. Characteristics unknown. Known uses limited to assist the Soviet fishing fleet.

TRIESTE II. Built by U.S. Navy in 1959 in conjunction with A. Picard. Dove to 36,000 feet (10,973 m) in the Mariana Trench in 1960 with a crew of three. For general oceanographic research, has mechanical arms. Connected by cable to surface ship. No mode of propulsion [1.6].

MORAY. Built by U.S. Naval Ordnance Test Center, China Lake, California, in 1960. Carries two individuals and is suitable for oceanic acoustic research. No viewports. Can dive to 6000 feet (1830 m) [1.7].

Figure 1.1, DENISE (DIVING SAUCER) (Photo © The Cousteau Society, a membership supported, non-profit environmental organization.)

DENISE. The original name of a submersible designed under the direction of J.Y. Cousteau in 1956. Although christened DENISE, that name is rarely used. Captain Cousteau coined the term SOUCOUPE PLONGEANTE (DIVING SAUCER) and that name has persisted. The true name is SOUCOUPE PLONGEANTE 350, referring to the maximum depth of 350 meters. The pressure hull consisted of two steel semi-ellipsoidal shells, each 0.75 inches (19.05 mm) thick, welded together. Several small jets squirt sea water propelling and guiding the vehicle. Peak submerged speed is 1.5 knots (1.73 miles per hour). Built in France in conjunction with Westinghouse Electric Corp., see [1.8], [1.9], to carry two individuals for general oceanographic research. See Figure 1.1.

ALVIN. Built by Litton Systems, Inc. in 1964 for Office of Naval Research, in conjunction with Woods Hole Oceanographic Institute. HY–100 steel pressure hull with depth capability of 6000 feet (1,829 m). Space for two crew members. Modified in 1973 with a titanium pressure hull having depth capability of 11,500 feet (3505 m) [1.6], [1.10].

ALUMINAUT. Constructed by Reynolds Metals, International, in 1964, all aluminum pressure hull. Dives to 15,000 feet (4570 m) with up to six crew including observers. Used for general oceanographic research [1.6], [1.12].

DEEPSTAR 4000. Built in 1965 by Westinghouse Electric Corp. Can dive to 4000 feet (1220 m) with three individuals on board. Has manipulator arm and is suitable for general oceanic research [1.6].

DEEP SUBMERGENCE RESCUE VEHICLE. Built in 1965 by Lockheed Missiles and Space Co. Can dive to 3500 feet (1067 m) employing a crew of three plus up to 24 individuals rescued from another submersible in distress. Can be flown to site of disabled vehicle [1.10], [1.11].

STAR III. Built by Electric Boat Co. in 1967. Can dive to 2000 feet (610 m) with a crew of two. Suitable for general oceanographic research. Has manipulator arms. [1.12].

DEEP DIVER. Built in 1967 by Ocean Systems of Union Carbide; design by Edwin Link and John Perry. Capable of diving to 1250 feet (381 m) carrying a total of four crew including observers. Has been used for observations during laying of underseas pipelines [1.7].

DEEP QUEST. Built in 1967 by Lockheed Missiles and Space Co. Can dive to 8000 feet (2438 m) with four on board. Designed for deep ocean exploration, including mineral surveys. Has manipulator arms. Was first vehicle to use a multisphere hull [1.7].

BENTHOS. Developed in 1967 at Pennsylvania State University and fabricated at the Corning Glass Works. The material is high-strength Pyroceram and the configuration consisted of a ring-stiffened cylindrical closed at the forward end by a hemisphere and at the after end by a truncated conical shell. Operating depth was 20,000 feet (6100 m) but cyclic resistance of joints was unsatisfactory after only five cycles of hydrostatic loading [1.13].

DEEP OCEAN WORK BOAT. Built in 1967 by AC Electronics Division of General Motors. Can dive to 6500 feet (1981 m) with two individuals on board. Has manipulator arm, 360° viewing ports, and is suitable for general oceanic research [1.12].

SHINKAI. Built in Japan in 1968 for operating depths of 1969 feet (600 m). Constructed at Kobe Shipyard by Kawasaki Heavy Industries for research associated with fisheries and geological surveys [1.5].

JOHNSON SEA LINK. Built in 1969 by the Link Division of the Singer Company, in conjunction with Alcoa. The vehicle consists of an aluminum cylindrical shell closed at its after end by an aluminum hemisphere and at its forward end by a transparent acrylic plastic hemisphere in which the pilot sits and has 180° visibility. Can dive to 400 feet (122 m) for shallow water explorations [1.12].

STAR II. Built by Electric Boat Co. in conjunction with University of Pennsylvania in 1969. Carries a crew of two, can descend to 1200 feet (366 m) for general oceanographic research [1.7].

KUMUKAHI. First transparent-hulled submersible. Built in 1969 by the Oceanic Institute, Hawaii for explorations at 450 feet (137 m). Two carefully constructed hemispheres of acrylic plastic were fabricated and joined to form the pressure hull [1.14].

BEN FRANKLIN. (PX–15). Built under supervision of Grumman Aircraft in Monthey, Switzerland in conjunction with Jacques Piccard and the U.S. Navy in 1969. Dives to 2000 feet (610 m) with six crew plus observers. Used for general oceanographic research, particularly ocean currents and

marine life investigations. See Figure 1.2, 1.3 [1.15].

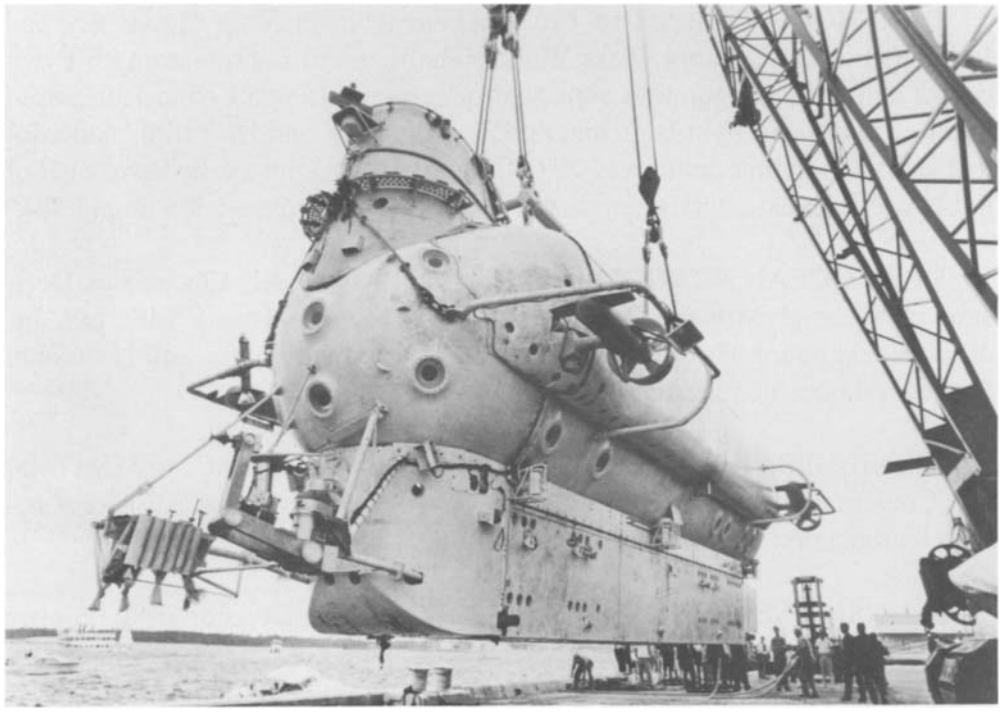

Figure 1.2, BEN FRANKLIN [From The Grumann Corp., Bethpage, NY]

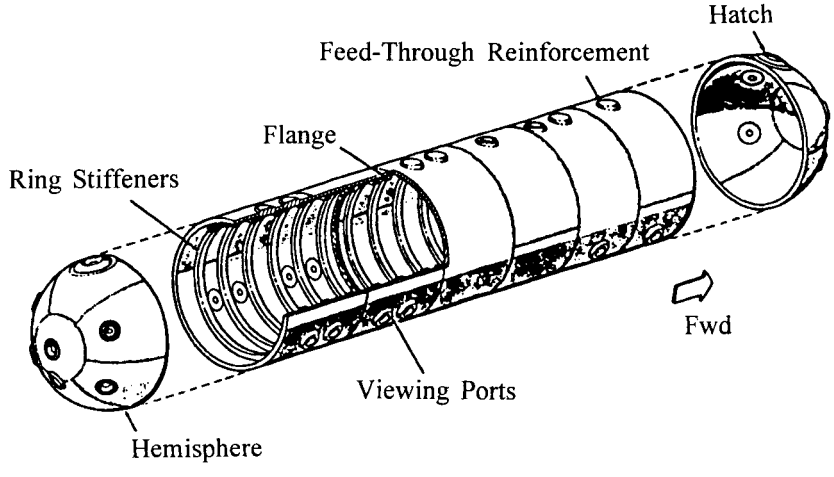

Figure 1.3, BEN FRANKLIN [From The Grumann Corp., Bethpage, NY]

Figure 1.4, BEAVER IV [From The North American Rockwell Corp. Courtesy of Cambridge Scientific Abstracts, Bethesda, Md.]

BEAVER IV. Built for North American Rockwell Corp. in 1969. Dives to 2000 feet (610 m) with up to three crew including observers. Used for viewing undersea oil drilling observations. [1.6], [1.7]. Figure 1.4.

PISCES II. Built in 1969 by the International Hydrodynamic Co. of Canada. Designed for salvage operations at depths to 3600 feet (1097 m) with several viewing ports and a versatile manipulator. A later version was intended for depths up to 6500 feet (1981 m) [1.6].

SOUCOUPE PLONGEANTES 350. See DENISE, page 4.

SHIMANSKIY. Built in the Soviet Union, about 1970. Characteristics unknown.

NEMO MOD 2000. Spherical pressure hull of transparent acrylic, 1975. Inside diameter is 58 inches (1.47 m) with aluminum hatches. Considered acceptable for manned explorations at depths of 3000 feet (915 m). Rated at life of 1000 dives [1.16].

PC3B. Built in 1977 by Perry Oceanographics, Inc. in Riviera Beach, Florida. Has a depth rating of 984 feet (300 m) and length of 22 feet (6.70 m) for carrying four individuals. Intended for maintenance of undersea oil drilling systems and pipeline inspections [1.17].

SHINKAI 2000. Spherical pressure hull of inside diameter 86.6 inches (2.2 m) of ultra-high strength steel, capable of carrying three individuals to a maximum operating depth of 6560 feet (2000 m). Launched in 1981 [1.18].

ATLANTIS IV. Built by Atlantic Aquatics Development Corp., British Columbia, Canada, in 1984. Carries 48 sightseeing passengers at a depth of 150 feet (45.7 m) in the Cayman Islands [1.19].

SEA SHUTTLE SAGA–N. Built in 1985 by International Submarine Engineering, Port Moody, British Columbia, Canada. It is a 125 foot (38.1 m) long vessel, having nuclear power with depth capability of 11,000 feet (3353 m), and carries 13 individuals [1.20].

DEEP ROVER I. Built in 1985 at Deep Ocean Engineering Co., Oakland, California. One-person vehicle for depths as great as 3300 feet (1006 m). Has manipulator arms.

JASON JR. Robot (unmanned) explorer tethered to ALVIN, built in 1985 and used in 1986 to video the remains of the TITANIC, sunk in 12,500 feet (3810 m) of water in 1912. Remotely controlled [1.21].

K–BOATS. Designed and built by George Kittredge, Warren, Maine, 1989. One-person submersible for depths as great as 350 feet (107 m). For sightseeing, has transparent portholes [1.22].

GEMINI. Built in 1989 by Hyco Technologies, Vancouver, B.C., Canada. Can dive to 2580 feet (786 m). Employed in Grand Cayman region for passenger under-sea sightseeing. Eight person vehicle composed of three acrylic spheres surrounded by a stainless steel/fiberglass cylindrical framework [1.19].

DOLPHIN 3K. Japanese built in 1991 for undersea research to depths of 9840 feet (3000 m). Has sampling as well as video capabilities [1.23].

DEEP FLIGHT. Built in 1991 by Deep Ocean Engineering Co., San Leandro, California. Designed for operation at 4000 feet (1219 m) and has a

Figure 1.5, SHINKAI [From Mitshbishi Heavy Industries, Tokyo, Japan]

transparent hemispherical forward end closure on the cylindrical shell which is fiberglass reinforced epoxy. Peak speed is 15 knots [1.24].

SHINKAI 6500. Built by Mitsubishi Heavy Industries in 1989, Kobe Shipyard, Japan. Pressure hull is a 6.56 foot (2 m) inside diameter sphere of titanium alloy with three observation ports. Acoustic navigation system and facilities to detect and image obstacles and targets. Operated by three-person crew, has descended to 21,300 feet (6527 m) [1.25], [1.26]. Figure 1.5

MIR. Built in Finland by Rauma Oceanics in 1992 for the former Soviet Union. Designed for ocean exploration up to 19,680 feet (6000 m) with metallic cylindrical pressure hull capped at one end by a hemisphere of transparent acrylic [1.27].

NAUTILE. Built in 1992 for the French Oceanographic Institute IFREMER, can explore ocean floor at depths as great as 19,680 feet (6000 m). It carries a crew of three in a 5.90 foot diameter (1.8 m) titanium sphere having several viewports. It also has a manipulative arm for collecting rock samples [1.28].

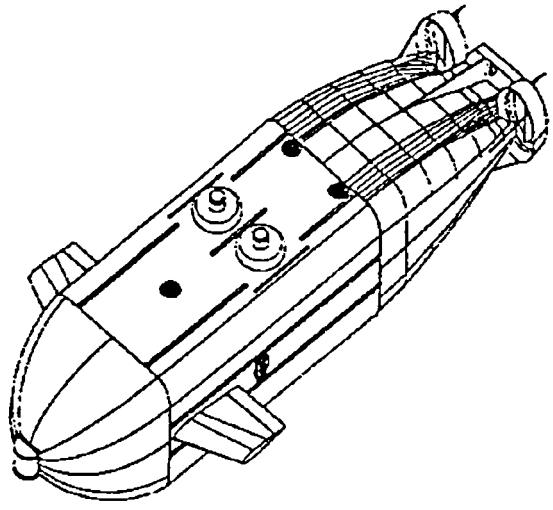

Figure 1.6, MAURIUS [From Office of Naval Research, London, UK]

ROVER. A remote-operated vehicle developed at the University of Michigan by Professor Guy A. Meadows and launched in 1992. Designed specifically for underwater exploration in the Laurentian Great Lakes with depth capability of 1475 feet (450 m) with low-light color video imaging capability, horizontal as well as vertical thrusters, speeds up to 0.86 miles per hour when submerged and 3.45 miles per hour on the surface, and articulated arm ability.

MARIUS. A European Union (EU) vehicle capable of seabed inspections and environmental surveys in coastal waters up to 1970 feet (600 m) deep. Battery powered and scheduled to be operational by late 1994. A subsequent version, composed of filamentary composite materials, will be suitable for 19,680 feet (6000 m) dives) [1.29]. Figure 1.6.

REFERENCES

1.1 Sheppard, R., "Early History of Submarines," Susquehanna, March, 1986, pp. 12–19.

1.2 Philip, C. O., "Robert Fulton," *Mechanical Engineering*, November, 1985, pp. 44–54.

1.3 Marx, R. F., "An Illustrated History of Submersibles," *Oceans,* November, 1978, Vol. 11, No. 6, pp. 22–27.

1.4 Reesink, M., "Nuclear Subs as Underwater Tankers?" *We,* Vol. 3, No. 3, February, 1994, page 1 (Washington, D.C.).

1.5 Sasaki, T. "On Underwater Observation Vessels in Japan," *Marine Technology,* 1970, pp. 227–262.

1.6 Ballard, R. D. and Emery, K. O., "Research Submersibles in Oceanography," Woods Hole Oceanographic Institution, Woods Hole, MA, published by Marine Technology Society, 1970.

1.7 Leary, F., "Vehicles for Deep Submergence," *Space/Aeronautics,* April, 1968, pp. 52–66.

1.8 Cousteau, J. Y., "Diving Saucer Takes to the Deep," *National Geographic,* April, 1960, pp. 571–586.

1.9 Church, R., "French Deep Diving Vehicles," *Marine Technology,* 1970, pp. 199–226.

1.10 Woodland, B. T., "Structures for Deep Submergence," *Space/Aeronautics,* March, 1967, pp. 100–108.

1.11 Feldman, S., "Developing a New Breed of Deep-Submergence Vehicles," *Aeronautics and Astronautics,* July, 1967, pp. 44–49.

1.12 Conway, J. C., "Benthos—Deep Submergence Pyroceram Test Vehicles," American Society of Mechanical Engineers, Paper 67–DE–5.

1.13 Gauren, J. A. and Pritzlaff, J.A., "Undersea Vehicle Operations and Development in the United States," *Marine Technology,* 1970, pp. 297–320.

1.14 Forman, W. R., "Kukuhaki," American Society of Mechanical Engineers, Paper 70–WA–Unt. 11.

1.15 Frewer, G. C., "Challengers of the Silent Depths," *Mechanical Engineering,* May, 1969, pp. 75–80.

1.16 Stachiw, J. D., "NEMO Type Acrylic Plastic Spherical Hull for Manned Operation to 3000 ft. Depth," American Society of Mechanical Engineers Paper No. 75–WA/OcE–3, 1975.

1.17 Sweeney, J. B., Pictorial History of Oceanographic Submersibles, Crown Publishers, New York, 1970.

1.18 Yokata, K. and Nanba, N., "2000 m Deep Submergence Research Vehicle Shinkai 2000," Mitsubishi Heavy Industries—Technical Reviews, Vol. 18, Number 3, 1981, pp. 4–12.

1.19 Anon., History of the American Bureau of Shipping, 1991.

1.20 Saunders, A., "Conquering Our Deepest Frontiers," *Popular Mechanics,* January, 1985, pp. 84–90, 12–134.

1.21 Baer, T., "Viewing Jason's Voyages to the Bottom of the Sea," *Mechanical Engineering,* November, 1989, pp. 36–42.

1.22 Haas, A., "Singular Subs," *U.S. Air Journal,* May, 1989, pp. 105–110.

1.23 Kalvaitis, A. N. and Stone, G., "Technical Assessment of Two Unmanned Vehicles for Undersea Research," Office of Naval Research, Asian Division, June, 1992, pp. 85–89.

1.24 Pope, G. T., "Deep Flight," *Popular Mechanics,* April, 1990, pp. 71–72.

1.25 Hayakawa, H., Takahashi, H., Kaihou, I., Barada, K., and Takahashi, H., "Development of Acoustic Support System for Submersible 'Shinkai 6500'," *OKI Technical Review,* No. 138, Tokyo, June, 1991, pp. 79–86.

1.26 Anon, "Brut aus der Urzeit," *der Spiegel,* Hamburg, Germany, No. 5, 1992, page 195.

1.27 Ashley, A., "Voyage to the Bottom of the Sea," *Mechanical Engineering,* December, 1993, pp. 50–58.

1.28 Bonatti, E., "The Earth's Mantle Below the Ocean," *Scientific American,* March, 1994, pp. 44–51.

1.29 Sampson, J. A. (Cdr.), "European Community Autonomous Underwater Vehicle Program," Office of Naval Research, European Office, ESNIB, No. 93–08, 1993, pp. 552–554.

BIBLIOGRAPHY

Anon., "Deutsche Tauchboote sind Weld-Klasse," *Hobby, magazin der Technik,* July, 1988, pp. 12–20.

Anon., "Subsea Work Boats," Mechanical Engineering, October, 1977, page 58.

Geyer, R. A., *Submersibles and Their Use in Oceanography and Ocean Engineering,* Elsevier, New York, 1977, 384 pp.

Kelsey, R. A. and Dolan, R. B., "The 'Johnson Sea Link', The First Deep Diving Welded Aluminum Submersible," SME Paper 70–WA–Unt–6.

Pritzlaff, J. A., "Submersibles," *Oceanology International,* June, 1970, pp. 36–44.

Weber, J., "Minnesota Welder Builds Mini-Sub for Great Lakes Shipwreck Venture," *Welding Journal,* December, 1984, pp. 57–59.

This Page Intentionally Left Blank

CHAPTER 2

GENERAL THEORY OF SHELLS

Any singly or doubly curved body one of whose dimensions, the thickness, is small compared to the other lateral dimensions of the body, is termed a *shell.* The curved surface midway between the bounding faces and therefore at the midpoint of the thickness at every point is termed the *middle surface* of the shell. In the limiting case of a flat (plane) middle surface the body is called a *plate.*

Figure 2.1 illustrates a portion of the middle surface of a doubly curved shell. At an arbitrary point of this element a normal n is drawn to the middle surface. Evidently an infinite number of planes may be passed through the normal and each of these planes intersects the middle surface in some plane curve, such as C for the plane P. Curves such as C, all formed by intersections of planes through $\bar{n}$ and the middle surface are termed *normal sections.* Each curve will have some curvature associated with it and in general this curvature will be different for each of the planes passing through the normal $\bar{n}$. We state, without proof, that there are two curves associated with the *perpendicular* planes P and P_1 for which curvatures are maximum and minimum at the point of intersection of $\bar{n}$ and the middle surface. The directions associated with these maximum and minimum curvatures are termed *principal directions* for any specified point on the middle surface, and the curvatures corresponding to these directions are called *principal curvatures.* Since it is presumably possible to find the principal directions at every point of the middle surface of an arbitrary shell, it is possible to draw curves which connect every point coinciding with these directions. These curves are termed *lines of curvature.* Thus, at every point along lines of curvature the middle surface curvatures are always maximum and minimum of all possible curvatures at that point. There are always two lines of curvature through every point on the middle surface of a shell and it is convenient to employ the lines of curvature of the undeformed middle surface as coordinate curves of the middle surface. In this way positions of points such as A on the middle surface may be described as indicated by the coordinates x_1 and y_1 in Figure 2.2, where x and y are lines of curvature. It will usually be convenient to refer various measures of strain and deformation of the middle surface to the same lines of curvature.

For most simple geometries, such as cylindrical, spherical, or conical shells the principal directions are immediately evident. Having selected x and y axes as coinciding with lines of curvature of the middle surface it is necessary to specify the location of an arbitrary point in the shell and this is

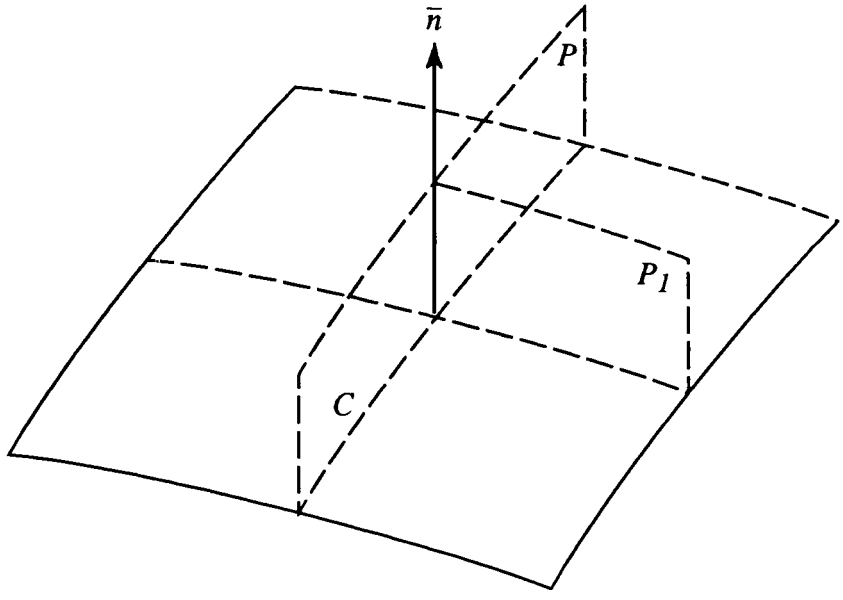

Figure 2.1

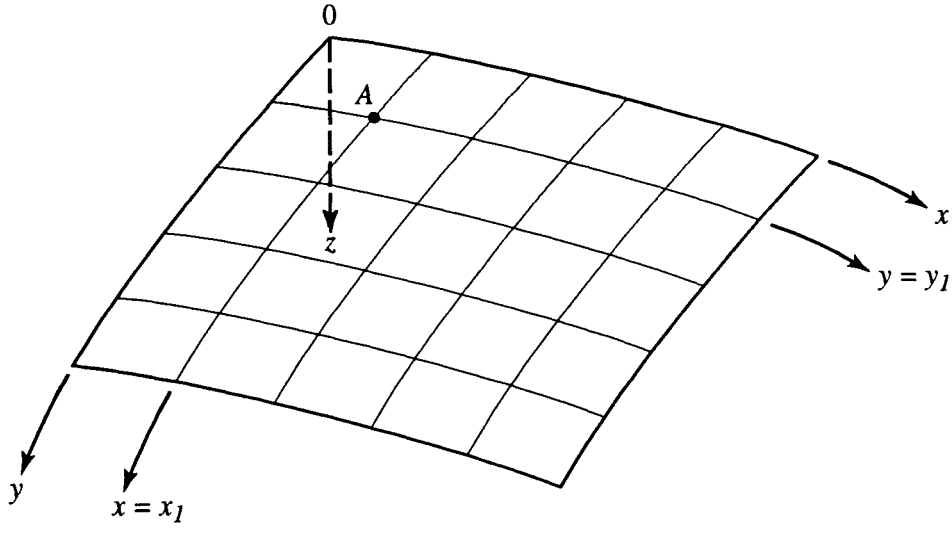

Figure 2.2

accomplished by introducing a z-axis coinciding with the normal $\bar{n}$ and having its positive direction directed toward the center of curvature of the shell. (We omit consideration of those unusual surfaces for which the centers of curvature corresponding to the principal directions lie on *opposite* sides of the shell middle surface, such as a hyperbolic paraboloid.)

Strain-Displacement Relations

Let us denote the x, y, and z components of displacement of a point on the shell middle surface by u, v, and w respectively, as the shell deforms under the action of applied loads. Further, let us denote *middle surface* normal strains in the x and y directions (remembering that these are lines of curvature) by ε_x and ε_y respectively and the *middle surface* shear strain by γ_{xy}. The determination may proceed in three phases.

(a) First, we consider the projection of an infinitesimal middle surface element $ABCD$ of dimensions dx and dy prior to any deformation of the shell on a plane which is tangent to the middle surface at some corner of the element, such as A, as shown in Figure 2.3.

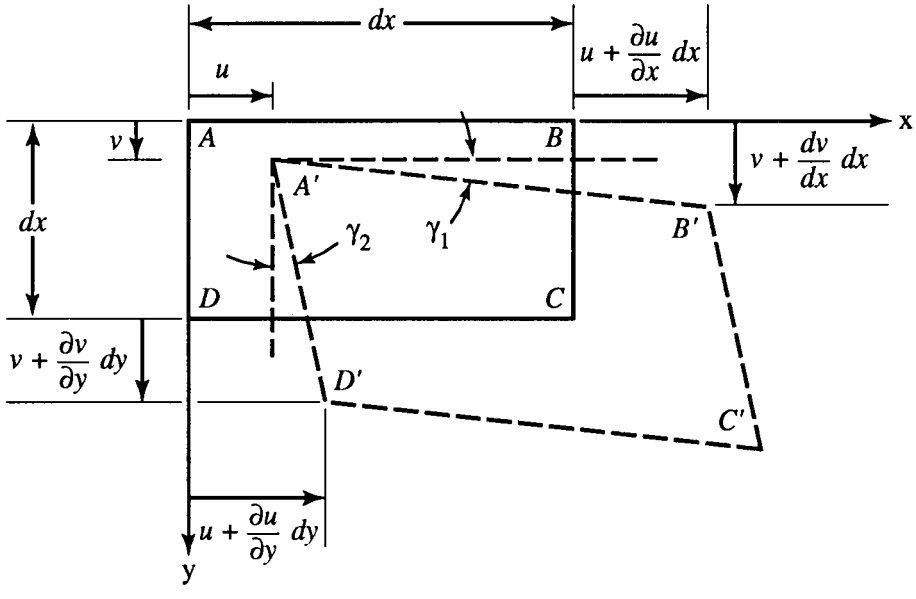

Figure 2.3

As may be seen from Figure 2.3, the point A displaces (during middle surface deformation) an amount u in the x direction, and v in the y direction to the position A'. Point B displaces to B' but instead of the displacement components in the x and y directions being u and v respectively they are $u + (\partial u/\partial x)\, dx$ and $v + (\partial v/\partial x)\, dx$ respectively, i.e. the *increments* of displacement $(\partial u/\partial x)\, dx$ and $(\partial v/\partial x)\, dx$ must be considered since, in general, the displacement at B is different than that at A even though the points A and B are only a distance dx apart. These displacement increments are small, but not negligible. Similarly point C displaces to C' and D to D' as indicated in Figure 2.3.

The originally rectangular element $ABCD$ has changed in both size and

shape during the deformation process. The side AB, originally of length dx after deformation is represented by $A'B'$ whose length is

$$\overline{A'B'} = \sqrt{\left(dx + \frac{\partial u}{\partial x}dx\right)^2 + \left(\frac{\partial v}{\partial x}\right)^2}$$

$$= dx\left[1 + 2\left(\frac{\partial u}{\partial x}\right) + \left(\frac{\partial u}{\partial x}\right)^2 + \left(\frac{\partial v}{\partial x}\right)^2\right]^{\frac{1}{2}}$$

Expanding the right side of this expression, and retaining only the first few terms, the final length is:

$$\overline{A'B'} = dx\left[1 + \left(\frac{\partial u}{\partial x}\right) + \frac{1}{2}\left(\frac{\partial u}{\partial x}\right)^2 + \frac{1}{2}\left(\frac{\partial v}{\partial x}\right)^2\right]$$

The normal strain ε_x' in the x-direction (due to u and v displacements *only*) is by definition:

$$\varepsilon'_x = \frac{\overline{A'B'} - \overline{AB}}{\overline{AB}}$$

$$= \frac{dx\left[1 + \frac{\partial u}{\partial x} + \frac{1}{2}\left(\frac{\partial u}{\partial x}\right)^2 + \frac{1}{2}\left(\frac{\partial v}{\partial x}\right)^2\right] - dx}{dx}$$

$$= \frac{\partial u}{\partial x} + \frac{1}{2}\left(\frac{\partial u}{\partial x}\right)^2 + \frac{1}{2}\left(\frac{\partial v}{\partial x}\right)^2 \tag{2.1}$$

An analogous consideration of $A'D'$ leads to the normal strain ε_y in the y-direction:

$$\varepsilon_y = \frac{\partial v}{\partial y} + \frac{1}{2}\left(\frac{\partial v}{\partial y}\right)^2 + \frac{1}{2}\left(\frac{\partial u}{\partial y}\right)^2 \tag{2.2}$$

As an approximation (which greatly simplifies future mathematical con-

siderations) let us henceforth neglect the square of the derivatives of displacements u and v occurring in (2.1) and (2.2) to obtain:

$$\varepsilon_x' = \frac{\partial u}{\partial x} \tag{2.3}$$

$$\varepsilon_y' = \frac{\partial v}{\partial y} \tag{2.4}$$

The middle surface shear strain (due to u and v displacements only) denoted by γ_{xy}' is by definition the change of the original right angle existing at point A between AB and AD. As may be seen from Figure 2.3, this is given by

$$\begin{aligned} \gamma_{xy}' &= \gamma_1 + \gamma_2 \\ &= \frac{\left(v + \frac{\partial v}{\partial x} dx\right) - v}{dx} + \frac{\left(u + \frac{\partial u}{\partial y} dy\right) - u}{dy} \\ &= \frac{\partial v}{\partial x} + \frac{\partial u}{\partial y} \end{aligned} \tag{2.5}$$

where, as an approximation, the projections of $A'B'$ and $A'D'$ on the x and y axes respectively have been replaced by the original lengths dx and dy. This is permissible because of the small magnitudes of the angles γ_1 and γ_2.

It is to be observed that the expressions (2.3), (2.4) and (2.5) have been derived through a consideration of only the u and v components of displacement of a point on the shell middle surface, i.e. only displacements *in* the middle surface have been considered.

(b) Next, it is necessary to consider the influence on normal and shear strains of the component of displacement of a point on the middle surface in the direction *normal* to that surface, i.e. one must examine the effect of the z-component of displacement which is denoted by w. This may be accomplished by re-examining the element $ABCD$ of Figure 2.3 taking into account the displacement w of point A to A'' as shown in Figure.2.4. In general the z-components of displacement of points B and D to the positions B'' and D'' will be slightly different than w, and, as indicated in Figure 2.4 are given by $w + (\partial w/\partial x)\, dx$ and $w + (\partial w/\partial y)\, dy$ respectively.

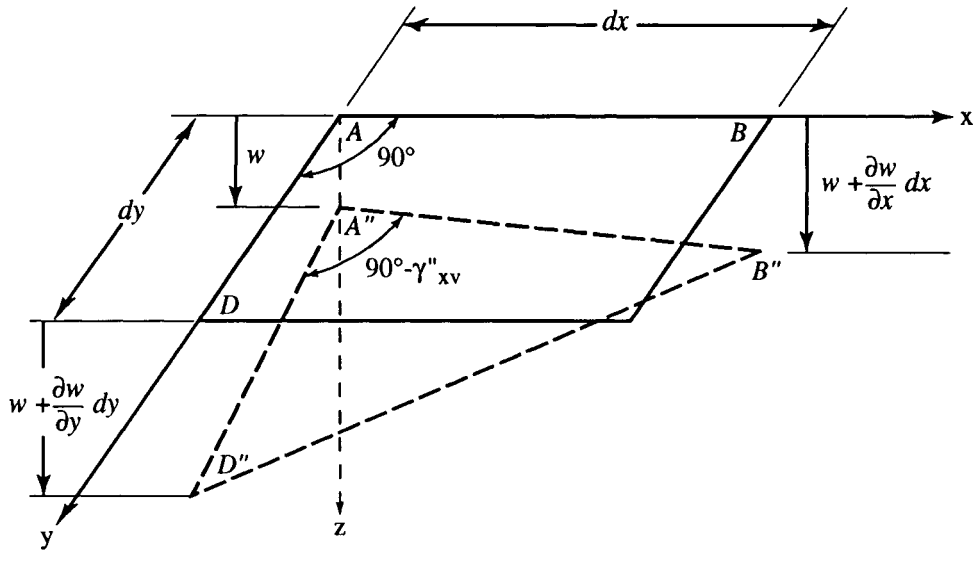

Figure 2.4

Because of deformations characterized by w, the side AB originally of length dx becomes, after deformation,

$$\overline{A''B''} = \sqrt{(dx)^2 + \left(\frac{\partial w}{\partial x}\right)^2 (dx)^2}$$

$$= dx\left[1 + \left(\frac{\partial w}{\partial x}\right)^2\right]^{\frac{1}{2}}$$

$$= dx\left[1 + \frac{1}{2}\left(\frac{\partial w}{\partial x}\right)^2 + \ldots\right]$$

The additional terms of the binomial expansion (indicated by dots) will henceforth be dropped. The normal strain ε''_x in the x direction (due to w displacements only) is:

$$\varepsilon''_x = \frac{\overline{A''B''} - \overline{AB}}{\overline{AB}}$$

$$= \frac{dx\left[1 + \frac{1}{2}\left(\frac{\partial w}{\partial x}\right)^2\right] - dx}{dx} \tag{2.6}$$

$$= \frac{1}{2}\left(\frac{\partial w}{\partial x}\right)^2$$

An analogous consideration of $A''D''$ leads us to the normal strain ε''_y in the y-direction:

$$\varepsilon''_y = \frac{1}{2}\left(\frac{\partial w}{\partial y}\right)^2 \tag{2.7}$$

The middle surface shear strain (due to w displacements only) is denoted by γ''_{xy} and is by definition the change of the original right angle DAB of Figure 2.4. To determine γ''_{xy} it is only necessary to consider the application of the law of cosines to triangle $A''B''D''$:

$$\overline{D''B''}^2 = \overline{D''A''}^2 + \overline{A''B''}^2 - 2\overline{D''A''}\,\overline{A''B''}\cos\left(90° - \gamma''_{xy}\right) \tag{2.8}$$

Substituting into (2.8) the various geometric relationships evident from Figure 2.4 we obtain:

$$\overline{D''B''}^2 = (dx)^2 + (dy)^2 + \left[\frac{\partial w}{\partial y}dy - \frac{\partial w}{\partial x}dx\right]^2$$

$$+\left[(dy)^2 + \left(\frac{\partial w}{\partial y}dy\right)^2\right]^2 + \left[(dx)^2 + \left(\frac{\partial w}{\partial x}dx\right)^2\right]^2 \tag{2.9}$$

$$-2\left[(dy)^2 + \left(\frac{\partial w}{\partial y}dy\right)^2\right]\left[(dx)^2 + \left(\frac{\partial w}{\partial x}dx\right)^2\right]\cos\left(90° - \gamma''_{xy}\right)$$

Since the angle γ'_{xy} is very small compared to a right angle, we have, approximately:

$$\cos\left(90-\gamma''_{xy}\right)\approx\gamma''_{xy}$$

If this relation is substituted in (2.9) and all terms involving squares of derivatives of displacements are dropped, we obtain:

$$\gamma''_{xy}=\frac{\partial w}{\partial x}\bullet\frac{\partial w}{\partial y} \tag{2.10}$$

(c) Finally, it is necessary to consider the effects of change of curvature on the desired strain-displacement relations. Let us examine the element AB of length dx shown in Figure 2.3. It may reasonably be assumed that the radius of curvature of AB is constant everywhere along the length dx and is given by ρ_x as indicated in Figure 2.5. Also, dx subtends a central angle $d\theta$ as shown there. In that figure the original position of AB prior to deformation is indicated by the solid line and after deformation it has displaced to the position $A'''B'''$, i.e. toward the center of curvature by an amount w, as

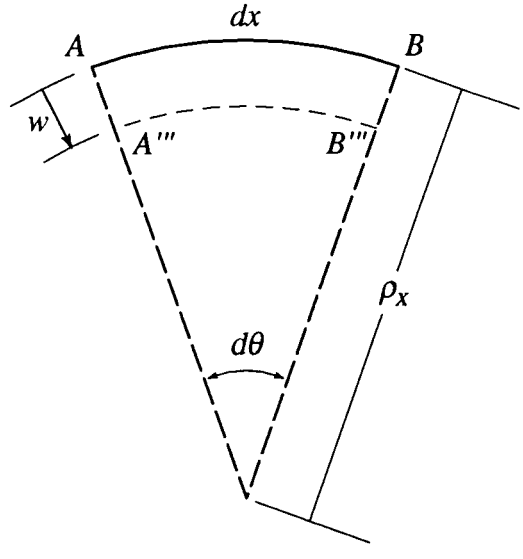

Figure 2.5

indicated by the dotted line. (Since the z-axis has already been specified as being directed toward the center of curvature, the displacement w is positive in that same direction.) Let us denote the principal curvature corresponding

to AB by k_x, which is related to the corresponding radius of curvature ρ_x by the relation $\rho_x = 1/k_x$. After deformation the radius of curvature is $(\rho_x - w)$ and the curvature is the reciprocal of that quantity. This *change of curvature* produces a normal strain ε'''_x given by:

$$\varepsilon'''_x = \frac{(\rho_x - w)d\theta - \rho_x d\theta}{\rho_x d\theta} = -\frac{w}{\rho_x} = -wk_x \tag{2.11}$$

Similarly, in the y-direction, the change of curvature produces a normal strain ε'''_y given by:

$$\varepsilon'''_y = -\frac{w}{\rho_x} = -wk_y \tag{2.12}$$

The changes of curvature do not influence the shear strain.

Now, it will be assumed that the deformations of the shell middle surface are sufficiently small that it is permissible to add the corresponding normal and shear strain components computed separately in (a), (b) and (c). This yields the desired middle surface strain-displacement relations:

$$\varepsilon_x = \frac{\partial u}{\partial x} + \frac{1}{2}\left(\frac{\partial w}{\partial x}\right)^2 - wk_x \tag{2.13}$$

$$\varepsilon y = \frac{\partial v}{\partial y} + \frac{1}{2}\left(\frac{\partial w}{\partial y}\right)^2 - wk_y \tag{2.14}$$

$$\gamma_{xy} = \frac{\partial v}{\partial x} + \frac{\partial u}{\partial y} + \frac{\partial w}{\partial x} \bullet \frac{\partial w}{\partial y} \tag{2.15}$$

An extremely useful result is obtained by differentiating (2.13) twice with respect to y, (2.14) twice with respect to x, and (2.15) once with respect to x then once with respect to y and subtracting this last result from the sum of the first two to obtain

$$\frac{\partial^2 \varepsilon_x}{\partial y^2} + \frac{\partial^2 \varepsilon_y}{\partial x^2} - \frac{\partial^2 \gamma_{xy}}{\partial x \partial y} =$$

$$\left(\frac{\partial^2 w}{\partial x \partial y}\right)^2 - \frac{\partial^2 w}{\partial x^2} \bullet - \frac{\partial^2 w}{\partial y^2} - k_x \frac{\partial^2 w}{\partial y^2} - k_y \frac{\partial^2 w}{\partial x^2} \tag{2.16}$$

Equation (2.16) is called the *equation of compatibility* (written in terms of strains) and clearly indicates that the strains ε_x, ε_y and γ_{xy} are *not independent.*

Equilibrium Relations

Let us consider the equilibrium of an element of a general, doubly curved shell. It is convenient to retain the element used in Figure 2.3 with dimensions *dx* and *dy* in the *x* and *y*-directions respectively. Such an element is considered to be removed from a shell structure and the action of the remainder of the shell structure on the element *dx, dy* is represented by various forces and moments. It will be convenient to treat these in two distinct groupings and with that objective we first examine the normal and shear forces acting in the shell middle surface. These forces are constant through the shell thickness and are most conveniently represented in terms of the normal stresses σ_x and σ_y and the shear stress τ_{xy}. The resultant forces for a shell of thickness *h* are represented in Figure 2.6. As may be seen from that figure, the normal force on the face *AB* is $\sigma_y hdx$ and the force on *AD* is $\sigma_x hdy$. Analogous to the situation concerning displacements (mentioned with regard to Figure 2.3) the forces on faces *BC* and *CD* will be somewhat different even though these faces are only distant *dx* and *dy* from *AD* and

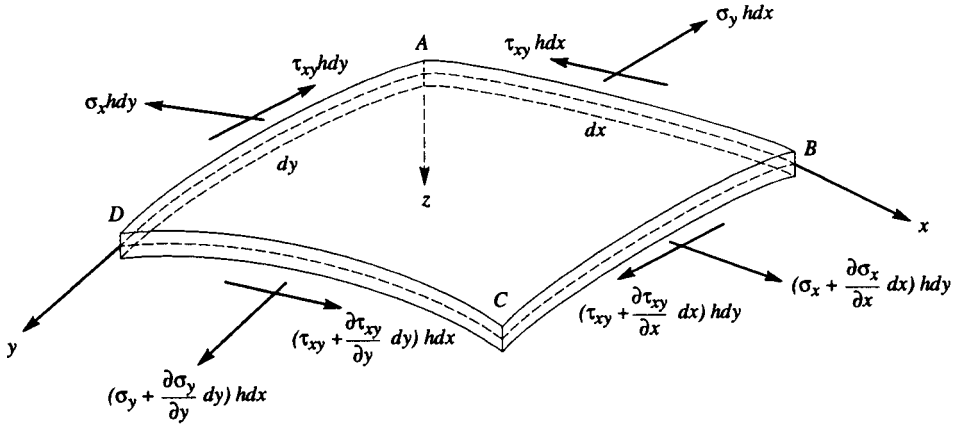

Figure 2.6

AB respectively. Just as in the case of the displacements, the normal stresses on *CD* and *BC* will be

$$\left(\sigma_y + \frac{\partial \sigma_y}{\partial_y} dy\right) \text{ and } \left(\sigma_x + \frac{\partial \sigma_x}{\partial_x} dx\right) \text{ respectively.}$$

Similar remarks hold for shearing stresses τ_{xy}. It is to be emphasized that equilibrium equations for the element must be written for the *forces* in various directions, but that it is convenient to represent these forces as the product of stress and area as indicated in Figure 2.6.

The first equilibrium equation may be obtained by summing forces acting on the element ABCD in the x-direction. Since the element is extremely small, all angles of inclination are likewise very small, and we obtain:

$$\left(\sigma_x + \frac{\partial \sigma_x}{\partial x} dx\right) \text{hdy} - \sigma_x h dy + \left(\tau_{xy} + \frac{\partial \tau_{xy}}{\partial y} dy\right) h dx - h dx = 0$$

which becomes

$$\frac{\partial \sigma_x}{\partial x} + \frac{\partial \tau_{xy}}{\partial y} = 0 \tag{2.17}$$

Similarly, we obtain the second equilibrium equation pertaining to forces in the y-direction in the form:

$$\frac{\partial \sigma_y}{\partial y} + \frac{\partial \tau_{xy}}{\partial x} = 0 \tag{2.18}$$

In Figure 2.7, bending moments per unit length of shell middle surface are designated by M_x and M_y, the twisting moment per unit length by M_{xy} and transverse shear forces, per unit length by Q_x and Q_y as illustrated. The vector representations of moments are particularly convenient for development of moment equilibrium equations. For example, from Figure 2.7 moment equilibrium about the y-axis leads to the equation

$$-M_x dy + \left(M_x + \frac{\partial M_x}{\partial x} dx\right) dy - M_{xy} dx + \left(M_{xy} + \frac{\partial M_{xy}}{\partial y} dy\right) dx$$

$$-\left(Q_x + \frac{\partial Q_x}{\partial x} dx\right) dy dx - q dx dy \left(\frac{dx}{2}\right)$$

$$+Q_y dx\left(\frac{dx}{2}\right)-\left(Q_y+\frac{\delta Q_y}{\delta y}dy\right)dx\left(\frac{dx}{2}\right)=0$$

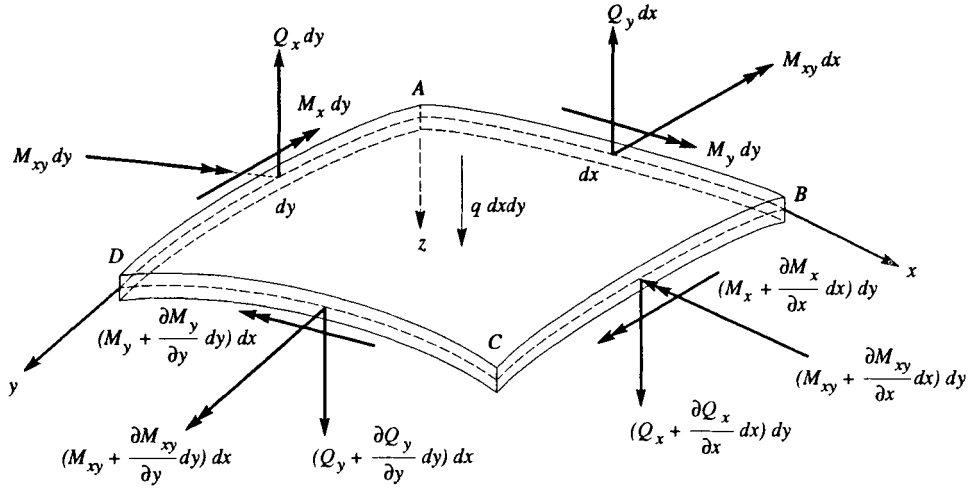

Figure 2.7

If terms involving products of three differentials are dropped in comparison to those involving only two differentials, this becomes

$$\frac{\partial M_x}{\partial x}+\frac{\partial M_{xy}}{\partial y}-Q_x=0 \tag{2.19}$$

Similarly, moment equilibrium about the x-axis yields:

$$\frac{\partial M_y}{\partial y}+\frac{\partial M_{xy}}{\partial x}-Q_y=0 \tag{2.20}$$

Prior to writing the next equilibrium equation involving forces in the z-direction, it is necessary to ascertain the angles of inclination of the various normal and shear forces shown in Figure 2.6. To find these angles, let us first examine the trace of the element $ABCD$ on a plane parallel to the x-z plane and located a distance $dy/2$ from A, as designated by EF in Figure 2.8. Prior to undergoing any displacement EF would have the appearance indicated in Figure 2.8 where it is convenient to regard the left end at E as hor-

izontal, and the right end at F as having an angle of inclination with the horizontal given by $d\theta$, where

$$d\theta = \frac{dx}{\rho_x} = k_x dx \tag{2.21}$$

Due to w displacements in the z-direction the element EF also undergoes further changes of slope. As indicated in Figure 2.9 the change of slope at the left end is $(\partial w/\partial x)$ but at the right end there is a somewhat different value given by

$$\frac{\partial w}{\partial x} + \frac{\partial}{\partial x}\left(\frac{\partial w}{\partial x}\right)dx$$

or:

$$\frac{\partial w}{\partial x} + \frac{\partial^2 w}{\partial x^2}dx \tag{2.22}$$

Evidently from (2.21) and (2.22) the net change of slope between the ends of the element EF is

$$\left(k_x + \frac{\partial^2 w}{\partial x^2}\right)dx \tag{2.23}$$

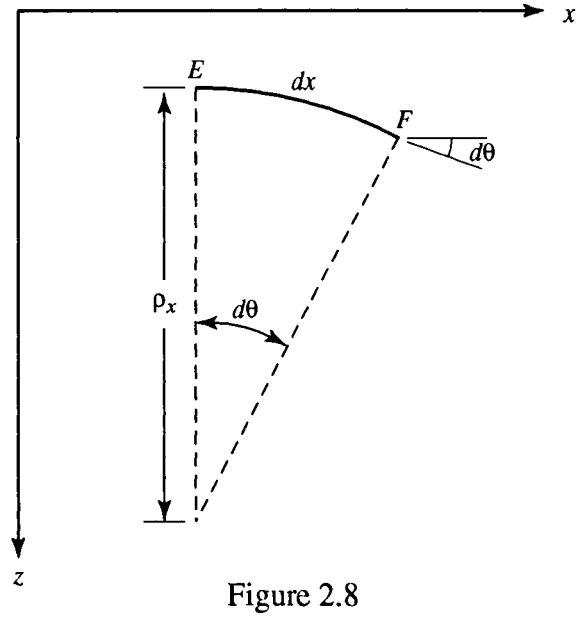

Figure 2.8

For the comparable element GH in the y-direction, the net change of slope is

$$\left(k_y + \frac{\partial^2 w}{\partial y^2}\right) dy \tag{2.24}$$

The second term in (2.22) is a measure of the change of slope (due to w-displacement) with respect to change of the x-coordinate. There is a comparable change of this same slope with respect to change of the y-coordinate. This may be illustrated by referring to the shear force $\tau_{xy}h dx$ acting on face AB of the element in Figure 2.6. If we take the slope of this force vector to be $\partial w/\partial x$ (which neglects certain higher order corrections introduced in (2.23) then it is reasonable to expect the slope of the shear force $(\tau_{xy} + (\partial\tau_{xy}/\partial y)h dx$ on CD to be given by $[\partial w/\partial x + \partial/\partial y\ (\partial w/\partial x) dy]$ or $(\partial w/\partial x) + (\partial^2 w/\partial x \partial y)\ dy$. Thus, the change of slope with respect to the y-coordinate is given by $\partial^2 w/\partial x \partial y$ per unit length in the y-direction. Analogously, if the slope of the shear force acting on face AD of the element in Figure 2.6 is $\partial w/\partial y$, then the change of this slope with respect to the x-coordinate is given by $\partial^2 w/\partial x \partial y$ per unit length in the x-direction.

A simple geometric interpretation may be attached to the second derivative occurring in (2.23). In the elementary theory of bending of beams the same term $\partial^2 w/\partial x^2$ arose and there may be shown to be an approxima-

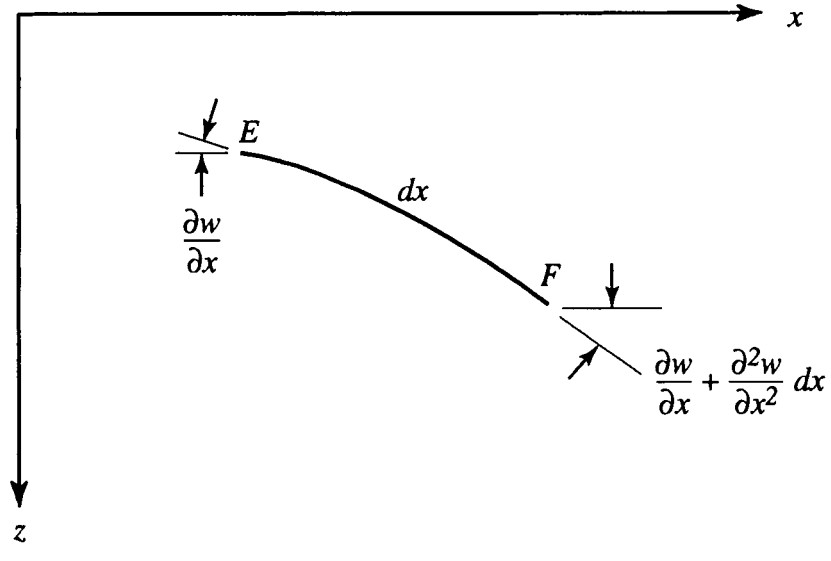

Figure 2.9

tion to the curvature of the beam at any point along the length of the beam. Here, in the case of a shell, there is an initial curvature in the x-direction, so the second derivative must be regarded as *change of curvature* per unit length in that direction. Likewise, $\partial^2 w/\partial y^2$ in (2.24) may be regarded as change of curvature per unit length in the y-direction. It will be seen shortly that each of these second derivatives $\partial^2 w/\partial x^2$ and $\partial^2 w/\partial y^2$ are related to bending of the shell. The mixed second derivative $\partial^2 w/\partial x \partial y$ is not related to bending of the shell but rather to so-called *twist*, i.e. the twist χ is defined by the relation

$$\chi = -\frac{\partial^2 w}{\partial x \partial y} \tag{2.25}$$

Knowledge of the above geometric relations now makes it possible to write the equation of equilibrium of forces in the z-direction. The middle surface normal and shear forces shown in Figure 2.6, and the transverse shears and normal loading shown in Figure 2.7 may be projected on the z-axis using appropriate components as given by the angles of Figure 2.9 and the relations (2.23), (2.24) and (2.25) to obtain:

$$-\sigma_x h dy \bullet \frac{\partial w}{\partial x} + \left(\sigma_x + \frac{\partial \sigma_x}{\partial x} dx\right) h dy \left[\frac{\partial w}{\partial x} + \left(k_x + \frac{\partial^2 w}{\partial x^2}\right) dx\right]$$

$$-\sigma y h dx \frac{\partial w}{\partial y} + \left(\sigma_y + \frac{\partial \sigma_y}{\partial y} dy\right) h dx \left[\frac{\partial w}{\partial y} + \left(k_y + \frac{\partial^2 w}{\partial y^2}\right) dy\right]$$

$$-\tau_{xy} h dx \frac{\partial w}{\partial x} + \left(\tau_{xy} + \frac{\partial \tau_{xy}}{\partial y} dy\right) h dx \left[\frac{\partial w}{\partial x} + \left(\frac{\partial^2 w}{\partial x \partial y}\right) dy\right]$$

$$-\tau_{xy} h dy \frac{\partial w}{\partial y} + \left(\tau_{xy} + \frac{\partial \tau_{xy}}{\partial x} dx\right) h dy \left[\frac{\partial w}{\partial y} + \left(\frac{\partial^2 w}{\partial x \partial y}\right) dx\right]$$

$$+\left(Q_x + \frac{Q_x}{\delta x} dx\right) dy - Q_x dy - Q_y dx + \left(Q_y + \frac{\theta Q_x}{\delta y}\right) dx$$

$$+q dx dy + 0 \tag{2.26}$$

In (2.26) the cosines of the angles of inclination of the transverse shears Q_x and Q_y have been replaced by unity since these are small angles. Simplifying (2.26) and dropping terms (a) containing products of three or more differentials in comparison to those containing products of two differentials, and (b) involving products of derivatives, we obtain the desired equilibrium equation:

$$\frac{\partial Q_x}{\partial x}+\frac{\partial Q_y}{\partial y}+\sigma_x h\left(k_x+\frac{\partial^2 w}{\partial x^2}\right)+\sigma_y h\left(k_y+\frac{\partial^2 w}{\partial y^2}\right)$$
$$+2\tau_{xy}h\frac{\partial^2 w}{\partial x\partial y}+q=0 \tag{2.27}$$

As mentioned previously the stresses σ_x, σ_y, and τ_{xy} are constant through the shell thickness h and give rise to the forces depicted in Figure 2.6, termed *membrane* effects. The membrane effects evidently correspond to extension or compression together with shearing of the shell middle surface as well as all surfaces in the shell parallel to the middle surface. Superposed upon these membrane effects the shell is, in general, subject to *bending* and *twisting* effects. These are illustrated in Figure 2.7 where M_x and M_y represent bending moments per unit length of the shell middle surface and M_{xy} represents twisting moment per unit length of the shell middle surface. In simplest terms, shell behavior (due to membrane and bending effects) may be likened to behavior of the beam-column, i.e. an initially straight bar subject to lateral as well as axial loading. Just as in the case of the beam it is customary in simplified shell analysis to assume that the stress in the direction normal to the shell middle surface is everywhere zero. To obtain relations between shell bending moments and lateral displacements it is first necessary to examine the behavior of the side AB of the element of Figure 2.4 and 2.5, but with a consideration of the shell thickness h. This side, prior to any deformation, is shown in Figure 2.10, where, as in Figure 2.5 the radius of curvature of the middle surface is ρ_x. Just as in the case of simple beam analysis we will assume the straight lines normal to the shell middle surface prior to deformation remain straight and normal to the deformed middle surface.

For simplicity, let us assume that no deformations occur at the left end A but that due to applied loads end B has distorted to the position B' shown in Figure 2.11. It is to be observed that the deformation from B to B' corresponds to a positive value of w, which is the z-component of displacement. The original configuration of the side AB is indicated by solid lines in Figure

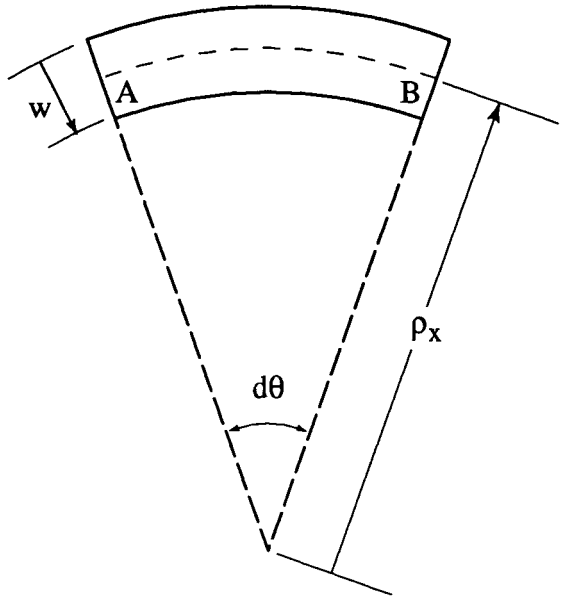

2.10

2.11 and the deformed position by dotted lines. The right end of the side is denoted by *a-a* in the undeformed state, and by *a'-a'* in the deformed configuration. Accompanying the deformed state is shown an auxiliary dotted line *a"-a"* which is parallel to *a-a*. If the left end *b-b* of the side *AB* were not rigidly clamped, the normal to the middle surface would rotate through an angle $\partial w/\partial x$ during deformation, and the right end *a-a* would rotate through a somewhat different angle $\partial w/\partial x + \partial/\partial x\,(\partial w/\partial x)\,dx$, indicating a relative angle of rotation of $\partial^2 w/\partial x^2\,dx$ in the length *dx*. However, since *b-b* is presumed to be rigidly secured then the absolute angle of rotation of *a-a* is also given by $-\partial^2 w/\partial x^2\,dx$ as indicated by the angle between *a-a* and *a'-a'* in Figure 2.11. Let us next consider a fiber oriented parallel to the shell middle surface as indicated by *c-c* which is located a distance *z* from the shell middle surface. During deformation, this fiber extends an amount $[-z\,(\partial^2 w/\partial x^2)\,dx]$ and since its original length prior to deformation was *dx* the normal strain corresponding to this shortening is

$$\varepsilon_{xB} = -z\frac{\partial^2 w}{\partial z^2} \tag{2.28}$$

where the subscript b has been attached to denote bending action. An analogous consideration of the side *AD* of Figure 2.4 leads to a corresponding

normal strain ε_{yb} in the y-direction given by

$$\varepsilon_{yB} = -z\frac{\partial^2 w}{\partial x^2} \tag{2.29}$$

Accompanying these normal strains of fibers a distance z from the middle surface there is also a shear strain denoted by γ_B. This may be calculated by consideration of Figure 2.12 which again shows the side AB of the element. Now, however, it is necessary to take into consideration the fact that during deformation b-b and a-a also rotate about the x-axis (i.e. rotate in planes parallel to the y-z plane) whereas previously rotations of these ends in

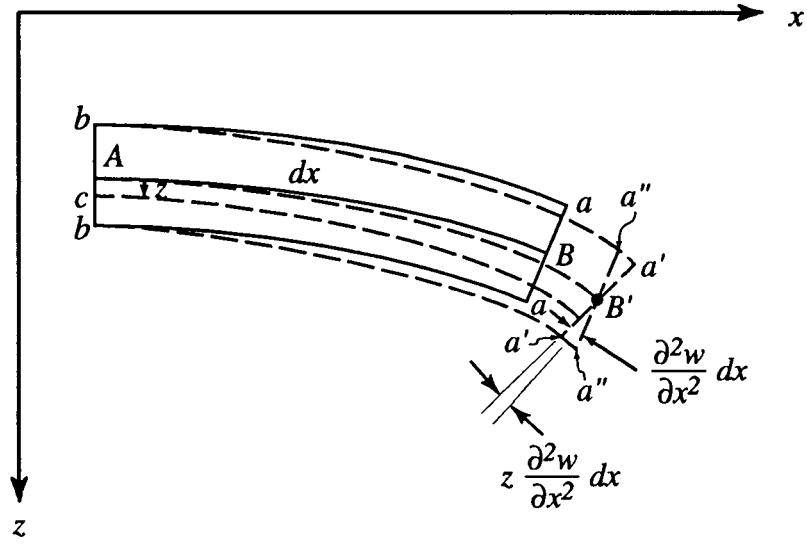

Figure 2.11

the x-z plane were considered. In general, end b-b, if not rigidly clamped, would rotate through an angle $\partial w/\partial y$ during deformation, and the right end a-a would rotate through a somewhat different angle $\partial w/\partial y - \partial/\partial x\,(\partial w/\partial y)\,dx$, indicating a relative angle of rotation of $-\partial^2 w/\partial x\partial y\,dx$ in the length dx. (Observe that for the deformation of a-a to a'''-a''' there is a *decrease* of $\partial w/\partial y$.) However, since b-b is presumed to be rigidly fixed then the absolute angle of rotation of a-a is also given by $-\partial^2 w/\partial x\partial y\,dx$ as indicated by the angle between a-a and a'''-a''' in Figure 2.12. The fiber c-c located a distance z from the shell middle surface now displaces laterally an amount $-z\,\partial^2 w/\partial x\partial y\,dx$ as indicated in Figure 2.12 thus giving rise to an angle of distortion (shear) indicated by γ_{B_1} in Figure 2.12.

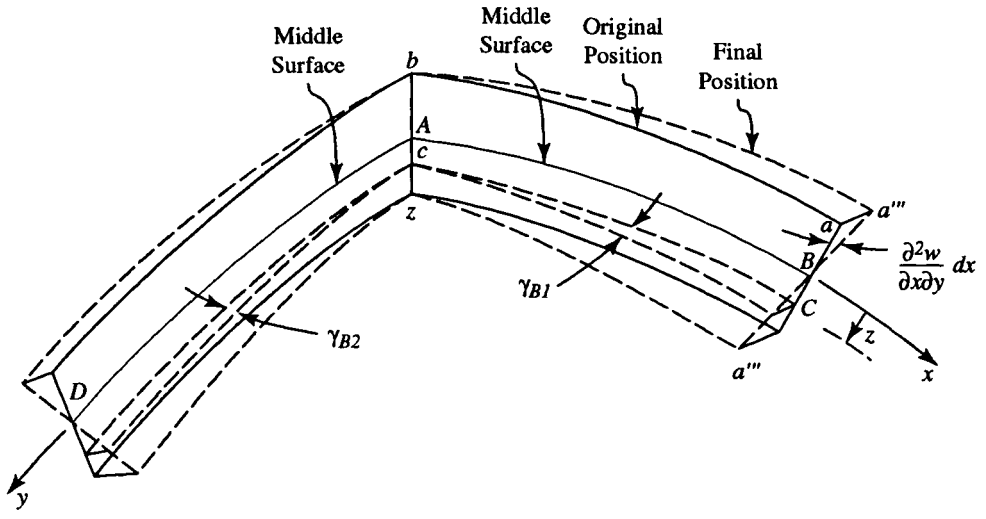

Figure 2.12

Previously rotations of these ends in the x-z plane were considered. In general, end b-b, if not rigidly clamped, would rotate through an angle $\partial w/\partial y$ during deformation, and the right end a-a would rotate through a somewhat different angle $\partial w/\partial y - \partial/\partial x\,(\partial w/\partial y)\,dx$, indicating a relative angle of rotation of $-\partial^2 w/\partial x \partial y\,dx$ in the length dx. (Observe that for the deformation of a-a to a'''-a''' there is a *decrease* of $\partial w/\partial y$.) However, since b-b is presumed to be rigidly fixed then the absolute angle of rotation of a-a is also given by $-\partial^2 w/\partial x \partial y\,dx$ as indicated by the angle between a-a and a'''-a''' in Figure 2.12. The fiber c-c located a distance z from the shell middle surface now displaces laterally an amount $-z\,\partial^2 z/\partial x \partial y\,dx$ as indicated in Figure 2.12 thus giving rise to an angle of distortion (shear) indicated by γ_{B_1} in Figure 2.12. An analogous consideration of the side AD leads to the angle of distortion indicated by γ_{B_2}. The shear strain γ_B is by definition the deviation from the original right angle and is thus

$$\gamma_B = \gamma_{B_1} = \gamma_{B_2} = -2z\frac{\partial^2 w}{\partial x \partial y} \tag{2.30}$$

The bending and twisting moments shown in Figure 2.7 are resultants of bending and shear stresses ($\sigma_x B, \sigma_y B$ and $\tau_{xy} B$ respectively) indicated in Figure 2.13. These bending and shearing stresses on fibers a distance z from the shell middle surface correspond to the normal and shear strains given by

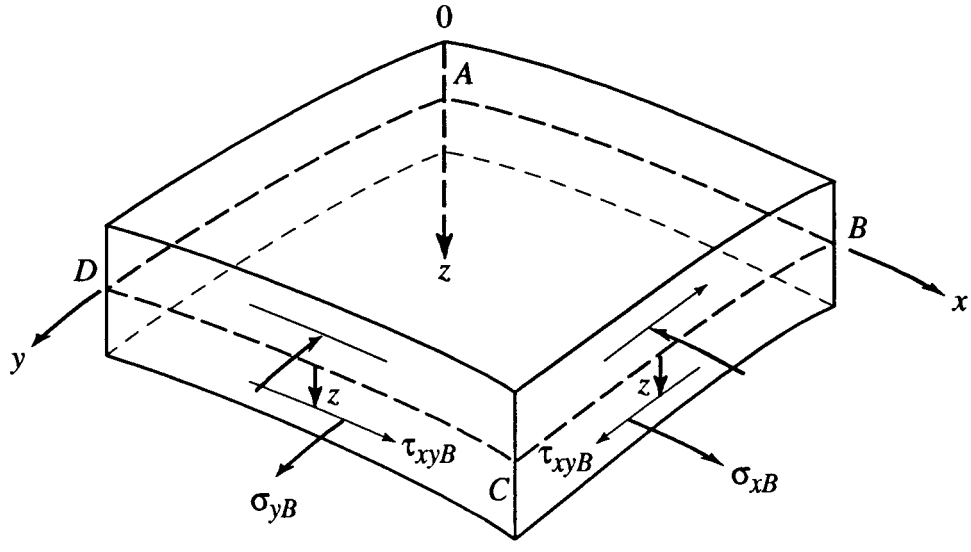

Figure 2.13

(2.28), (2.29) and (2.30). From Figure 2.13, just as in simple beam theory, but remembering that M_x and M_y represent bending moments per unit length of the shell middle surface, we have:

$$M_x = \int_{-h/2}^{h/2} \sigma_{xB} z(1) dz \tag{2.31}$$

$$M_y = \int_{-h/2}^{h/2} \sigma_{yB} z(1) dz \tag{2.32}$$

The twisting moment per unit length of the middle surface is

$$M_{xy} = \int_{-h/2}^{h/2} \tau_{xyB} z(1) dz \tag{2.33}$$

It had already been mentioned that it is customary to assume that there is no stress acting normal to the shell middle surface. Consequently, the relations between normal strains ε_{xB} and ε_{yB} of fibers a distance z from the middle surface and the normal stresses (which we will denote by σ_{xB} and σ_{yB}) acting on these same fibers are given by the two-dimensional form of Hooke's law:

$$\varepsilon_{xB} = \frac{1}{E}\left(\sigma_{xB} - \mu\sigma_{yB}\right) \tag{2.34}$$

$$\varepsilon_{yB} = \frac{1}{E}\left(\sigma_{yB} - \mu\sigma_{xB}\right) \tag{2.35}$$

where E is Young's modulus and μ denotes Poisson's ratio. These relations are readily solved for the normal stresses to yield:

$$\sigma_{xB} = \frac{E}{1-\mu^2}\left(\varepsilon_{xB} + \mu\varepsilon_{yB}\right) \tag{2.36}$$

$$\sigma_{yB} = \frac{E}{1-\mu^2}\left(\varepsilon_{yB} + \mu\varepsilon_{xB}\right) \tag{2.37}$$

The shear strain γ_B given by (2.30) of an element a distance z from the shell middle surface is related to the shear stress τ_{xyB} shown in Figure 2.13 by the relation $G = \tau_{xyB}/\gamma_B$ where G is the shear modulus. Since for isotropic materials we have

$$G = \frac{E}{2(1+\mu)} \tag{2.38}$$

then the shear stress acting in a surface a distance z from the middle surface is related to the shear strain by

$$\tau_{xyB} = \frac{E}{2(1+\mu)}\gamma_B \tag{2.39}$$

The relations (2.28), (2.29) and (2.30) may now be introduced into (2.36), (2.37), (2.39) to yield:

$$\sigma_{xB} = \frac{Ez}{\left(1-\mu^2\right)}\left(\frac{\partial^2 w}{\partial x^2} + \mu\frac{\partial^2 w}{\partial y^2}\right) \tag{2.40}$$

$$\sigma_{yB} = \frac{Ez}{(1-\mu^2)}\left(\frac{\partial^2 w}{\partial y^2} + \mu\frac{\partial^2 w}{\partial x^2}\right) \tag{2.41}$$

$$\tau_{xyB} = \frac{Ez}{(1+\mu)} \bullet \frac{\partial^2 w}{\partial x \partial y} \tag{2.42}$$

The stresses given by (2.40), (2.41), and (2.42) may now be substituted into (2.31), (2.32), and (2.33). In this operation it is to be observed that the various derivatives of w are independent of the thickness coordinate z, hence the derivatives may be brought outside the integrals to yield the moment-change of curvature relationships:

$$M_x = -D\left(\frac{\partial^2 w}{\partial x^2} + \mu\frac{\partial^2 w}{\partial y^2}\right) \tag{2.43}$$

$$M_y = -D\left(\frac{\partial^2 w}{\partial y^2} + \mu\frac{\partial^2 w}{\partial x^2}\right) \tag{2.44}$$

$$M_{xy} = -D(1-\mu)\frac{\partial^2 w}{\partial x \partial y} \tag{2.45}$$

where, for brevity, the symbol D has been introduced to represent the quantity:

$$D = \frac{Eh^3}{12(1-\mu^2)} \tag{2.46}$$

D is termed the flexural rigidity of the shell and is analogous to EI of simple beam theory where here, for the shell, I corresponds to a section of the shell of unit length along the middle surface, the shell thickness being given by h. Because of the biaxial field action of the shell the Poisson's ratio is present in (2.46) whereas it is absent in beam theory. Such a section in the direction of the y-axis is shown in Figure 2.14

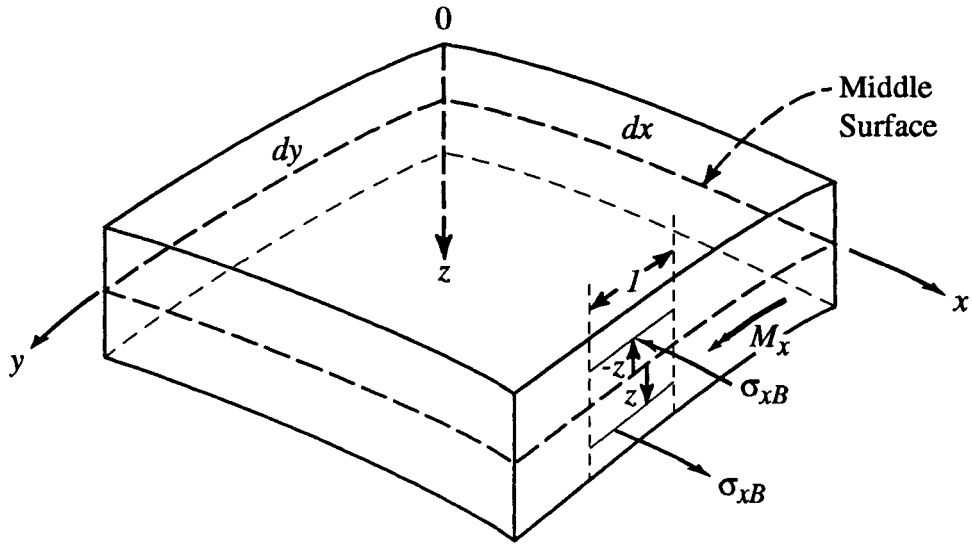

Figure 2.14

together with the normal stresses and their resultant, i.e. the bending moment M_x. Just as in simple beam analysis, the bending stresses on this side are given by

$$\sigma_{xB} = \frac{M_x z}{I}$$

But, for the section of unit length

$$I = \frac{1}{12}(1)h^3$$

hence the bending stresses are given by

$$\sigma_{xB} = \frac{12M_x z}{h^3} \tag{2.47}$$

The bending action is thus analogous to that of a beam, with the bending stresses being zero at the shell middle surface and increasing to a maximum at the outer faces. For purposes of stress determination it is not necessary to

consider the increments to M_x and M_y that are indicated in Figure 2.7. Consideration of a section in the direction of the x-axis yields a like expression:

$$\sigma_{yB} = \frac{12M_y z}{h^3} \tag{2.48}$$

The stresses σ_x, σ_y, and τ_{xy} appearing in Figure 2.6, the membrane stresses, are constant through the shell thickness h. For clarity, the subscript M will henceforth be attached to these stresses. As was mentioned previously the membrane and bending effects must be superposed to obtain the true description of shell action under load with the result that the actual (total stresses denoted by T) are given by:

$$\sigma_{xT} = \sigma_{xM} + \frac{12M_x z}{h^3} \tag{2.49}$$

$$\sigma_{yT} = \sigma_{yM} + \frac{12M_y z}{h^3} \tag{2.50}$$

The transverse shear forces Q_x and Q_y shown in Figure 2.7 are actually resultants (per unit length of shell middle surface) of shear stresses distributed over the shell thickness and oriented normal to the shell middle surface. Such stresses are indicated in Figure 2.15 for a section in the direction of the y-axis. Evidently:

$$Q_x = \int_{-h/2}^{h/2} \tau_{xz}\, dz \tag{2.51}$$

Likewise, for a section in the direction of the x-axis:

$$Q_y = \int_{-h/2}^{h/2} \tau_{yz} dz \tag{2.52}$$

Expressions for Q_x and Q_y are readily determined by substituting (2.43), (2.44) and (2.45) in (2.19) and (2.20):

$$Q_x = -D\left(\frac{\partial^3 w}{\partial x^3} + \frac{\partial^3 w}{\partial x \partial y^2}\right) \tag{2.53}$$

$$Q_y = -D\left(\frac{\partial^3 w}{\partial x^2 \partial y} + \frac{\partial^3 w}{\partial y^3}\right) \tag{2.54}$$

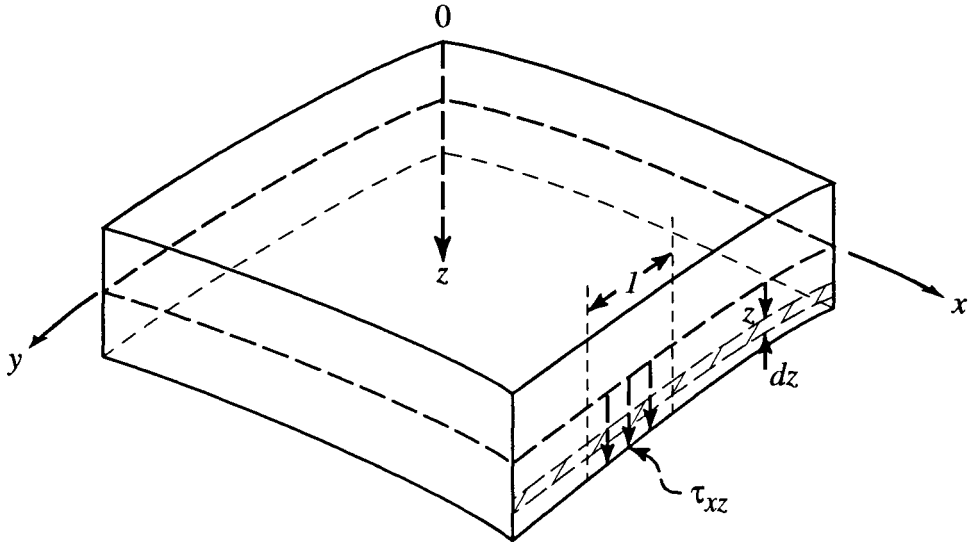

Figure 2.15

The relations (2.53) and (2.54) may now be introduced into the equilibrium equation (2.27) to yield:

$$D\left(\frac{\partial^4 w}{\partial x^4} + 2\frac{\partial^4 w}{\partial x^2 \partial y^2} + \frac{\partial^4 w}{\partial y^4}\right) = \sigma_{xM} h\left(k_x + \frac{\partial^2 w}{\partial x^2}\right)$$

$$+\sigma_{yM} h\left(k_y + \frac{\partial^2 w}{\partial y^2}\right) + 2\tau_{xyM} h \frac{\partial^2 w}{\partial x \partial y} + q \tag{2.55}$$

It is customary, for brevity, to introduce the operator ∇^4 defined by the relation:

$$\nabla^4(\ ) = \frac{\partial^4(\ )}{\partial x^4} + 2\frac{\partial^4(\ )}{\partial x^2 \partial y^2} + \frac{\partial^4(\ )}{\partial y^4} \tag{2.56}$$

At this point, it is desirable to modify the equation of compatibility

(2.16) by replacing strains by stresses through introduction of relations analogous to (2.34), (2.35) and (2.39) but written for membrane, rather than bending, effects, viz:

$$\varepsilon_{xM} = \frac{1}{E}\left(\sigma_{yM} - \mu\sigma_{yM}\right) \tag{2.57}$$

$$\varepsilon_{yM} = \frac{1}{E}\left(\sigma_{yM} - \mu\sigma_{xM}\right) \tag{2.58}$$

$$\gamma_{xyM} = \frac{2(1+\mu)}{E}\tau_{xyM} \tag{2.59}$$

With these substitutions, (2.16) becomes:

$$\frac{\partial^2\sigma_{xM}}{\partial y^2} - 2\frac{\partial^2\tau_{xyM}}{\partial x\partial y} + \frac{\partial^2\sigma_{yM}}{\partial x^2} - \mu\left(\frac{\partial^2\sigma_{xM}}{\partial y^2} + 2\frac{\partial^2\tau_{xyM}}{\partial x\partial y} + \frac{\partial^2\sigma_{yM}}{\partial x^2}\right)$$

$$= E\left[\left(\frac{\partial^2 w}{\partial x\partial y}\right)^2 - \frac{\partial^2 w}{\partial x^2}\bullet\frac{\partial^2}{\partial y^2} - k_x\frac{\partial^2 w}{\partial y^2} - k_y\frac{\partial^2 w}{\partial x^2}\right] \tag{2.60}$$

It is extremely convenient to introduce a so-called *stress function* $\phi(x,y)$ which is related to the membrane stresses by the following equations that essentially define ϕ:

$$\sigma_{xM} = \frac{\partial^2\phi}{\partial y^2};\ \sigma_{yM} = \frac{\partial^2\phi}{\partial x^2};\ \tau_{xyM} = -\frac{\partial^2\phi}{\partial x\partial y} \tag{2.61}$$

It is evident that these definitions of ϕ imply automatic satisfaction of the equilibrium equations (2.17) and (2.18). Thus, if we henceforth work with the function ϕ it will not be necessary to give further consideration to satisfaction of (2.17) and (2.18).

Introduction of the stress function into the equation of equilibrium (2.55) and the equation of compatibility (2.60) yields the desired forms of the governing equations, viz:

$$\frac{D}{h}\nabla^4 w = \frac{\partial^2 w}{\partial x^2}\bullet\frac{\partial^2 \phi}{\partial y^2} + \frac{\partial^2 w}{\partial y^2}\bullet\frac{\partial^2 \phi}{\partial x^2} - 2\frac{\partial^2 w}{\partial x \partial y}\bullet\frac{\partial^2 \phi}{\partial x \partial y}$$

$$+k_x\frac{\partial^2 \phi}{\partial y^2} + k_y\frac{\partial^2 \phi}{\partial x^2} + \frac{q}{h} \tag{2.62}$$

$$\frac{1}{E}\nabla^4 \phi = \left(\frac{\partial^2 w}{\partial x \partial y}\right)^2 - \frac{\partial^2 w}{\partial x^2}\bullet\frac{\partial^2 w}{\partial y^2} - k_x\frac{\partial^2 \phi}{\partial y^2}$$

$$-k_y\frac{\partial^2 w}{\partial x^2} \tag{2.63}$$

Equations (2.62) and (2.63) are the equations of equilibrium and compatibility, respectively, of a doubly curved shell subject to normal loading. The equations contain the two unknowns w and ϕ, are coupled and are nonlinear.

For dynamic situations, if one considers only inertial effects in the z-direction (neglecting inertia forces tangential to the shell middle surface) then the normal load q may be replaced by the inertia force and the above equations then become equations of motion. This approach neglects wave propagation effects in the system.

Also Equations (2.62) and (2.63) may be employed to treat behavior of shells having initial (no-load) geometric imperfections in the z-direction. This is accomplished by regarding w as the normal displacement from the unloaded shell having some known (or assumed) imperfection $w_0(x,y)$ at every point in the shell middle surface.

Internal Strain Energy

When a thin shell deforms under the action of applied loads, the various applied forces perform work which is stored in the shell as internal strain energy. It is convenient to determine the strain energy corresponding to membrane effects and that corresponding to bending effects separately then add these to determine the total internal strain energy. Since energy is a scalar quantity this addition is possible.

Let us first examine the energy due to membrane effects. If a simple bar is subject to axial tension with a stress σ_x and a corresponding axial strain of ε_x, then the work done on a unit volume of the bar is the product of the mean value of force per unit area, i.e. $\sigma_x/2$, times the displacement in the direction

of the force, or ε_x. The work is thus $U = \sigma_x\, \varepsilon_x/2$ and this work is stored as internal strain energy. For an element of a thin shell, such as in Figure 2.6, the stress field is biaxial and for this case the membrane strain energy per unit volume due to stresses σ_{xM} and σ_{yM} and corresponding normal strains ε_{xM} and ε_{yM} is

$$dU'_M = \frac{1}{2}\sigma_{xM}\varepsilon_{xM} + \frac{1}{2}\sigma_{yM}\varepsilon_{yM}$$

Analogously, the shear stress τ_{xyM} and corresponding shear strain γ_{xyM} give rise to work of magnitude $dU''_M = 1/2\ \tau_{xyM}\ \gamma_{xyM}$ which is also stored as internal strain energy. Thus, the membrane strain energy of the entire shell is given by

$$U_M = \frac{h}{2}\iint\left[\sigma_{xM}\varepsilon_{xM} + \sigma_{yM}\varepsilon_{yM} + \tau_{xyM}\gamma_{xyM}\right]dxdy \tag{2.64}$$

where the limits of integration are set so as to cover the entire shell.

A somewhat more convenient form is obtained by introducing the strains from (2.57) and (2.58) into (2.64) to obtain:

$$U_M = \frac{h}{2E}\iint\left[\sigma_{xM}{}^2 + \sigma_{yM}{}^2 - 2\mu\sigma_{xM}\sigma_{yM} + 2(1+\mu)\tau_{xyM}{}^2\right]dxdy \tag{2.65}$$

An alternative form that will frequently be attractive is obtained from (2.65) by introducing the stress function $\phi(x,y)$ as defined in (2.61):

$$U_M = \frac{h}{2E}\iint\left\{\left(\frac{\partial^2\phi}{\partial x^2} + \frac{\partial^2\phi}{\partial y^2}\right)\right\}^2 - 2(1+\mu)\left[\frac{\partial^2\phi}{\partial x^2}\frac{\partial^2\phi}{\partial y^2} - \left(\frac{\partial^2\phi}{\partial x\partial y}\right)^2\right]dxdy \tag{2.66}$$

To determine the strain energy due to bending effects, let us first consider a unit volume of material subject to the stresses σ_{xB}, σ_{yB}, and τ_{xyB} shown in Figure 2.13. For the stress σ_{xB} for example, the work done by it during bending is given by the product of its mean value (as it gradually increases from zero) i.e. $(0 + \sigma_{xB})/2$, and the displacement in the direction of σ_{xB} which is of course the normal strain ε_{xB}, since a unit volume is under consideration. The work is thus $1/2\ \sigma_{xB}\ \varepsilon_{xB}$ and this is stored in the shell as

internal strain energy. Since the stress field is biaxial the bending strain energy per unit volume due to the stresses σ_{xB} and σ_{yB} is

$$dU'_B = \frac{1}{2}\sigma_{xB}\varepsilon_{xB} + \frac{1}{2}\sigma_{yB}\varepsilon_{yB}$$

The shear stress τ_{xyB} and corresponding shear strain γ_{xyB} give rise to work of magnitude $dU''_B = 1/2\ \tau_{xyB}\ \gamma_{xyB}$ which is also stored as internal strain energy of bending. Thus, the bending energy of the entire shell is given by

$$U'_B = \iiint \left[\sigma_{xB}\varepsilon_{xB} + \sigma_{yB}\varepsilon_{xB} + \tau_{xyB}\gamma_{xyB}\right] dxdydz \tag{2.67}$$

where the limits of integration are adjusted so as to cover the entire volume of the shell. The normal and shear strains due to bending as given by (2.34), (2.35), and (2.39) may now be introduced into (2.67) to give the bending energy entirely in terms of stresses, viz:

$$U'_B = \frac{1}{2}\iiint \left[\sigma_{xB}\varepsilon_{xB} + \sigma_{yB}\varepsilon_{xB} + \tau_{xyB}\gamma_{xyB}\right] dxdydz \tag{2.68}$$

The stresses in (2.68) may now be expressed in terms of displacements by the introduction of (2.40), (2.41), and (2.42 in (2.68). The expression inside the integral is then in terms of various derivatives of w together with powers of z and this is immediately integrable through the shell thickness between the limits $-h/2$ and $h/2$ to obtain the bending energy:

$$U_B = \frac{D}{2}\iint \left\{ \left(\frac{\partial^2 w}{\partial x^2} + \frac{\partial^2 w}{\partial y^2} \right)^2 - 2(1-\mu)\left[\frac{\partial^2 w}{\partial x^2}\frac{\partial^2 w}{\partial y^2} - \left(\frac{\partial^2 w}{\partial x \partial y} \right)^2 \right] \right\} dxdy \tag{2.69}$$

Buckling of Thin Elastic Shells

It is desirable for the sake of simplicity to consider a column, plate, or a shell as a system with one degree of freedom and plot the relationships between load and some parameter f representing deflection. The deflections are taken to be small compared to characteristic lengths of the structure, but may be equal to the shell thickness or column section depth. The plots for the column and plate are indicated in Fig. 2.16, where OA pertains to initial equilibrium states, considered to be bending-free whereas AD and AC refer to the bent, moment-carrying equilibrium configurations. For the column P, (f) has the form of a horizontal line CD which corresponds to neutral equi-

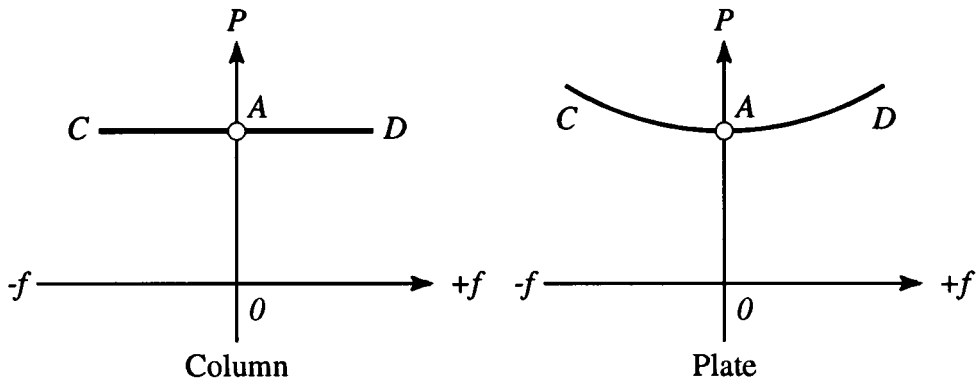

Figure 2.16

librium. For the plate we obtain a curve of postcritical stable states symmetric with respect to the ordinate axis, so that as in the case of an initially straight column, both plus and minus values of "f" are equally likely.

The most significant aspect of the behavior of compressed shells of length/radius ratios usually found in engineering practice is that they tend to fail at loads considerably below the values predicted by linearized theory. This is usually attributed to the influence of sensitivity of the shell to even very small initial geometric imperfections from perfect shape, e.g. cylindrical, spherical, etc. Experimental evidence, as well as utilization of nonlinear geometric analysis, indicates that compressed shells usually exhibit the type of load-deflection behavior shown in Fig. 2.17. There, the case of a geometrically perfect shell is indicated by the upper curve and that of a shell with initial imperfections by the lower dotted curve. In each case it is clear that equilibrium is possible in a slightly deformed configuration at loads considerably below the critical load found from linear thory and indicated by P_{cr}. In reality, the initially imperfect shell never attains the critical load P_{cr} given by linear theory for a perfect shell. The point corresponding to P_{cr} is termed the bifurcation point *(A)*.

Computerized Analysis of Shells

Once the physical aspects of shell analysis are well understood and confirmed by experiments, it is logical to carry out specific invesgitations by modern computer technology. This is a lengthy and detailed topic and space does not permit its exposition here. Indeed, it is not necessary since two recent and still timely books, one by D. Bushnell [2.5] and the other by P. Gould [2.6] offer concise developments of this topic together with many pertinent references. The reader is urged to consult these treatments for expositions of the computerized approach.

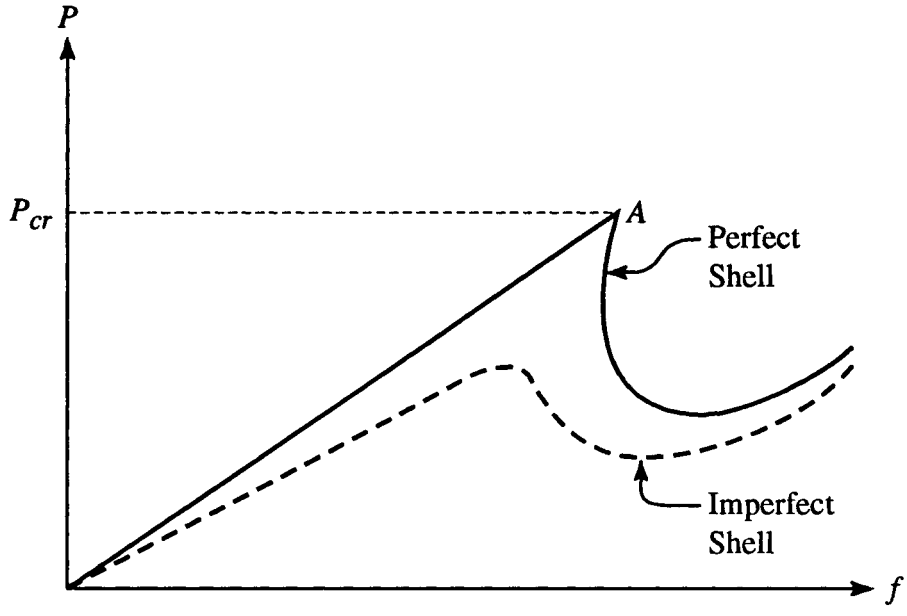

Figure 2.17

REFERENCES

2.1 Vol'mir, A.S., *Flexible Plates and Shells,* (in Russian), Moscow. Available in English as *Flexible Plates and Shells,* AFFDL-TR-66-216, 1966. 489 pages.

2.2 Vol'mir, A.S., *Stability of Elastic Systems,* (in Russian), Moscow, 1963. Available in English as *Stability of Elastic Systems,* FTD-MT-63-335, 1964. 1003 pages.

2.3 Weatherburn, C.E., *Differential Geometry of Three Dimensions,* Cambridge University Press, 1955. 268 pages.

2.4 Wempner, G., *Mechanics of Solids with Applications to Thin Bodies,* Kluwer Academic Publishers, 1990.

2.5 Bushnell, D., "Computerized Buckling Analysis of Shells," Nijhoff Publishers, Dordrecht, The Netherlands, 423 pages, 1985.

2.6 Gould, P.L., "Finite Element Analysis of Shells of Revolution," Pitman Advanced Publishing Program, Boston, MA, 1985, 210 pages.

BIBLIOGRAPHY

Anonymous, *Collected Papers on Instability of Shell Structures,* NASA-TN-D-1510, 1962, 761 pages.

Arbocz, J., Potier-Ferry, M., Singer, J., and Tvergaard, V., "Buckling and Post-Buckling Lecture Notes in Physics," Number 288, Springer-Verlag, Berlin, 1987, 246 pages.

Brush, D.O., and B.O. Almroth, *Buckling of Bars, Plates and Shells,* McGraw-Hill Publishing Co., 1975, 379 pages.

Budiansky, B., (ed.) *Buckling of Structures,* Springer-Verlag, Berlin, 1976, 398 pages.

Calladine, C.R., *Theory of Shell Structures,* Cambridge University Press, 1983, 1983, 763 pages.

Chajes, A., *Principles of Structural Stability Theory,* Prentice-Hall, 1974, 336 pages.

Chien, W.Z., "The Intrinsic Theory of Thin Plates and Shells," *Quarterly of Applied Mathematics,* Vol. 1, No. 4, pp. 297-327, Vol 2, No. 1, pp. 43-59,

1944, and Vol 2, No. 2, pp. 120-135, 1945.

Donnell, L.H., *Beams, Plates, and Shells,* McGraw-Hill., Inc., New York, 1976, 453 pages.

Dym, C.L., *Introduction to the Theory of Shells,* Pergamon Press, Oxford, England, 1974. 159 pages.

Galambos, *T.V., Guide for Stability Design Criteria for Metal Structures,* Fourth Edition, John Wiley & Sons, New York, 1988, 786 pages.

Goldenveizer, A.S., *Theory of Thin Elastic Shells,* (in Russian), 1958. Available in English, Pergamon Press, New York, 1961. 651 pages.

Grigolyuk, E.I., and Kabanov, V.Yu., *Stability of Shells,* Nauka Publishing House, Moscow, 1978, 359 pages. Available in English as FTD-ID-(RS)T-0600-80.

Gould, P.L., *Analysis of Shells and Plates,* Springer-Verlag, New York, Berlin, Heidelberg, 1988, 493 pages.

Guz, A.N., (ed.) *Methods of Analysis of Shells,* Nauka Dumka Publishing House, Kiev, Vol. 1. *Theory of Thin Shells Weakened by Holes,* A.N. Guz, I.S. Chernyshenko, V.N. Chekhov, and K.I. Shnerenko, 1980; Vol. II. *Theory of Ribbed Shells,* I.Ya. Amiro, and V.A. Zarutskiy, 1980; Vol. III. *Theory of Elasto-Plastic Shells Subject to Nonisothermal Loadings,* Yu.N. Shevchenko and I.V. Prokhorenko, 1981: Vol. IV. *Theory of Shells of Variable Thickness,* Y. M. Grigorenko, and A.T. Vasizenko, 1981, and Vol. V. *Theory of Nonstationary Aerohydroelastic Shells,* A.N. Guz and V.D. Kubenko, 1982. (In Russian.)

Hoff, N.J., *The Analysis of Structures,* John Wiley and Sons, New York, 1956. 492 pages.

Kraus, H., *Thin Elastic Shells,* J. Wiley and Sons, 1967. 476 pages.

Mushtari, Kh.M., and Galimov, K.V., *Nonlinear Theory of Thin Elastic Shells,* (in Russian), 1957. Available in English as NASA-TT-F-62, 1061. Also, U.S. Department of Commerce, Publication No. 61-31227, 1961.

Naghdi, P.M., "The Theory of Plates and Shells," in S. Flugge, Ed., *Encyclopedia of Physics,* 62/2. *Mechanics of Solids-2,* pp. 425-640. Springer-Verlag, 1972.

Niordsen, F.I., *Shell Theory,* vol. 29 in Applied Mathematics and Mechanics,

Elsevier, The Netherlands, 1985.

Novozhilov, V.V., *Thin Shell Theory,* 2nd Ed., P. Noordhoff Ltd., 1964. 417 pages.

Pogorelev, A.G., *Geometric Methods in the Nonlinear Theory of Elastic Shells,* Nauka Publishing House, Moscow, 1967, 280 pages. (In Russian.)

Pogorelev, A.G., *Geometric Shell Stability Theory,* Nauka Publishing House, Moscow, 1966, 296 pages. Available in English as FTD-ID-(RS)-T22-78.

Samuelson, L.A., and Eggwertz, S., *Shell Stability Handbook,* Elsevier Applied Science, London, 1992, 278 pages. Originally published in Swedish, 1990.

Seide, P., *Small Elastic Deformations of Thin Shells,* Noordhoff International Publishing, 1975. 654 pages.

Thompson, J.M.T., and Hunt, G.W., *A General Theory of Elastic Stability,* John Wiley and Sons, London, 1973, 317 pages.

Timoshenko, S., and Woinowsky-Krieger, S., *Theory of Plates and Shells,* 2nd Ed., Mc-Graw Hill Book Co., Inc., New York, 1959.

Vinson, J.R., *Behavior of Thin Walled Structures: Plates and Shells,* Kluwer Publishing Co., The Netherlands, 1989.

Vlasov, V.Z., *General Theory of Shells and its Applications in Engineering,* (in Russian), 1949, (Available in English, NASA, TT-F-99, 1964.)

Codes Pertinent to Shell Design

API RP2A, American Petroleum Institute, Wasington, D.C., 1982.

ASME Code Case N-284. Boiler and Pressure Vessel Code, considered by DASt, 1980, continually updated. Unique in that it indicates how various proprietary computer programs for pressure vessel buckling should be regarded.

British Standard Rules for Pressure Vessels (BS 5500) BSI, 1977. Contains allowable stress levels in many hydrostatically loaded structures, as well as buckling loads.

DASt, Deutscher Ausschuss Für Stahlbau, Richtlinin 013, 1980. Design of containment vessels and vessels subject to external pressure.

DIN 18,800, Teil 4, Stahlbauten, Stabilitätsfalle, Beulen von Schalen, 1990, Berlin, Germany.

DNV, Den Norske Veritas, considers design rules for surface vessels as well as various configurations of offshore structures, 1984, Trondheim, Norway.

ECCS, European Convention for Constructional Steelwork, 1988. Contains recommendations for design of shells to avoid bucking. Dusseldorf, Germany.

This Page Intentionally Left Blank

CHAPTER 3

STRUCTURAL BEHAVIOR OF CYLINDRICAL SHELLS

Cylindrical shells subject to hydrostatic loading occur as structural components of moving undersea vehicles as well as chambers fixed to the floor of the sea. The pressure hull of most submersibles consists of a cylindrical shell, capped at the ends by a spherical, torispherical, or ellipsoidal shell. To furnish necessary strength and rigidity at great depths the pressure hull is almost always reinforced by circular rings which may be interior or exterior to the cylindrical portion. In the present discussion it is assumed that the submersible is at a sufficiently great depth that the hydrostatic pressure is, as an approximation, taken to be constant over the entire exterior cylindrical surface.

Stress Analysis of Cylindrical Shells

In the early part of our discussion we will assume that the cylindrical shell is free of initial (no-load) geometric imperfections and free of initial stresses due to all aspects of fabrication, including welding effects. Neglecting localized effects due to the closures at each end the external hydrostatic loading produces membrane stresses in both the longitudinal as well as circumferential directions given by elementary analysis of strength of materials. However, the presence of the circular reinforcing rings, usually welded to the cylindrical pressure hull greatly changes the structural behavior of the system. These rings are often structural I-sections, WF sections, or sometimes T-sections.

Let us consider a perfectly circular cylindrical shell reinforced by a number of equally spaced identical reinforcing rings. One bay between adjacent rings is shown in Figure 3.1 where the distance between centers of adjacent rings is denoted by L_f and the unsupported length of the shell between adjacent rings is represented by L. This is a repeating section, i.e. there are many more bays to the left and right of the one shown. It will be convenient to introduce the (x,y,z) coordinate system with its origin midway between adjacent rings and with the x-direction in the direction of a shell generator, y running circumferentially, and z directed positive inward. The shell thickness is designated by h.

The equation governing the axisymmetric structural behavior of that portion of the shell between adjacent rings may be obtained from the general equation (2.62). For axisymmetric deformation, all partial derivatives of w with respect to the circumferential coordinate y vanish in (2.62) and it is then possible to employ ordinary derivatives. Further, if R denotes the mean

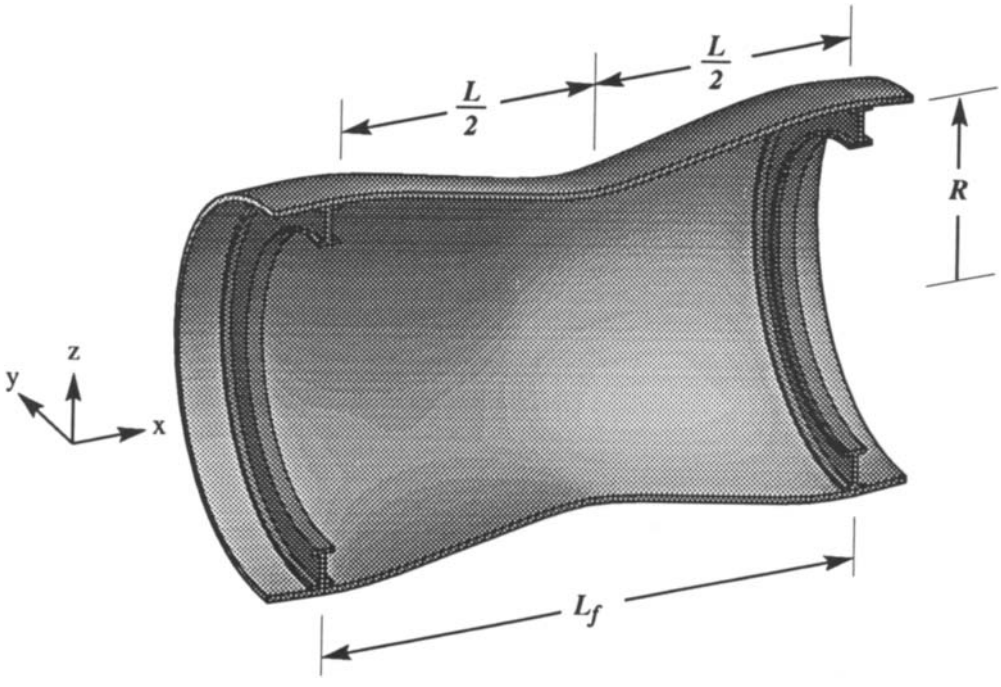

Figure 3.1

radius of the cylindrical shell, then $k_y = 1/R$, and $k_x = 0$. Also, the mean axial stress is that found by elementary analysis, namely

$$\sigma_{XM} = -\frac{pR}{2h} = \frac{\partial^2 \Phi}{\partial y^2} \tag{3.1}$$

where the negative sign has been introduced because tensile membrane stresses were assumed to be positive in Figure 2.6 and here the hydrostatic pressure obviously sets up compressive axial stresses. Thus (2.62) becomes

$$\frac{D}{h}\frac{d^4 w}{dx^4} = \frac{d^2 w}{dx^2} \bullet \sigma_{XM} + \frac{1}{R} \bullet \sigma_{YM} + \frac{p}{h} \tag{3.2}$$

where D is defined in Equation (2.46). It is not permissible to take the value of the circumferential stress σ_{yM} from elementary analysis which indicates a

value of *-qR/h* since that expression is obtained by assuming that the radial displacement *w* is constant along the shell length which is not the case here because of the influence of the reinforcing rings. Instead, it is necessary to employ (2.58) which may be written in the form

$$\sigma_{YM} = E\varepsilon_{YM} + \mu\sigma_{XM} \tag{3.3}$$

But from (2.12) for axisymmetric deformation $\varepsilon_{yM} = -w/R$ hence (3.2) may be expressed as:

$$D\frac{d^4w}{dx^4} + \frac{pR}{2}\frac{d^2w}{dx^2} - \frac{h}{R}\left[E\left(\frac{w}{R}\right) + \mu\left(-\frac{pR}{2H}\right)\right] = +p$$

or:

$$D\frac{d^4w}{dx^4} + \frac{pR}{2}\frac{d^2w}{dx^2} + \frac{Eh}{R^2}w = p\left(1 - \frac{\mu}{2}\right) \tag{3.4}$$

Equation (2.4) describes axisymmetric elastic deformations of a perfectly circular cylindrical shell of finite length subject to external hydrostatic pressure *p*. The equation has also been derived by *ad hoc* analyses of a cylindrical shell in References [3.1] and [3.2]. It is of considerable interest to observe that for some years a much-used theory due to K. von Sanden and K. Gunther [3.3] and modified by F. Viterbo [3.4] neglected the term $pR/2\ d^2w/dx^2$ in (3.4). This term essentially represents a beam-column effect.

The general solution of Equation (3.4) may be written as the sum of solutions of the corresponding homogeneous equation together with a particular solution of (3.4). Realizing that the tangent to the deflected shell shown in Figure 3.1 must be horizontal at $x = 0$ because of symmetry of deformation between adjacent rings, this leads to the solution

$$w = B\cosh\lambda_1 x + F\cosh\lambda_3 x + \frac{pR^2}{Eh}\left(1 - \frac{\mu}{2}\right) \tag{3.5}$$

where *B* and *F* are constants of integration to be determined from boundary conditions. Also, λ_1 and λ_3 are characteristic roots of the auxiliary equations corresponding to (3.4). Physically, these boundary coniditions are (a) zero change of slope of the shell adjacent to each end ring of the section shown in Figure 3.1, and (b) compatibility of shell and ring radial displacements at juncture of shell plating and ring. The axisymmetric radial displacement of the ring may be found from elementary strength of materi-

als, realizing that the radial load acting per unit circumferential length of the ring consists of the hydrostatic pressure on the horizontal flange of width *"b"* of the ring plus transverse (radially directed) shear exerted on the ring by the adjacent material of the shell.

Imposition of these boundary conditions leads to lengthy and complicated representations of the constants of integration B and F in Equation (3.5). For analytical representations of these, the reader is referred to [3.5].

With constants B and F in Equation (3.5) determined for a specific geometry, it is then possible to determine numerical values of significant stresses in the bay shown in Figure 3.1. In [3.5] it is demonstrated that the significant normal stresses in any bay are: in the circumferential direction at the outer fibers of the shell midway between adjacent rings ($x = 0$), and in the longitudinal direction at the shell inside fibers adjacent to the rings ($x = L/2$). These are, of course, the sum of bending and membrane effects.

Which of the two streses is greater depends upon shell and ring geometry, but in many cases of practical interest the longitudinal stress is more important than the circumferential one. For materials usually found in submersibles, the von Mises-Hencky criterion for yield in biaxial loading is most suitable for determination of load carrying capability once the significant stresses are found at the two above-mentioned points.

Fortunately, it is not necessary for the designer to employ Equation (3.5) and its attendant complicated relations for B and F. In 1959, M. Krenzke and R.D. Short [3.6] presented a graphical approach based upon [3.5] and leading to stresses that do not deviate from those found from a tedious, precise solution, by more than 0.2 percent. In [3.6] the authors introduce the various auxiliary parameters:

$$\alpha = \frac{A_f}{hL_f} \tag{3.6}$$

$$\beta = \frac{b}{L_f} \tag{3.7}$$

$$\gamma = \frac{p}{2E}\left(\frac{R}{h}\right)^2 \sqrt{3\left(1-\mu^2\right)} \tag{3.8}$$

$$\theta = \frac{L\sqrt[4]{3\left(1-\mu^2\right)}}{\sqrt{Rh}} \tag{3.9}$$

where A_f denotes the area of the ring stiffener, assumed to be concentrated at the middle surface of the shell, and the remaining symbols are defined in Figure 3.1, with b being effective width of the ring stiffener in contact with the shell. Reference [3.6] continues to define four more dimensionless parameters F_1, F_2, F_3, and F_4 in terms of circular and hyperbolic functions of θ. Then, it was possible to present four plots of the F_i each involving a family of curves for a range of values of θ. A typical plot appears as in Figure 3.2, indicating only one of the family of curves for a range of gamma from zero to unity. With geometric and materials characteristics of a ring-stiffened cylindrical shell one can enter the plots for F_i and set up simple linear combinations of the F_i to determine numerical values of significant longitudinal and circumferential stresses for a specified hydrostatic pressure.

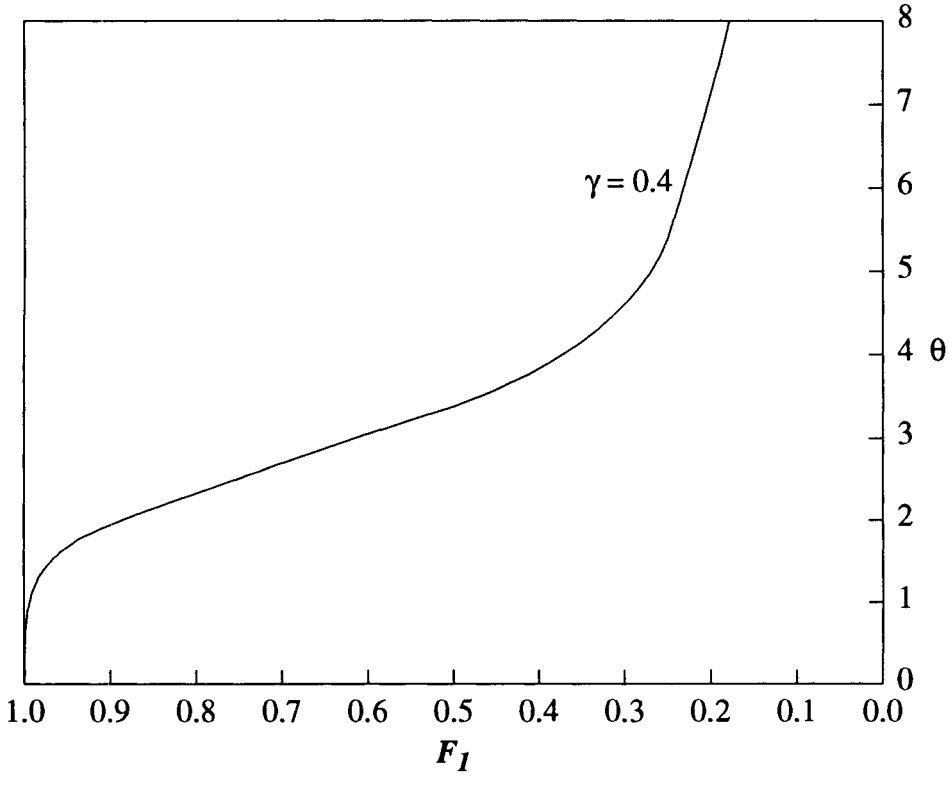

Figure 3.2

Buckling of Smooth (Unreinforced) Cylindrical Shells

Experimental investigations of the buckling characteristics of unreinforced cylindrical shells subject to external hydrostatic pressure began as early as 1858 at which time W. Fairbairn [3.7] presented an empirical relation for the buckling load of relatively long shells that were not reinforced

by any rings. An analytical solution of buckling of a long, non-reinforced cylindrical shell was presented by G.H. Bryan in 1888 [3.8]. Additional experiments were carried out by A.P. Carman in 1905 [3.9] which indicated that there exists a minimum length for any cylindrical shell beyond which the buckling pressure is essentially constant and for lengths less than this minimum "critical length" the buckling pressure increases. In 1913 R.V. Southwell [3.10] published the first of a series of three papers on the elastic buckling of a geometrically perfect cylindrical shell. This first work essentially rederived Bryan's result [3.8] but in a different manner. For the first time Southwell introduced the concept of reinforcing rings and discussed, qualitatively, their influence on buckling. In [3.10] an expression was obtained for the minimum length of shell for which the effect of the rings may be neglected. This is Carman's "critical length." Southwell's work also presented, for the first time, an analytical treatment of the problem of the number of waves that would form around the circumference upon buckling under the influence of external hydrostatic pressure. A second work by Southwell [3.11] offered an explanation of the discrepancies between predictions of the theories of Bryan [3.8] and Southwell [3.10] and the experimental results of Carman [3.9] as being caused by a reduced value of elastic limit of the shell material brought about by annealing. To substantiate this hypothesis, Southwell presented his own test results involving buckling of annealed as well as unannealed drawn steel tubes which indicated that the unannealed specimens withstood greater hydrostatic pressures. A third contribution by Southwell [3.12] suggested a safety factor to be applied to the predictions of Bryan's expression [3.8] as well as presenting a criteria for most advantageous use of reinforcing rings.

The first analysis of buckling of a thin elastic cylindrical shell with specific consideration of boundary conditions at the shell ends was presented in 1914 by R. von Mises [3.13]. This treatment was limited to consideration of radial pressure acting on the exterior of the shell, which was presumed to be of finite length. In 1929 von Mises [3.14] extended his original treatment to account for combined axial and radial loading, thus leading to a proper representation of hydrostatic pressure. His work was based upon the three linearized partial differential equations representing elastic shell action in terms of the three orthogonal displacements at any point in the shell [3.1]. These equations were treated using assumed displacements in the axial as well as circumferential directions in the form of products of harmonic functions in each direction. For example, in the circumferential direction von Mises took the radial buckling displacement to be

$$w = C \sin n\theta \sin \frac{m\pi x}{L} \tag{3.10}$$

where C is an amplitude constant, θ represents the circumferential coordinate, x the longitudinal coordinate, L the shell length, and n and m are integers denoting the number of full waves around the circumference and the number of half waves in the longitudinal direction, respectively. Comparable expressions were adopted for the axial displacement u and tangential displacement v. Amplitude coefficients A and B, respectively, were employed. After substituting the displacements comparable to (3.10) into the differential equations of equilibrium the determinant of the coefficients A, B and C must vanish. Expanding the determinant, and dropping various small terms, the von Mises buckling pressure is obtained in the form:

$$p = \frac{Eh}{R}\left[\frac{1}{n^2 + \frac{1}{2}\left(\frac{\pi R}{L}\right)^2}\right]\left\{\frac{\left(\frac{\pi R}{L}\right)^4}{\left[n^2 + \left(\frac{\pi R}{L}\right)^2\right]^2} + \frac{\left(\frac{h}{R}\right)^2}{12\left(1-\mu^2\right)}\left[n^2 + \left(\frac{\pi R}{L}\right)^2\right]^2\right\} \tag{3.11}$$

Examination of (3.11) indicates that the buckling pressure p depends upon n, the number of waves around the circumference. This means that for a given geometry of shell and for a given material, calculations must be made for different integral values of n in order to find that value of n which minimizes the pressure. This pressure is the desired buckling pressure. A very convenient chart based upon solutions of (3.11) has been offered by D.F. Widenburg and C. Trilling [3.15] wherein the chart is entered from known geometry of the shell and the number n is immediately found. With n known, the buckling pressure is immediately found from (3.11).

Another approach to this minimization is to do it analytically and thus find an expression for p which is independent of n. This was done in [3.15] with the result that a very convenient expression is obtained:

$$p = \frac{2.42E}{\left(1-\mu^2\right)^{3/4}}\left[\frac{\left(\frac{h}{2R}\right)^{5/2}}{\frac{L}{2R} - 0.45\left(\frac{h}{2R}\right)^{1/2}}\right] \tag{3.12}$$

Usually buckling pressures determined by use of (3.12) differ by no more than about 3.5 percent from those found from (3.11). It is to be observed that neither of these expressions takes specific account of the elastic

characteristics of the reinforcing rings. However (3.11) and (3.12) indicate buckling pressures considerably in excess of most experiments conducted on shells made of rolled sheet material with a longitudinal seam.

The analyses of von Mises [3.13] and [3.14] were for cylindrical shells having simply supported ends and no reinforcing rings. In 1954 W.A. Nash [3.16] extended these results to the same configuration having clamped ends. It was found that this change in boundary conditions led to elastic buckling loads as much as forty percent greater than for simply supported ends, the exact change depending upon shell geometry. In 1955, that same author [3.17] examined the elastic buckling of a hydrostatically loaded shell having nearly simply supported ends with no reinforcing rings. The analysis was based upon a slightly simplified version of the finite deformation equations (2.62) and (2.63), frequently termed the Donnell equations. These were developed earlier by L.H. Donnell [3.18] and [3.19]. It was necessary to introduce into the analysis [3.17] an "unevenness" factor describing the initial no-load deviations of the cylindrical shell from perfect circularity. Although there were no experimentally determined values of its factor, a range of values extending from half the shell thickness to the entire shell thickness was investigated and it was concluded that radial imperfections slightly less than the shell thickness could account for the deviation of load carrying capacity from that of an initially perfect cylindrical shell. In 1956, L.H. Donnell (3.20) presented a somewhat different approach to the same problem, based upon finite displacements and consideration of initial geometric imperfections. His treatment was cast in terms of volume inside the closed cylindrical shell and pressure-volume change relationships were obtained for a wider range of unevenness factors characteristic of realistic cylindrical shells. It was found that failure loads initiated by yielding agree well with test results. Another investigation along these lines was carried out by G.D. Galletly and R. Bart [3.21] at the David Taylor Model Basin in Washington, D.C. in 1957. They employed the shell equations of classical small deformation shell theory which they modified for clamped end shells, and also another slightly different version due to S. Bodner and W. Berks [3.22] for simply supported ends. Experimental tests were carried out on nine steel cylinders and it was found that if determination of initial (no-load) out-of-roundness is carried out in accordance with a method proposed by M. Holt [3.23] agreement between experimental and analytical results is quite good.

Buckling of Ring-Reinforced Cylindrical Shells - Axisymmetric

There are several modes in which a ring-reinforced cyclindrical shell subject to hydrostatic loading may fail. These modes are:

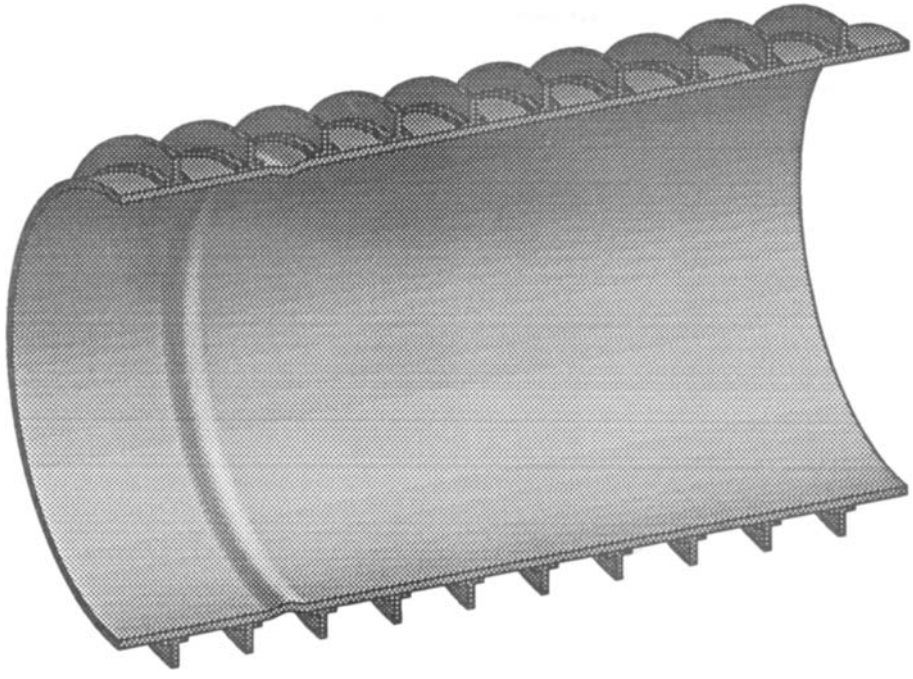

Figure 3.3

a) Inelastic axisymmetric shell instability between adjacent rings, i.e. axisymmetric collapse between adjacent rings. It is a combination of *yielding* and *axisymmetric buckling*. Experiments have indicated that this mode is characterized by an accordion-type pleat which may extend partially, or completely, around the circumference of some bay between adjacent rings. It may also occur in more than one bay of the ring-reinforced cylindrical shell. Figure 3.3 represents this mode of failure.

Note that the pleat is represented by a V-shaped ring extending fully or partially around the shell circumference.

b) *Asymmetric* collapse of the shell between adjacent rings, often termed *lobar* buckling, see Figure 3.4. This is, strictly, inelastic asymmetric shell instability between adjacent rings. The indentations, (lobes), seldom extend around the entire 360° circumference of the shell. This corresponds to *asymmetric* shell instability between adjacent rings.

For a particular ring-shell geometry, failure in mode (a) or (b) will prevail depending on shell thickness/radius ratio, ring spacing/shell radius ratio, the ratio of ring cross-sectional area to shell cross-sectional area, and stress-strain relations of the materials involved. Initial (no-load) geometric imperfections of the shell may also be of importance. A typical asymmetric

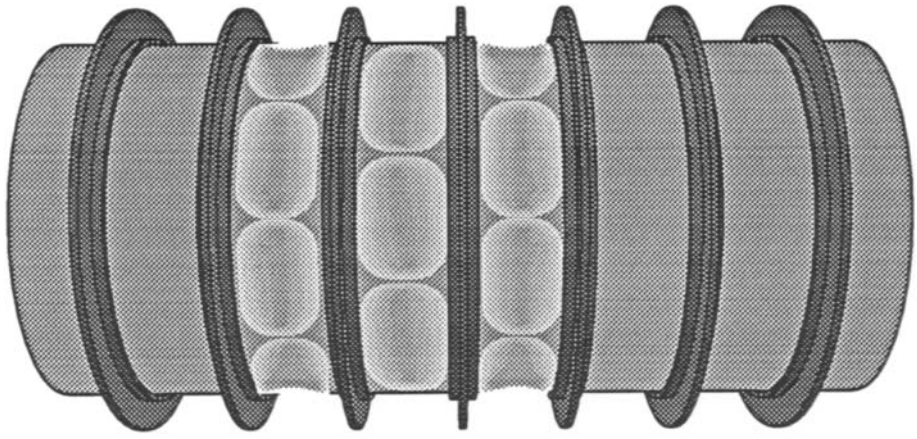

Figure 3.4

collapse between adjacent rings is shown in Figure 3.4.

With regard to formation of mode (a) i.e., inelastic axisymmetric collapse between adjacent rings, resulting in the accordion-type wrinkle extending more or less completely around the shell circumference, it is necessary to consider the circumferential as well as longitudinal normal stresses corresponding to the deflected configuration (3.5). These are offered in coplete detail in [3.5]. Failure under the biaxial state of stress existing everywhere in the cylindrical shell indicates that one must employ the Huber-von Mises-Hencky criteria to determine the collapse pressure. In [3.5] the authors considered the point on the shell outer surface midway between adjacent rings and determined longitudinal as well as circumferential streses. These were then introduced into the Huber-von Mises-Hencky equation for a biaxial stress field to lead to a collapse pressure of

$$p = \frac{\sigma_y h/R}{\{A-B\}^{1/2}}$$

where

$$A = \frac{3}{4} + a^2\left[F_2^2 + F_2F_4(1-2\mu)\sqrt{\frac{0.91}{1-\mu^2} + F_4^2\left(1-\mu+\mu^2\right)\left(\frac{0.91}{1-\mu^2}\right)}\right] \quad (3.13)$$

$$B = \frac{3}{2}a\left[F_2 - \mu F_4\sqrt{\frac{0.91}{1-\mu^2}}\right]$$

where σ_y denotes yield strength of the material.

Alternately, if we assume that the yield zone extends completely through the shell thickness at this point midway between rings, one obtains a collapse pressure of

$$p = \frac{\sigma_y h / R}{\left[\frac{3}{4} + a^2 F_2^2 - \frac{3}{2} a F_2\right]^{1/2}} \tag{3.14}$$

where, for a tentative design, the F_i may be found from the plots in [3.6].

An alternate approach to determination of the pressure causing plastic action through the shell thickness at a critical point was offered by M. Lurichick [3.24] in 1959. This theory is equivalent to treating the shell as a three-hinge mechanism and leads to predictions of collapse pressure which agree well with experimental data for certain ranges of geometry.

A comprehensive treatment of the elastic phase of buckling into the accordion-like wrinkle, mode (a), was offered by J.G. Pulos, and V.L. Salerno [3.5]. This considered biaxial effects in the shell and rings of finite rigidity. Various dimensionless parameters were introduced and plotted for practical geometric values of interest in submersibles. In this manner it became possible to readily determine the pressure required to develop extremely large radial displacements. This determined the hydrostatic loading required to cause elastic buckling.

Mode (b), i.e. buckling into a number of lobes extending from one ring to an adjacent ring and usually only over a portion of the circumference of the cylindrical shell was considered by T.E. Reynolds [3.25] in 1962. He developed a rigorous solution in which the influence of the elastic rings on both prebuckling as well as buckling deformations was included. Bending, torsional, and axial deformation energies were considered. Strain energy in the deformed shell was determined through use of quadratic terms in the strain-displacement relations and then the strain energy of the shell formulated with displacement terms through third order retained. Shell, and consequently ring, buckling displacements were represented by several terms of a Fourier series in each of the three orthogonal directions at any point in the shell. This permitted consideration of various degrees of support offered to the shell by the rings and ranging from simple support to complete fixity.

This formulation led to very lengthy and involved expressions for energy in the shell and rings together with work done by the external pressure forces. Complete details of these energies are to be found in [3.25]. Application of the Rayleigh-Ritz technique led to an equation that is transcendental in the pressure. The author suggested a semi-graphical approach for

extraction of the lowest value of pressure that caused buckling.

Further, Reynolds [3.25] discussed experimental results obtained at the David Taylor Model Basin. Tests of ring-stiffened cylindrical shells fabricated from flat steel plate by welding and in the absence of stress relieving, resulted in collapse pressure well below the predictions of linearized small deformation shell theory. It was hypothesized that these discrepancies were due to weakening effects of no-load deviations from perfect circularity together with residual stresses due to welding as well as to rolling of the flat sheet into a cylindrical form. To investigate these hypotheses several additional ring-stiffened cylindrical shells of identical geometry and material properties were machined (with integral rings) from a stress-relieved thick cylindrical shell. Both of these test specimens collapsed at hydrostatic pressures approximately forty percent greater than for the case of the models with welded rings plus a welded longitudinal seam in the absence of stress-relieving. Thus, the weakening effects of initial imperfections together with residual stresses were demonstrated, at least for the parameters concerned. These test specimens had been heavily instrumented with electric strain gages to be certain that no yielding took place prior to buckling. Typical lobar patterns developed as indicated in Figure 3.4, but the lobes did not extend completely around the shell circumference. Normal strains varied approximately with pressure up to loading close to the collapse load. Strain gage data indicated that the material behavior was elastic so that the collapse pressure was not seriously affected by inelastic action.

(c) General instability of shell and rings. If the rings are relatively "light" or "weak" in comparison to the shell, i. e., if the rings lack sufficient cross-sectional area and/or inertia it is possible that each ring will "follow" the deforming shell during collapse. This is termed general instability of the shell and rings. It usually initiates elastically but the final configuration is in the plastic range of action of the material. General instability usually occurs in that portion of the cylindrical shell lying between two essentially rigid bulkheads (a circular plate or very heavy ring) that offer near-fixity to the shell. Such collapse is shown in Figure 3.5 and usually consists of a cosine-like curve describing the buckled shell along a generator between end bulkheads, upon which is superposed additional localized radial deformations in each bay between rings.

The first analysis of such collapse was offered by T. Tokugawa [3.26] in 1929. This was based upon the method of "split rigidities," i. e., the critical pressure is represented as the sum of the pressure required to buckle the cylindrical shell plus that needed to buckle the rings. Interaction between shell and rings is not specifically considered. In 1954 A.R. Bryant [3.27] at the Naval Construction Research Establishment in Dunfermline, Scotland, ob-

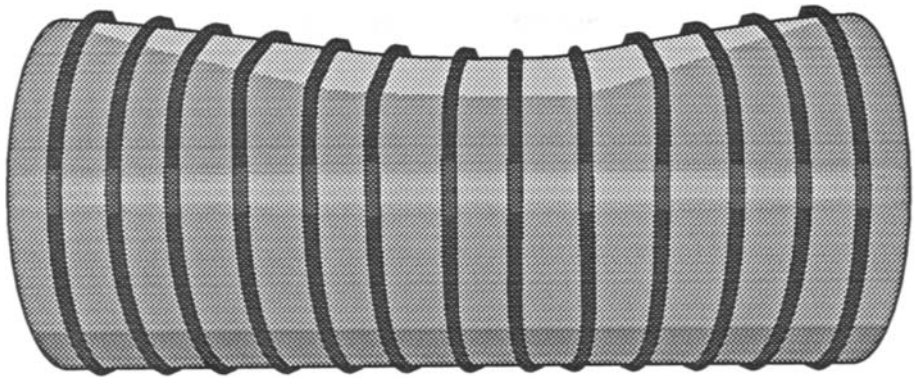

Figure 3.5

tained nearly the same result, but by a much different approach. These studies led to a buckling pressure given by

$$p = \frac{Eh}{R}\left[\frac{\lambda^4}{\left(n^2 - 1 + \frac{\lambda^2}{2}\right)}\right] + \left(n^2 - 1\right)\frac{EI_e}{R^3 L_f} \tag{3.15}$$

where $\lambda = pR/L_b$, and, as shown in Figure 3.5, L_b represents shell length (along a generator) between edges of flanges of adjacent rings, L_f denotes the distance (along a generator) between centers of adjacent rings, I_e is the moment of inertia of the combined section of one ring plus an "effective" length of the adjacent shell, and n is the number of full waves circumferentially. The first term of (3.15) corresponds to the shell and the second to the ring in the spirit of the "split rigidity" approach. One must determine the minimum buckling pressure by evaluating (3.15) for various values of n and selecting that n leading to minimum pressure.

In 1951, V.L. Salerno and B. Levine [3.28] presented a rigorous elastic analyis of collapse in the general instability mode. This was based upon the principle of minimization of the potential energy, which accounted for bending and membrane energies in the shell and rings, and energy of the external loading. The same energy approach was utilized by S. Kendrick [3.29] in 1953, but with significantly different expressions which described the collapsed system. A comparable approach was offered by W.A. Nash [3.30] in 1954. It employed different expressions for the buckled configuration than [3.28] or [3.29], and in addition, considered torsional elastic energy in the rings. Also, in 1954, E. Wenk, Jr., R.C. Slankard, and W.A. Nash [3.31]

presented results of an extensive experimental program on hydrostatic buckling of ring-stiffened cylindrical shells. The photographs [3.31] furnish a clear impression of the general instability mode of collapse.

Because of the complexity of applying the results of [3.30] to a proposed design, T.E. Reynolds [3.32] in 1957 developed a graphical approach. The significant parameters of the problem were grouped in terms of dimensionaless variables and it was possible to enter the several charts offered to determine the buckling load for the geometry under consideration. Confidence was gained in this technique by test results due to T.E. Reynolds and W.F. Blumenberg in 1959 [3.33]. Alternately, one may employ the results of a 1956 study by G.D. Galletly and T.E. Reynolds [3.34], which extended the approach developed by R.V. Southwell for determination of buckling load of a column based upon test data on imperfect (non-straight) columns.

The completely analytical approaches described in the past sections have led to a comprehensive understanding of the physical aspects of the general instability problem for the ring-stiffened cylindrical shell. Clearly application to specific geometries is extremely tedious. A significant step forward in design was offered by D. Bushnell [3.35] in 1976 with development of the BOSOR 5 computer code. This code calculates elastic instability pressures of axisymmetric shells with generalized shape of generator to permit initial imperfections. The code permits consideration of various combinations of cylinders, cones, and cone ends in the cylindrical region. Any arrangement of ring stiffeners may be treated. In 1983 S. Kendrick [3.36] published a comparison of BOSOR 5 predictions with results obtained from use of the British Standard Rules for Pressure Vessels (BS 5500) code of 1977. The BOSOR 5 yielded many eigenvalues for each integral number of circumferential waves formed during general instability. For geometries occurring in submersibles, the minimum of the BOSOR 5 pressures agreed well with the values predicted by the BS 5500 code. For certain ring-shell geometries BOSOR 5 may yield several closely spaced eigenvalues and great care must be taken in interpretation of computer results. In general, use of this computer code requires considerable skill as well as the presence of a large main-frame computer system. The BOSOR 5 system also permits determination of the hydrostatic pressure required to produce ring tripping [3.37]. This term denotes a type of instability in which the line of connection of the ring stiffener to the shell remains very nearly circular but the stiffener displaces sideways into a wavy deformation mode. T-type stiffeners as well as bar type (i.e., hollow circular plates) acting as rings are subject to this type of failure. A detailed investigation of this type of collapse was offered by M. Esslinger and H.P. Weiss [3.38] in 1988, on the basis of a computer code developed by the authors at Braunschweig, Germany.

A new approach to hydrostatic buckling of stiffened cylindrical shells has been offered by H.S. Shen, P. Zhou, and T.Y. Chen [3.39] at the Shanghai Jiao Tong University. This analysis employs a boundary layer theory which includes edge fixity conditions in the post-buckling shell analysis. A singular perturbation analysis leads to the buckling load as well as post-buckling equilibrium paths. These analytical results were in modest agreement with limited available experimental evidence on ring-stiffened cylinders available to the author.

A novel pressure hull design has been considered by C.T.F. Ross and A. Palmer [3.40] at Portsmouth University, England. They presented finite element as well as experimental data for pressure hulls having cross-sections such as indicated in Figure 3.6a and 3.6b. It was found that such a system is structurally more efficient than the traditional ring-stiffened cylinder from considerations of general instability. These geometries are termed "swedge-stiffened" and further work on their desirability is now in progress. Longitudinal profiles corresponding to trapezoidal, triangular, and sinusoidal shapes are under investigation.

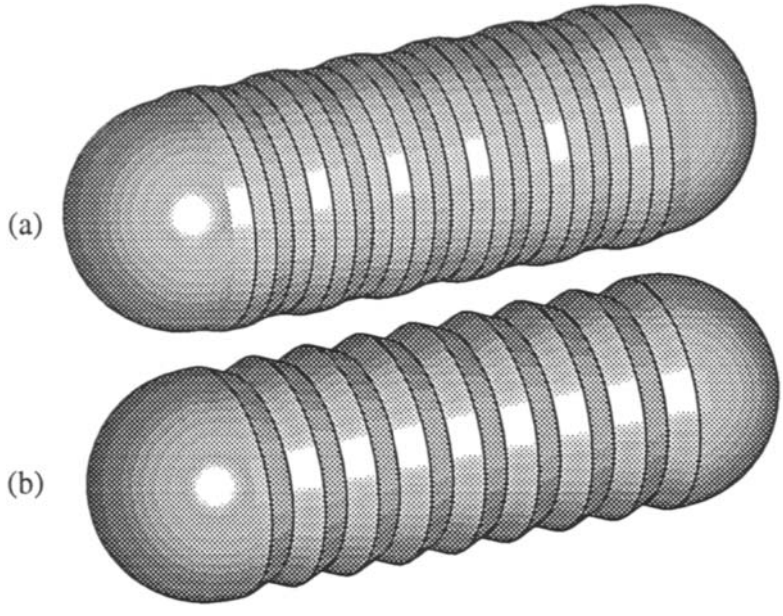

Figure 3.6

Another reliability-based approach to design criteria of hydrostatically loaded cylindrical shells has recently been offered by A.C. Morandi, P.K. Das, and D. Faulkner [3.41] at the University of Glasgow. The authors considered four methods for evaluation of failure probability: three of these

were based upon various statistical analyses of data and the fourth consisted of Monte Carlo simulation. In all cases the general purpose finite element program ABAQUS was employed to represent structural behavior in the linear range of action of the material. This approach could also be used to evaluate safety of in-service submersibles.

Because of the relatively large data bank pertinent to behavior of geometrically imperfect axially compressed cylindrical shells it has been possible to determine a reliability function leading to a "knock-down" factor commonly employed by designers of thin-walled systems. This work has been pioneered by J. Arbocz [3.42] and I. Elishakoff. Unfortunately data pertinent to structural behavior of hydrostatically loaded imperfect cylindrical shells is not as plentiful, and what does exist has not always been obtained using like geometries and boundary conditions.

REFERENCES

3.1 Timoshenko, S.P., and Woinowsky-Krieger, S., *Theory of Plates and Shells,* 2nd ed., McGraw-Hill Book Co., 1959.

3.2 Pulos, J.G., and Salerno, V.L., "Axisymmetric Elastic Deformations and Stresses in a Ring-Stiffened, Perfectly Circular Cylindrical Shell under External Hydrostatic Pressure," David Taylor Model Basin Report 1497, 1961.

3.3 von Sanden, K., and Gunther, K., "The Strength of Cylindrical Shells, Stiffened by Frames and Bulkheads, under Uniform External Pressure on all Sides," (in German), *Werft und Reederei,* 1920. Vol. 9, pp. 189-198; Vol. 10, pp. 216-221. English translation published by David Taylor Model Basin, Translation No. 38, 1952.

3.4 Viterbo, F., "Sul Problema Della Robustezza di Cilindri Cavi Rinforzati Transversalmente Sottopsti da Ogni Parte a Pressione Esterna," *l'Ingegnere,* Vol. IV, pp. 446-456 and 531-540, 1930.

3.5 Pulos, J.G., and Salerno, V.L., "Axisymmetric Elastic Deformations and Stresses in a Ring-Stiffened, Perfectly Circular Cylindrical Shell under External Hydrostatic Pressure," David Taylor Model Basin, Department of the Navy, Washington, D.C., 1961. Report 1497. See also Polytechnic Institute of Brooklyn Report 171-A, Department of Aeronautical Engineering, 1951.

3.6 Krenzke, M., and Short, R.D., "Graphical Method for Determining Maximum Stresses in a Ring-Stiffened Cylinder Under External Hydrostatic Pressure," David Taylor Model Basin, Department of the Navy, Washington, D.C., 1959. Report 1348.

3.7 Fairbairn, W., "On the Resistance of Tubes to Collapse," *Philosophical Transactions,* Vol. 148, pp. 389-413, 1858.

3.8 Bryan, G.H., "Application of the Energy Test to the Collapse of a Thin Long Pipe under External Pressure," *Proceedings of the Cambridge Philosophical Society,* Vol. 6, pp. 287-292, 1888.

3.9 Carman, A.P., "Resistance of Tubes to Collapse," *Physical Review,* Vol. 21, pp. 381-387, 1905.

3.10 Southwell, R.V., "On the Collapse of Tubes by External Pressure I," *Phil. Magazine,* pp. 687-698, 1913.

3.11 Southwell, R.V., "On the Collapse of Tubes by External Pressure,

II," *Philosophical Magazine,* pp. 502-511, 1913.

3.12 Southwell, R.V., "On the Collapse of Tubes by External Pressure, III," *Philosophical Magazine,* pp. 67-77, 1915.

3.13 von Mises, R., "Der Kritische Aussendruck Zylindrischer Rohre," *Zeitschrift Vereiniger Deutscher Ingenieur,* Vol. 58, pp. 750-755, 1914.

3.14 von Mises, R., "Der Kritische Aussendruck fuer allseits Belastete Zylindrische Rohre," *Festschrift zum 70 Geburstag von Prof. Dr. A. Stodola,* Zurich, pp. 418-430, 1929. Available in English as Experimental Model Basin Report 366, Department of the Navy, Washington, D.C. August, 1933.

3.15 Windenburg, D.F., and Trilling, G., "Collapse by Instability of Thin Cylindrical Shells under External Pressure," *Transactions of the A.S.M.E.*, Vol. 56, No. 11, 1934.

3.16 Nash, W.A., "Buckling of Thin Cylindrical Shells Subject to Hydrostatic Pressure," *Journal of the Aeronautical Sciences,* Vol. 21, No. 5, 1954, pp. 354-355.

3.17 Nash, W.A., "Effect of Large Deflections and Initial Imperfections on the Buckling of Cylindrical Shells Subject to Hydrostatic Pressure," *Journal of the Aeronautical Sciences,* Vol. 22, No. 4, 1955, pp. 264-268.

3.18 Donnell, L.H., "Stability of Thin-Walled Tubes under Torsion," National Advisory Committee for Aeronautics, Washington, D.C., Report No. 874, 1947.

3.19 Batdorf, S.B., "A Simplified Method of Elastic Stability Analysis for Thin Cylindrical Shells," National Advisory Committee for Aeronautics, Washington, D.C., Report No. 874, 1947.

3.20 Donnell, L.H., "Effect of Imperfections on Buckling of Thin Cylinders Under External Pressure," *Journal of Applied Mechanics,* Transactions of the American Society of Mechanical Engineers, Vol. 23, 1956, pp. 569-575.

3.21 Galletly, G.D., and Bart, R., "Effects of Boundary Conditions and Initial Out-of-Roundness on the Strength of Thin-Walled Cylinders Subject to External Hydrostatic Pressure," *Proceedings of the First U.S. National Congress on Applied Mechanics,* 1956. Published by the American Society of Mechanical Engineers.

3.22 Bodner, S., and Berks, W., "The Effect of Imperfections on the Stresses in a Circular Cylindrical Shell under Hydrostatic Pressure," Polytechnic Institute of Brooklyn, Department of Aeronautical Engineering, Report No. 210, December, 1952.

3.23 Holt, M., "A Procedure for Determining the Allowable Out-of-Roundness for Vessels under External Pressure," *Transactions of the American Society of Mechanical Engineers,* Vol. 74, 1952, pp. 1225-1230.

3.24 Lunchick, M.E., "Yield Failure of Stiffened Cylinders under Hydrostatic Pressure," David Taylor Model Basin, Department of the Navy, Washington, D.C. 1959. Report 1291.

3.25 Reynolds, T.E., "Elastic Lobar Buckling of Ring-Supported Cylindrical Shells under Hydrostatic Pressure," David Taylor Model Basin, Department of the Navy, Washington, D.C., 1962. Report 1614.

3.26 Tokugawa, T., "Model Experiments on the Elastic Stability of Closed and Cross-Stiffened Cylinders under Uniform External Pressure," *Proceedings of the World Engineering Congress,* Tokyo, Volume 29, 1929, pp. 249-279.

3.27 Bryant, A.R., "Hydrostatic Pressure Buckling of a Ring-Stiffened Tube," Naval Constructon Research Establishment, Dunfermline, Scotland, 1954. Report R-306.

3.28 Salerno, V.L. and Levine, B., "General Instability of Reinforced Shells under Hydrostatic Pressure," Polytechnic Institute of Brooklyn, Department of Aeronautical Engineering and Applied Mechanics, Report No. 189, 1951.

3.29 Kendrick, S., "The Buckling under External Pressure of Circular Cylindrical Shells with Evenly-Spaced Equal-Strength Circular Ring-Frames -- Part III," Naval Construction Research Establishment, Dumfermline, Scotland, 1953, Report R-244.

3.30 Nash, W.A., "General Instability of Ring-Reinforced Cylindrical Shells Subject to Hydrostatic Pressure," *Proceedings of the Second U.S. National Congress of Applied Mechanics,* 1954, published by the American Society of Mechanical Engineers, pp. 359-368.

3.31 Wenk, Jr. E.,Slankard, R.S., and Nash, W.A., "Experimental Analysis of the Buckling of Cylindrical Shells Subjected to External Hydrostatic Pressure," *Proceedings of the Society for Experimental Stress Analysis,* Vol. 12, No. 1, 1954, pp. 163-180.

3.32 Reynolds, T.E., "A Graphical Method for Determining the General Instability Strength of Stiffened Cylindrical Shells," David Taylor Model Basin, Department of the Navy, Washington, D.C., 1957. Report 1106.

3.33 Reynolds, T.E., and Blumbenberg, W.F., "General Instability of Ring-Stiffened Cylindrical Shells Subject to External Hydrostatic Pressure," David Taylor Model Basin, Department of the Navy, Washington, D.C., 1959. Report 1324.

3.34 Galletly, G.D., and Reynolds, T.E., "A Simple Extension of Southwell's Method for Determing the Elastic General Instability Pressure of Ring-Stiffened Cylinders Subject to External Hydrostatic Pressure," *Proceedings of the Society for Experimental Stress Analysis,* Vol. 13, No. 2, 1956, pp. 141-152.

3.35 Bushnell, D., "BOSOR 5-Program for Buckling of Elastic-Plastic Complex Shells of Revolution Including Large Deflections and Creep," *Computers and Structures,* Vol. 6, 1976, pp. 221-239.

3.36 Kendrick, S., "Vessels to Withstand External Pressure," published in *Developers in Pressure Vessel Technology,* Vol. 4, Applied Science Publishers, 1983, pp. 197-233.

3.37 Kennard, E.H., "Tripping of T-Shaped Stiffening Rings on Cylinders Under External Pressure," David Taylor Model Basin, Department of the Navy, Washington, D.C., 1959, Report No. 1079.

3.38 Esslinger, M., and Weiss, H.P., "Postbuckling Calculation of Extremely Thin-Walled Vessels Under External Pressure," published in *Buckling of Structures - Theory and Experiment (The Joseph Singer Anniversary Volume),* Elsevier Ltd., Amsterdam, 1988, pp. 211-220.

3.39 Shen, H.S., Zhou, P., and Chen, T.Y., "Postbucklling Analysis of Stiffened Cylindrical Shells under Combined External Pressure and Axial Compression," *Thin-Walled Structures,* Vol. 15, 1993, pp. 43-63.

3.40 Ross, C.T.F., and Palmer, A., "General Instability of Swedge-Stiffened Circular Cylinders Under Uniform External Pressure," *Journal of Ship Research,* Vol. 37, No. 1, 1993, pp. 77-85.

3.41 Morandi, A.C., Das, P.K., and Faulkner, D., "Computer Aided Reliability Based Design of Submersible Structures," Department of Naval Architecture and Ocean Engineering, Report NAOE-92-22, University of Glasgow, June, 1992.

3.42 Arbocz, J., "Towards an Improved Design Procedure for Buckling Critical Structures," published in *Structures on Land, in the Sea, and in the Air*, ed. by J.F. Jullian, published by Elsevier Applied Science, Ltd. 1991, pp. 570-577.

BIBLIOGRAPHY

Amiro, I. Ya., and Zarutskii, V.A., "Stability of Ribbed Shells," *Prikladnaya Mekhankia,* Vol. 19, No. 11, 1983, pp. 3-20 (in Russian). Available in English as Soviet Applied Mechanics, Plenum Publishing Corp.

Bijlaard, P.P., "Buckling under External Pressure of Cylindrical Shells Evenly Stiffened by Rings Only," *Journal of the Aeronautical Sciences,* Vol. 24, No. 6, 1957.

An application of the method of "split rigidities" to the ring stiffened shell, i.e. the critical pressure is represented as the sum of (a) pressure to the buckle the shell, and (b) pressure required to buckle the rings.

Bodner, S.R., and Berks, W., "The Effect of Imperfections on the Stresses in a Circular Cylindrical Shell Under Hydrostatic Pressure," Polytechnic Institute of Brooklyn, Dept. of Aeronautical Engineering and Applied Mechanics, PIBAL Report No. 210, December, 1952.

The effect of initial (no-load) deviations from circular cylindrical shape is investigated. An eighth order linear differential equation for radial deflection is derived which accounts for initial departures from perfect circularity. Stresses are obtained for the case when the initial deviations correspond to the buckled configuration.

Bodner, S.R., "General Instability of a Ring-Stiffened Circular Cylindrical Shell under Hydrostatic Pressure ," *Journal of Applied Mechanics, Transactions of the American Society of Mechanical Engineers,* Vol. 24, No. 2, 1957.

Croll, J.G.A., "Axisymmetric Collapse of Cylinders Including Deformation of Ring Stiffening," *Behavior of Thin-Walled Structures,* ed. by J. Rhodes and J. Spence, Elsevier Applied Science Publishers, London, 1984, pp. 211-233.

Axisymmetric elastic-plastic collapse estimates for cylindrical shells under arbitrary combinations of axial and radial pressure are based upon predictions of first surface yield and first full section plasticity.

DeHart, R.C., and Basdekas, N.L., "Yield Collapse of Stiffened Circular Cylindrical Shells," Southwest Research Institute, San Antonio, September, 1960.

Tests on ring-stiffened shells subject to hydrostatic loading ranging from

8000 to 10,000 lb/in^2 (68.95 MPa) were carried out and it was found that radial displacements of the shell at midbay were reduced from those in an unstiffened cylindrical shell. Also, peak strength-weight ratios were found to occur when some plastic strain is present in the stiffener at the time of collapse.

DeHart, R.C., and Basdekas, N.L., "Investigation of Yield Collapse of Stiffened Circular Cylindrical Shells with a Given out-of-Roundness," Southwest Research Institute, San Antonio, May, 1961.

A study of effect of initial geometric imperfections on strength of ring-reinforced cylindrical shells composed of material having a nonlinear stress-strain relation.

Galishin, A.Z., Merzlyakov, V.A., and Skosarenko, Yu.V., "Applicability of Different Approaches to the Determination of the Axisymmetric Stress-Strain State of Cylindrical Shells Reinforced by Annular Ribs," *Prikladnaya Mekhanika,* Kiev, Vol. 26, No. 10, 1990, pp. 50-55. Available in English as *Soviet Applied Mechanics,* Plenum Publishing Corp., New York.

A numerical investigation of hydrostatically loaded ring-reinforced cylindrical shells by means of (a) finite elements, (b) simplified representations of the rings followed by an energy approach, and (c) replacement of the rings by an elastic foundation.

Galletly, G.D., Slankard, R.C., and Wenk, E. Jr., "General Instability of Ring-Stiffened Cylindrical Shells Subject to External Hydrostatic Pressure - A Comparison of Theory and Experiment," Journal of Applied Mechanics, Transactions of the American Society of Mechanical Engineers, Vol. 25, 1958, pp. 259-266.

Tests are described on general instability of machined ring-stiffened cylindrical shells under hydrostatic pressure. Weakening effects of initial imperfections are determined. Electric strain gage data show nonlinear characteristics of deformation at the threshold of cubuckling.

Gavrilenko, G.D., and Matsner, V.I., "Stability of Cylindrical Shells with Spiral Stiffening," *Problemi Prochnosti,* (in Russian). No 2, 1990, pp. 110-113. Available in *English as Strength of Materials,* Plenum Publishing Corp. New York.

An energy approach to buckling loads of a hydrostatically loaded cylindrical shell reinforced by a spiral rib. An optimum angle of the spiral was determined and it was found that for certain shell geometries there may be an increase in load-carrying capacity of a spiral stiffener over a ring-stiffener of the same total weight.

Gerard, G., "Minimum Weight Design of Ring-Stiffened Cylinders Under External Pressure," *Journal of Ship Research,* September, 1961, pp. 44-49.

Ring-stiffened as well as unstiffened cylindrical shells subject to hydrostatic loading are compared with regard to stability as well as yield cri-

teria. The efficiency of the stiffening system is established.

Gerard, G., "Minimum Weight Design of Ring-Stiffened Cylinders under External Pressure," *Journal of Ship Research,* Vol. 5, No. 2, 1961.

Goldberg, J.E., Setlur, A.V., and Pathak, D.V., "Stability of Ring-Stiffened Cylindrical Shells with Closed Ends Under External Pressure," *Proceedings of the Pacific Symposium on Hydrodynamically Loaded Shells,* International Association of Shell Structures, University of Honolulu Press, Honolulu, 1971, pp. 400-411.

A very general computer program admitting any of five types of rotationally symmetric end closures and admitting unlike ring stiffeners. The program first calculates internal forces and moments, then carries out iteration to determine the eigenvalue and mode shape associated with each of a selected integral number of circumferential waves. The lowest eigenvalue represents buckling. Linearized shell theory is employed. The program permits thickness variation of the shell.

Gudramovich, V.S., and Demenkov, A.F., "Deformation and Carrying Capacity of Elastoplastic Cylindrical Shells with Imperfect Forms and Residual Stresses," *Prikadnaya Mekhanika,* Kiev, Vol. 21, No. 7, 1985, pp. 62-68. Available in English as *Soviet Applied Mechanics,* Plenum Publishing Corp., New York.

Analysis of hydrostatic load carrying capacity of elasto-plastic cylindrical shells having initial geometric imperfections of a random distribution. Several distributions of imperfections are studied.

Horton, W.H., "Imperfections, A Main Contribution to Scatter in Experimental Values of Buckling Load," U.S. Army Transportation Research Command, Fort Eustis, Virginia, May, 1964. Report 64-31.

Hodge, P.G. Jr., "Plastic Analysis of Cylindrical Shells," Polytechnic Institute of Brooklyn, Department of Aeronautical Engineering and Applied Mechanics, Report No. 242, January, 1954.

The case of a hydrostatically loaded long cylindrical shell reinforced by equally spaced rings is studied in detail to determine plastic collapse loadings.

Keefe, R.F., and Overby, J.A., "An Experimental Investigation of Effect of End Conditions on Strength of Stiffened Cylindrical Shells," David Taylor Model Basin, Department of the Navy, Washington, D.C., 1959. Report 1326.

Six pairs of ring-stiffened cylinders, machined from thick tubes and identical except for size and spacing of end rings, were subject to hydrostatic pressure to establish a design procedure for the end bays.

Keefe, R.F., and Short, R.D., Jr., "A Method for Eliminating the Effect of

End Conditions on the Strength of Stiffened Cylindrical Shells," David Taylor Model Basin, Department of the Navy, Washington, D.C., 1961, Report 1513.

A procedure was established for eliminating the effect of end conditions on strength of hydrostatically loaded ring-stiffened cylindrical shells.

Kempner, J., Pandalai, K.A., Patel, S.A., and Crouzet-Pascal, J., "Postbuckling Behavior of Circular Cylindrical Shells under Hydrostatic Pressure," *Journal of the Aeronautical Sciences,* Vol. 24, No. 4, 1957. Also Polytechnic Institute of Brooklyn Reports 256 and 343, October 1954 and January 1956.

Kirkwood, J.G., Richardson, J.M., and Frankel, E.M., "Buckling Instability of Thin Cylindrical Shells under External Static Loading," Office of Scientific Research and Development, Report No. 3780, 15 June, 1944.

Basic, linearized shell theory, as amended by Prof. P.S. Epsteiin (CalTech) in the Journal of Mathematics and Physics, 1942) is utilized to determine buckling loads of finite length cylindrical shells subject to hydrostatic pressure. Difference between these buckling loads and those found for like geometries through use of the vonMises method [3.14] are discussed.

Kuhn, E.J., III, and Huang, N.C., "Optimal Design of Submerged Elastic Cylindrical Shells," University of Notre Dame, College of Engineering, Technical Report UND-73-8, July 1973.

For a presumed form of shell thickness variation along the length of the submersible, optimal length/radius values are determined.

Langhaar, H.L., and Boresi, A.P., "Snap-Through and Post-Buckling Behavior of Cylindrical Shells Under the Action of External Pressure," University of Illinois Engineering Experiment Station, Bulletin No. 443, 1957.

A rigorous treatment, based upon energy considerations, of hydrostatic buckling of an unstiffened cylindrical shell. Terms through quadratic in the displacements are included in the strain expressions. Comparisons of buckling pressure obtained by this energy approach and those due to vonMises are presented in terms of dimensionless parameters.

Lee, S.D., "On the Axisymmetric Collapse of Cylindrical Shells Under External Hydrostatic Pressure," *Transactions of Chalmers University of Technology,* Gothenburg, Sweden, Number 314, 1967.

The von Karman approach for determination of the maximum allowable eccentrically applied axial load of an inelastic column has been extended to analyze a cylindrical shell stiffened by uniformly spaced rings and subject to hydrostatic loading. The technique applies only to plastic collapse in the axisymmetric mode. A one point collocation method is used to satisfy the governing equation in the plastic range.

Lunchick, M.E., and Overby, J.A., "An Experimental Investigation of the

Yield Strength of a Machined Ring-Stiffened Cylindrical Shell (Model BR-7M) Under Hydrostatic Pressure," David Taylor Model Basin, Department of the Navy, Washington, D.C., 1958. Report 1255.

A machined, stress-relieved ring-reinforced cylindrical shell was hydrostatically loaded to ascertain effects of initial imperfections and residual stresses. The experimental collapse pressure agreed well with such pressures computed from theories which account for reserve plastic strength. It was concluded that residual welding and rolling stresses did not adversely affect the collapse pressure.

Makhnenko, V.I., and Shekera, V.M., "Research into the Stresses and Strains Developing when Cylindrical Shells with Circumferential Stiffening Ribs are Welded," *Avt. Svarka* (in Russian). Available as *Automatic Welding,* for the American Welding Society, New York.

A step-by-step procedure for following development of elasto-plastic strains from inception of welding until completion.

Malik, Z.M., Morton, J., and Ruiz, C., "An Experimental Investigation into the Buckling of Cylindrical Shells of Variable Wall Thickness under Radial External Pressure," *Experimental Mechanics,* Vol. 36, No. 1, 1979, pp. 87-92.

Buckling of cylindrical shells having variable wall thickneses (in stepwise segments) ranging from 1/2000 to 1/500 with the system being subject to partial vacuum are investigated in detail experimentally.

Nash, W.A., "Buckling of Multiple-Bay Ring-Reinforced Cylindricl Shells Subject to Hydrostatic Pressure," *Journal of Applied Mechanics, Transactions of the American Society of Mechanical Engineers,* Vol. 20, 1953, pp. 469-474.

Pappas, M., and Allentuch, A., "Pressure Hull Optimization Using General Instability Equations Admitting More Than One Longitudinal Buckling Half-Wave," *Journal of Ship Research,* Vol. 19, No. 1, 1975, pp. 18032.

Often design procedures assume that the critical buckling shape in general instability contains only one longitudinal half-wave. This may be incorrect for optimal hulls if what appears to be a questionable independent ring buckling constraint is relaxed. A method for predicting general instability admitting more than one longitudinal half-wave is investigated and adapted to automated optimal design for ring-stiffened cylindrical shells. Substantial weight saving may be possible by these methods.

Raetz, R.V., "Analysis of Stresses at Junctures of Axisymmetric Shells with Flexible Insert Rings of Linearly Varying Thickness", David Taylor Model Basin, Department of the Navy, Washington, D.C., 1961, Report 1444.

Analysis of a tapered ring joining a conical shell to a cylindrical one on the basis of the Geckeler-type approximation for the analysis of the

cone. It was found that the taper significantly reduces stresses in the ring.

Reynolds, T.E., "Inelastic Lobar Buckling of Cylindrical Shells under Hydrostatic Pressure", David Taylor Model Basin, Department of the Navy, Washington, D.C., 1960. Report 1392.

A solution is developed for fully plastic action of a hydrostatically loaded cylindrical shell with right stiffeners. The solution is valid for (a) elastic-perfectly plastic action, and (b) elastic strain-hardening. A single eighth order differential equation was found to govern these actions.

Reynolds, T.E., "A Graphical Method for Determining the General-Instability Strength of Stiffened of Stiffened Cylindrical Shells," David Taylor Model Basin, Department of The Navy, Washington, D.C., 1957. Report 1106.

Reznikov, B.S., "Initial Failure of Cylindrical Ribbed Shells of Reinforced Materials," *Mekhanika Kompozitnykh Materilov,* No. 6, 1979, pp. 1031-1035 (in Russian). Available in English as *Soviet Composite Materials,* Plenum Publishing Corporation.

The effect of filamentary reinforcement (in the circumferential direction) of stiffening rings on a hydrostatically loaded composite material is evaluated on the basis of linearized orthotropic shell theory.

Roorda, J., "Pressurized Ring-Stiffened Shells: A Model Study," Journal of Structural Mechanics, Vol. 10, No. 1, 1982, pp. 33-48.

Interaction between general instability and interframe buckling in ring-stiffened cylindrical shells subject to hydrostatic loading is studied by use of a rigid link model. The model incorporates linear as well as bilinear springs with special properties to represent the rings. The model also permits a shift of stiffness from the shell to the rings. Thus, optimal weight distribution may be found in a relatively simple manner.

Ross, C.T.F., "Lobar Buckling of Thin-Walled Cylindrical and Truncated conical Shells under External Pressure," *Journal of Ship Research,* Vol. 18, No. 4, 1974, pp. 272-277.

A presentation of numerical solutions for asymmetric instability of cylindrical as well as truncated conical shells subject to hydrostatic pressure.

Rybakov, L.S., "Axisymmetric Elastic Deformation of a Circular Cylindrical Shell Reinforced by Frames," *Mekhanika Tverdogo Tela* (in Russian) Vol. 25, No. 3, pp. 132-140, 1990. Available in English as *Mechanics of Rigid Bodies,* Allerton Press Inc., New York.

The rings are treated as discrete, evenly spaced, and capable of only radial displacement. Using linearized shell theory a technique was developed for finding stresses at all points in the shell.

Shcherbakov, V.T., Pechorina, S.I., and Popov, A.G., "Stability of Cylindrical Shells Under Conditions of Creep," *Makhankia Kompozitnykh Materialov,* No. 2, 1982, pp. 279-283 (in Russian). Available in English as Soviet Composite Materials, Plenum Publishing Corp.

Shirakawa, K., and Morita, M., "Vibration and Buckling of Cylinders with Elliptic Cross Sections," *Journal of Sound and Vibration,* Vol. 84, pp. 212-131, 1982.

The case of free vibrations, as well as the limiting case of buckling, of a finite length cylinder of elliptic cross section subject to normal pressure is considered. The analysis is based upon linear, small deformation shell theory.

Singer, J., and Abramovich, H., "The Development of Shell Imperfection Measurement Techniques," Report TAE 712, The Technion, Haifa, Israel.

Stulhafer, D., "Stress Analysis of a Circular Cylindrical Shell," Reinforced by Equally Spaced Ring Frames under Uniform Pressure," *Proceeding of the Pacific Symposium on Hydromechanically Loaded Shells,* Part I, Honolulu, Hawaii. Published by the University of Hawaii for the International Association for Shell Structures, 1971, pp. 727-741.

This approach offers several refinements to the von Sanden-Gunther theory for stress analysis of ring-reinforced cylindrical shells under hydrostatic pressure.

Sunakawa, M., and Uemura, J.M, "Symmetric Buckling of Cylindrical Shells Under External Pressure," Aeronautical Research Institute, University of Tokyo, Report No. 356, 1960.

Numerical solutions of Equations (2.62) and (2.63) of this book were obtained in terms of dimensionless parameters of shell geometry.

Sundstrom, E., "Creep Buckling of Cylindrical Shells," *Transactions of the Royal Institute of Technology,* Stockholm, Sweden. Number 118, 1857.

Linearized shell theory, accompanied by the creep law due to F. Odqvist is employed to determine creep behavior of a cylindrical shell subject to hydrostatic pressure.

Vol'mir, A.S., "On the Influence of Initial Imperfections on the Stability of Cylindrical Shells under External Pressure," *Doklady,* Akad. Nauk, USSR, Vol. 112, No. 2, 1957, pp. 291-293. (In Russian).

Vol'mir modified Equations (2.62) and (2.63) of this book to include initial no-load geometric imperfections of the cylindrical shell. These are assumed to be harmonic in nature (in both circumferential and longitudinal directions) and the Galerkin procedure was employed to obtain pressure-radial deformation relationships in the shell.

Westergaard, H.M., "Stress Functions for Shells, Illustrated by a Problem of Buckling," Technical Memorandum No. 351, Bureau of Reclamation, De-

partment of the Interior, July, 1933.

The problem of structural behavior of a penstock (cylindrical shell) reinforced by circumferential rings and subject to normal loading is treated on the basis of an ad hoc simplified formulation of Equations (2.62) and (2.63) of the present book. The work was unpublished but furnished an interesting historical perspective of later works based upon the generalized vonKarman equations.

Yamaki, N., and Otomo, K., "Experiments in the Postbuckling Behavior of Circular Cylindrical Shells Under Hydrostatic Pressure", Experimental Mechanics, Vol. 13, No. 9, 1973, pp. 299-304.

Experimental results are reported on lap-jointed polyester cylinders of radius 3.94 inches (100 mm) and thickness of 0.001 inches. Test results followed the trends of small deflection theories, but buckling occurred at somewhat smaller values than predicted by such theories.

Yamaki, N., *Elastic Stablity of Circular Cylindrical Shells,* North-Holland Publishing Co., Amsterdam, 1984, 558 pages.

A comprehensive treatment of analytical and experimental approaches to buckling and postbuckling behavior of cylindrical shells subject to a variety of external static loadings. The effect of geometric imperfections is examined in detail. Behavior under combined loads, as well as behavior of partially liquid-filled shells is also examined.

Yamaki, N., and Tani, J., "Postbuckling Behavior of Circular Cylindrical Shells under Hydrostatic Pressure," *Zeitschrift fuer Angewandte Mathematik und Mechanik,* Vol. 54, 1971, pp. 709-714.

The author employs the Donnell equations for finite deformation of cylindrical shells and obtains an approximate solution through use of the Galerkin procedure based upon experimentally determined buckling configurations. The radial displacemennt thus obtained are in good agreement with experimental results reported by N. Yamaki and K. Otomo.

Yamamoto, Y., Homma, Y., Oshima, K., Mishiro, Y., Terada, H., Yoshikawa, T., Morihana, H., Yamauchi, Y., and Takenaka, M., "General Instability of Ring-Stiffened Cylindrical Shells under External Pressure," *Marine Structures,* Vol. 2, 1989, pp. 133-149.

The general instability of four machined low alloy steel having high yield strength was investigated experimentally as well as by several analytical approximations. The shell has ring-stiffeners machined so as to be integral with the cylindrical shell. Comparisons were offered with comparable studies on two welded models.

CHAPTER 4

STRUCTURAL BEHAVIOR OF CONICAL SHELLS

Stress Analysis of Conical Shells

Conical shells (usually truncated) occur frequently as components of deep submersibles. Often they are joined (with a common geometric axis of symmetry) to either cylindrical or spherical shells, as shown in Figure 4.1.

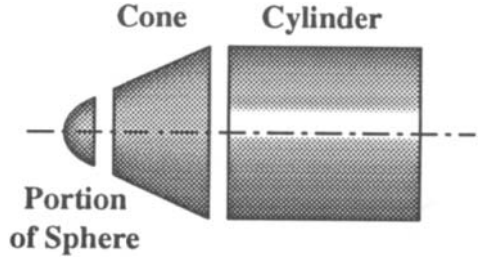

Figure 4.1

Linear as well as nonlinear behavior of hydrostatically loaded conical shells follows the formulation given in Equations (2.62) and (2.63). In the case of the conical shell (complete or truncated) the coordinate system usually employed is shown in Figure 4.2, where x is measured from the apex (or fictitious apex in the case of the truncated cone) in the direction of a shell generator, ϕ is the circumferential coordinate, and z is the radial coordinate directed toward the axis of symmetry of the shell and perpendicular to a generator. The corresponding components of displacement we will term u, v, and w respectively. The hydrostatic pressure is p. Thus, x, ϕ, and z correspond to x, y, and z in Equations (2.13), (2.14) and (2.15).

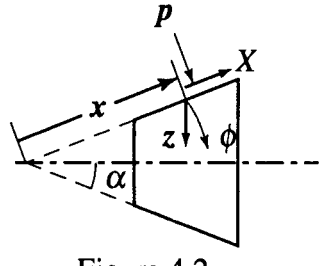

Figure 4.2

The axisymmetric membrane stresses in a hydrostatically loaded conical shell are indicated in Figure 4.3. For the nomenclature introduced above,

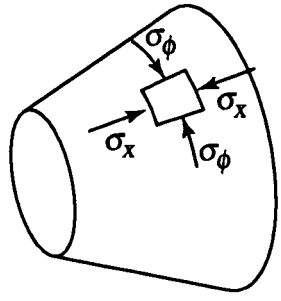

Figure 4.3

and since this stress situation is statically determinate, it is possible to show that membrane stresses are [4.1], [4.2]:

$$\sigma_x = \frac{px}{2h}\tan\alpha \tag{4.1}$$

$$\sigma_\phi = \frac{px}{h}\tan\alpha \tag{4.2}$$

$$\sigma_{x\phi} = 0 \tag{4.3}$$

In 1956 N. J. Hoff [4.3] presented an independent derivation of equations for static behavior of conical shells in the spirit of the Donnell approximation mentioned for cylindrical shells in Chapter 3. For general asymmetric deformations the strain-displacement relations were found to be

$$\varepsilon_x = \partial u/\partial x = u_{,x} \tag{4.4}$$

$$\varepsilon_\phi = (1/x \sin\alpha)\,[(dv/d\varphi) + u \sin\alpha - w\cos\alpha)] \tag{4.5}$$

$$\gamma = (\partial v/\partial x) - (1/x)\sin\alpha\,[(v\sin\alpha - (du/d\varphi) \tag{4.6}$$

for small half cone angles α, less than approximately 30°. Hoff formulated the strain energy of bending and twisting, the membrane energy, the potential of the hydrostatic pressure, then applied variational techniques to obtain the equations of equilibrium in the axial and circumferential directions:

$$[E/(1 - \nu^2)]\,[u_{,x}\,x \sin\alpha + \mu\,(v_{,\varphi} - w\cos\alpha)]_{,x} + [E/2(1+\nu)]\,[v_{,x} + (u_{,\varphi}/x \sin\alpha)]_{,\phi} + (X/h)\,x \sin a = 0 \tag{4.7}$$

$$[E/(1 - \nu^2)]\,[\mu u_{,x} + (1/x \sin\alpha)\,(v_{,\varphi} - w\cos\alpha)]_{,\phi} + [E/2(1+\nu)]\,[v_{,x}\,x \sin\alpha + u_{,\varphi}]_{,x} + (\Phi/h)\,x \sin a = 0 \tag{4.8}$$

where X, Φ and p denotes surface loads per unit area acting in the axial, circircumferential, and radial directions respectively as shown in Figure 4.2 and μ is Poisson's ratio. We let

$$H_1(z) = x \sin\alpha\{x \sin\alpha\,[x \sin\alpha(x \sin\alpha\, z_{,x})_{,x}]_{,x}\}_{,x} + 2x \sin\alpha\,(x \sin\alpha\, z_{,\varphi\varphi x})_{,x} + z_{,\varphi\varphi\varphi\varphi} \tag{4.9}$$

and

$$H_2(x) = x \sin\alpha\,(x \sin\alpha\,(x \sin\alpha\, z_{,xx})_{,xx} + z_{,xx\varphi\varphi} + x \sin\alpha\,[z_{,\varphi\varphi}/x \sin\alpha]_{,zz} + z_{,\varphi\varphi\varphi\varphi}/x^2 \sin^2\alpha - 2(1-\nu)\, z_{,\varphi\varphi}/x^2 \tag{4.10}$$

and utilize these in (4.7) and (4.8) we obtain the third (and last) equation describing equilibrium in the radial direction:

$$H_1[H_2(w)] + (Eh/D)\,(\cos^2\alpha)\,x \sin\alpha\{x \sin\alpha[x \sin\alpha(x \sin\alpha w_{,x})_{,x}]_{,x}\}_{,x} + (\cos\alpha/D)\Big|\mu x \sin\alpha\{x \sin\alpha\}x \sin\{\alpha(x^2 \sin^2\alpha\, X) - x \sin\alpha(x^2 \sin^2\alpha\, X_{,\varphi\varphi})_{,x} + (2+\mu)x \sin\alpha[x \sin\alpha(x^2 \sin^2\alpha\, \Phi_{,\varphi})_{,x}]_{,x} + x^2 \sin^2\alpha\, \Phi_{,\varphi\varphi\varphi}\Big| - (1/D)H_1(px^2 \sin^2\alpha) = 0 \tag{4.11}$$

Note that (4.11) contains only the radial displacement w so that this equation must be solved first. Then, this result is introduced into (4.7) and (4.8) to determine the displacements u and v. These equations describe the asymmetric displacements of the conical shell. They are, in point of fact, the generalization of the Donnell equations mentioned in Chapter 3 for a cylindrical shell, and indeed reduce to those relations for a half-cone angle α = 0, i.e. a cylindrical shell. Solution of these equations has proved difficult [4.4]. In 1957 P. Seide [4.5] modified the Hoff relations by retaining certain terms omitted by Hoff but even so the resulting equations are extremely dif-

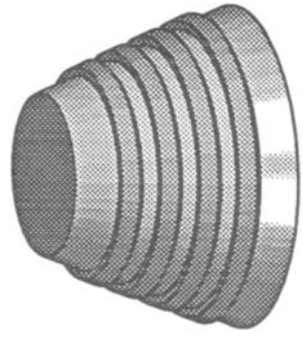

Figure 4.4

ficult to solve even for a simple loading, such as hydrostatic pressure.

Hydrostatically loaded conical shells are often reinforced by circumferential rings as indicated in Figure 4.4. Let us consider the case of a truncated conical shell with a single axisymmetric ring of radius a and supported at the right end to create equilibrium with the horizontal component of the hydrostatic loading that is axisymmetric around the system, as shown in Figure 4.5. In 1957 O. L. Bowie [4.6] offered an approximate analysis of the influence of the ring using the shell equations due to E. Reissner [4.7] which account for bending stiffness of the shell. In the Reissner relations the dis-

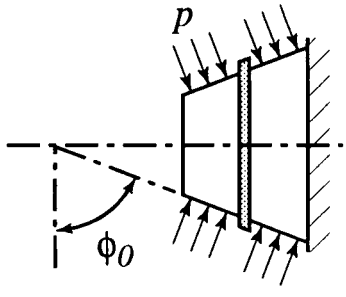

Figure 4.5

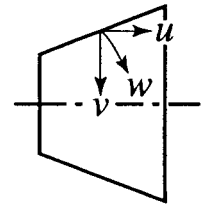

Figure 4.6

placement components constitute an orthogonal triad oriented horizontally, vertically, and tangentially as shown in Figure 4.6 instead of along the generator, radially, and tangentially as in the Hoff relations (4.7), (4.8), (4.9). Bowie considered axisymmetric deformations of the truncated shell with a single ring subject to external pressure p, having shell thickness h, Poisson's ratio μ, Young's modulus E, ring cross-sectional area A, and half-cone angle α. He then enforced compatibility of radial deformations where the ring is

joined to the conical shell but considered the dimension of the ring in the direction of a generator of the cone to be very small compared to the length of a generator of the cone. If one designates by F_r the normal force per unit of circumferential length acting between shell and ring, compatibility of deformations leads to

$$F_r\left\{\frac{\lambda}{2hE_s\sqrt[4]{1+p_1^2}}+\frac{1}{AE_r}\right\}=p\frac{\sqrt{1+p_1^2}(1)\mu/2}{E_S h} \tag{4.12}$$

where E_s and E_r denote moduli of the shell and ring respectively, and $p_1 = \cos \phi_0$.

Further, Bowie found that for the case of a truncated conical shell of thickness h reinforced by multiple, evenly spaced rings a distance d apart (measured along a shell generator) interaction effects between adjacent rings is less than approximately five per cent provided

$$d \geq \frac{2}{\lambda\sqrt{\cos\alpha}} \text{ where } \lambda=\frac{\sqrt[4]{3\left(1-\mu^2\right)}}{\sqrt{ah}} \text{ and } \mu \text{ is Poisson's ratio} \tag{4.13}$$

for the cone if there is only one adjoining ring, and

$$d \geq \frac{4}{\lambda\sqrt{\cos\alpha}} \tag{4.14}$$

if the ring has adjoining neighbors on both sides.

Bowie's analysis also indicates that the bending moment in the conical shell adjacent to the ring is given by

$$M_\xi \approx \frac{F_r\sqrt{\cos\alpha}}{4\lambda} \tag{4.15}$$

the hoop stress in the shell adjacent to the ring is

$$N_\xi \approx \pm 1/2 F_r \sin\alpha - \frac{pa}{2\cos\alpha} \tag{4.16}$$

and the radial displacement under the ring is

$$\frac{2a^2 sp(\sec\alpha)}{Eh}\left\{\frac{(1+4\nu)\tan^2\alpha}{64a\lambda^4(\sec\alpha)^{1/2}}+\frac{\mu\tan\alpha-a\lambda^4(\sec\alpha)^{1/2}}{2}\right\} \tag{4.17}$$

where a is the radius of the cone (measured perpendicular to the axis of symmetry) at a point a distance s of the reinforcing ring from the small end of the cone, measured along a generator.

In (4.11) the dimension of the reinforcing ring in the direction of a generator of the conical shell was assumed to be very small compared to the length of a generator of the cone. Often it is necessary to determine the structural influence of a relative large cross-section elastic ring used as a reinforcement on a closed end conical shell. In such a case it is necessary to first determine expresssions for the influence on the conical shell of axisymmetrically distributed transverse shearing forces H as well as bending moments M acting at the open end of a hydrostatically loaded conical shell as shown in Figure 4.7. In 1953 E. Wenk and C.E. Taylor [4.8] investigated axisymmetric behavior of such a constant thickness conical shell, which is governed by a fourth order differential equation, and found solutions in terms of Bessel functions which may be grouped in a convenient manner leading to the so-called tabulated Schleicher functions. With the notation of Figure 4.7 the displacement w perpendicular to a generator of the cone was shown to be:

$$w=\frac{-\sqrt{2x}}{D\lambda_3}\frac{\eta}{\eta_0}\{[x_0 H\cos\alpha+\frac{x_0^2\sin^2\alpha}{2}p+\sqrt{x_0}\lambda\left(\frac{2}{\xi_0}-\frac{\sqrt{2}}{2}\right)M]\cos\left(\frac{\xi_0-\xi}{\sqrt{2}}\right)$$

$$+\frac{\sqrt{2}}{2}\sqrt{x_0}\lambda M\sin\left(\frac{\xi_0-\xi}{\sqrt{2}}\right)\}+\frac{3}{4hE}px^2\tan^2\alpha \tag{4.18}$$

where

$$\lambda=\sqrt[4]{\frac{12(1-\mu^2)}{h^2\tan^2\alpha}} \tag{4.19}$$

$$\xi=2\lambda\sqrt{x} \tag{4.20}$$

$$\eta=\frac{e^{\xi/\sqrt{2}}}{\sqrt{2\pi\xi}} \tag{4.21}$$

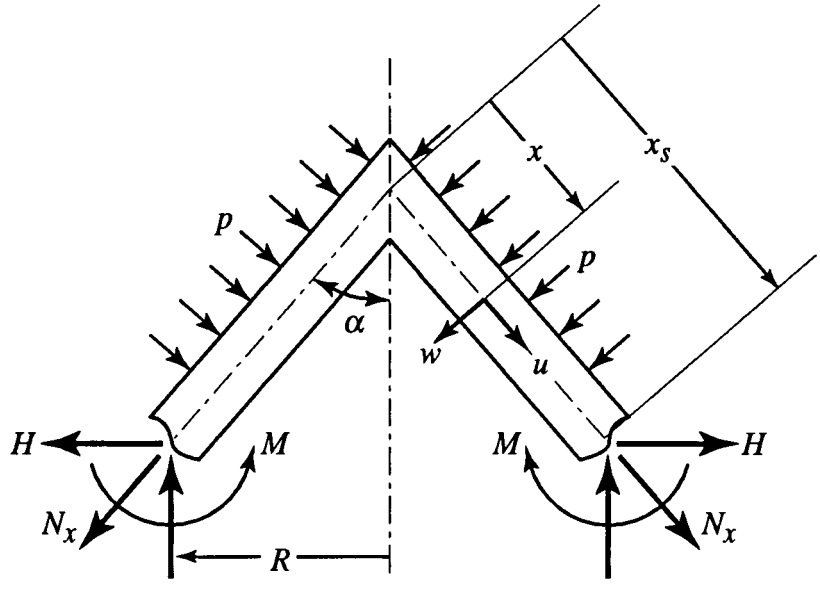

Figure 4.7

and x_0 for a truncated cone is measured from the fictitious vertex along a generator as in Figure 4.7.

From shell theory, the bending moments and in-plane normal forces as well as the transverse shearing force at any point x in the shell are found from

$$M_x = D\, w_{xx} \tag{4.22}$$

$$M_\phi = D\, v\, w_{xx} \tag{4.23}$$

$$N_x = D\,(\tan\alpha)\, w_{xxx} - \frac{px}{2}\tan\alpha \tag{4.24}$$

$$N_\phi = D\,(\tan\alpha)\, x\, w_{xxxx} - px\tan\alpha \tag{4.25}$$

$$Q_x = D\, w_{xxx} \tag{4.26}$$

For example, the meridional (longitudinal) bending moment (per unit of circumferential length at a station a distance x from the apex due to axi-symmetric loads H, M, and p was found to be

$$M_x = \frac{-\eta}{\eta_0 \xi}\left\{\left[2\sqrt{2}x_0 \,\mathrm{H}\cos\alpha + \sqrt{2}x_0^2 \,\mathrm{p}\sin^2\alpha\right.\right.$$

$$\left.\left.-\sqrt{x_0}\lambda\left(2 - \frac{4\sqrt{2}}{\xi_0}\right)M\right]\sin\left(\frac{\xi_0 - \xi}{\sqrt{2}}\right) - 2\sqrt{x_0}\,\lambda\,\mathrm{M}\cos\left(\frac{\xi_0 - \xi}{\sqrt{2}}\right)\right\} \tag{4.27}$$

The other bending moment, as well as the in-plane and transverse shearing forces are given in detail in [4.8]. The outer fiber stresses in the conical shell are then found as the sum of bending and normal stressess in the form (for outer fiber stresses along a generator):

$$\sigma_x = \frac{Q_x \tan\alpha}{h} - \frac{px}{2h}\tan\alpha \pm \frac{6M_x}{h^2} \tag{4.28}$$

A similar expression exists for outer fiber circumferential stresses. Thus, for given values of H, M, and pressure p, stresses may be readily determined at any point in the conical shell.

Often the conical shell is securely attached (perhaps welded) to some adjacent, coaxial, shell such as a cylinder or a sphere, see Figure 4.1, or possibly to a heavy reinforcing ring. Compatibility of displacements and rotations must be enforced at this juncture and H and M represent discontinuity shears and moments at the circumferential joint. The normal displacements and rotations at the open end of the conical shell are functions of H, M, p, and geometric and materials parameters of the conical shell. In [4.8] these influence coefficients for displacement and rotation of the end of a generator were shown to be

$$\theta_0 = aM + bH + cp \tag{4.29}$$

$$\overline{w}_0 = dM + gH + f_p \tag{4.30}$$

where

$$a = \frac{\theta_0^M}{M} \approx \frac{U^3}{E}\sqrt{\frac{2R}{h^5\cos\alpha}} \tag{4.31}$$

$$b = \frac{\theta_0^H}{M} = \frac{U^2}{E}\frac{R}{h^2} \tag{4.32}$$

$$c = \frac{\theta_0^p}{p} - \frac{U^2}{2E}\frac{R^2 \tan\alpha}{h^2} + \frac{3}{2E}\frac{R}{h}\frac{\tan\alpha}{\cos\alpha} \tag{4.33}$$

$$d = \frac{\overline{w}_0^M}{M} \approx \frac{U^2 R}{Eh^2} \tag{4.34}$$

$$f = \frac{\overline{w}_0^p}{p} = -\frac{U}{E}\sqrt{\frac{R^5}{2h^3}\frac{\sin^2\alpha}{\cos\alpha}} + \frac{(1-\nu/2)}{E}\frac{R^2}{h\cos\alpha} \tag{4.35}$$

$$g = \frac{\overline{w}_0^H}{H} = \frac{-\sqrt{2}U}{E}\sqrt{\frac{R^3}{h^3}\cos\alpha} \tag{4.36}$$

Analogous expressions for cylindrical as well as spherical shells are to be found in [2.5]. Thus, problems of joining of coaxial conical, cylindrical, and spherical shells subject to hydrostatic loading may be readily treated to ascertain the effects of the joint.

For example, the effect of a heavy, elastic ring at the junction between a conical and a cylindrical shell, has been examined by the use of the above influence functions by R.V. Raeta and J.G. Pulos [4.9]. The discontinuity shears and moments (uniformly distributed around the circumference of the system) appear as in Figure 4.8.

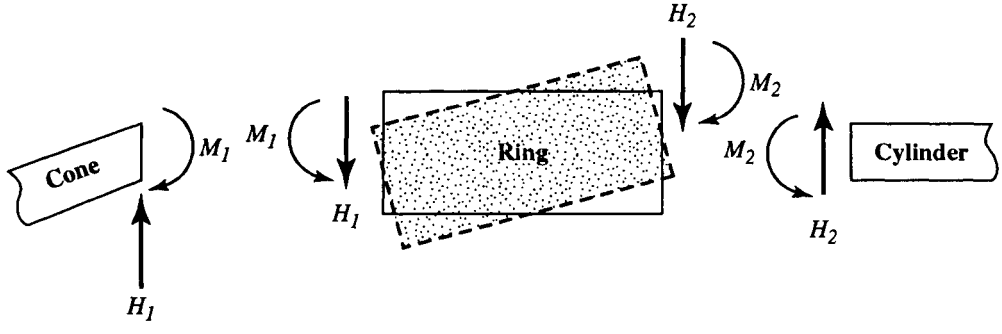

Figure 4.8

The conical shell involved in this example was assumed to be truncated and closed at the end remote from the cylindrical shell by a spherical dome. The length of the truncated conical shell was taken to be of the order of magnitude of the larger radius of the cone, so that it became necessary to generalize equation (4.18) to account for the interaction of displacements

and rotations due to both ends of the conical frustum being loaded simultaneously. Since the transverse shears and moments act on the ends of the ring shown in Figure 4.8 it is necessary to consider rotation of the ring cross-section as shown by dotted lines in Figure 4.8. This angle of rotation is uniform around the ring circumference and may be found from elementary ring theory.

In [4.10] Wenk and Taylor offered a numerical solution of a system consisting of a 27 inch diameter (68.6 cm) cylindrical shell joined coaxially to a 16 inch (40.6 cm) cylindrical shell by a conical shell with a heavy reinforcing ring at each end of the cone. Numerical tabulations of functions pertinent to the edge coefficients were offered.

Buckling of Conical Shells

Hydrostatically loaded complete as well as truncated conical shells may buckle elastically, plastically, or into the elasto-plastic range of action. The initial buckling configuration appears as in Figure 4.9 for a truncated conical shell. The buckled shape of a truncated conical shell consists of a number n of dents (lobes) of depth measured normal to the undeformed shell surface) at least several times the shell thickness. The lobes extend from one end of the truncated cone to the other and are rather regularly spaced around the circumference of the shell as in Figure 4.9. Because of initial geometric imperfections in the shell prior to loading, thickness variations occuring during production of the sheet metal from which the cone is fabricated, and possible small amplitude vibrations occuring during testing, the entire circumference may not be filled with lobes, as shown by the dot-dash line in Figure 4.10.

Perhaps the earliest analytical investigation of elastic buckling of hydrostatically loaded truncated as well as complete conical shells (with an apex) is due to A. Pflüeger [4.11] in 1937 of Hannover, Germany. This study involves application of simplified differential equations (lacking many terms presented by N.J. Hoff [4.3]) to each of these shells for the case where the shell thickness was taken to increase linearly from the apex for the complete shell or linearly from the fictitious vertex in the case of a truncated conical shell. The boundary conditions for either shell corresponded approximately to simple support, but not all displacement relations were satisfied at either boundary for the truncated cone. When applied to constant thickness conical shells, Pflüeger's solution leads to very conservative results even if a mean shell thickness is considered in his solution.

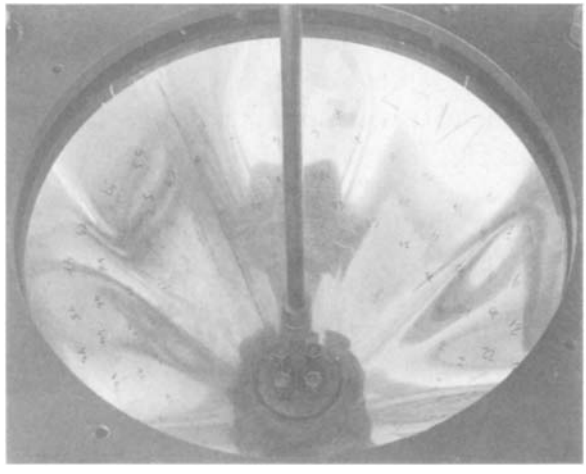

Figure 4.9 [From Prof. J. Singer, The Technion, Haifa, Israel]

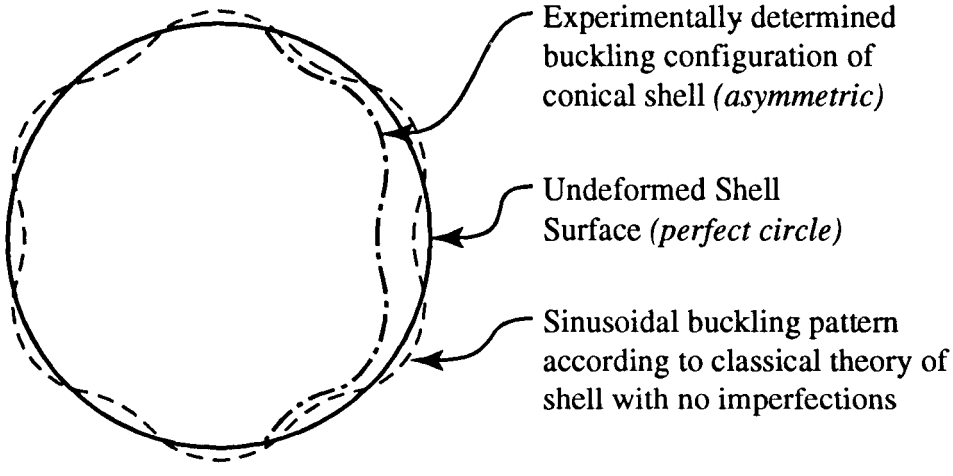

Figure 4.10

Several investigators have attempted to relate buckling of conical shells to buckling of "an equivalent cylindrical shell." The first of these is T. Tokugawa [4.12] who, in 1940, rather arbitrarily suggested that the equivalent cylindrical shell is one whose radius is equal to the radius of curvature of the cone at a point on a generator of the conical surface located at a distance of 0.6 times the length of a generator of a closed conical shell (having an apex). This leads to a hydrostatic buckling pressure p given by

$$\frac{p}{E} = 1.83 \tan \alpha \left(\frac{h}{\rho}\right)^{2.5} \tag{4.37}$$

where r has the significance shown in Figure 4.2, α is the half-apex angle, h the constant shell thickness, and E is the elastic modulus of the cone. In 1947 F.I.N. Niordson [4.13] developed a Ritz-type energy approach applicable to truncated conical shells and introduced an assumed deflection shape during buckling. This led to a hydrostatic buckling load:

$$\frac{p}{E} = 2.51 \tan \alpha \left(\frac{h}{\rho}\right)^{2.5} \tag{4.38}$$

This relation leads to higher values of buckling load than does Tokugawa's which, in turn, gives higher values than Pflüeger's relation. However, the Niordson approach is only applicable to truncated conical shells, and not to complete ones. In 1953 P.P. Bijlaard and R. Wong [4.14] employed the equivalent cylindrical shell concept where the cylinder is of thickness equal to that of the cone, whose radius is equal to the largest radius of curvature of the cone, see Figure 4.2, and whose length is equal to approximately 0.8 the length of a generator of the truncated conical shell. In all of these "equivalent cylindrical shell" investigations the authors referred to the buckling pressure of the cylinder as that given by the simple, linearized shell theory approach employed by R. von Mises (see Chapter 3).

In 1955 W.D. Jordan [4.15] investigated the buckling of complete conical shells experimentally as well as analytically and compared test results with the theoretical predictions of Pflüeger, Tokugawa, Niordson, and Bijlaard and Wong. Tests were conducted on 24S-T3 and 61S-T6 aluminum alloy models having a total cone angle of 20°, 30°, 40° and 50° with wall thicknesses ranging from 0.040 inches (1.02 mm) to 0.080 inches (2.04 mm). The greatest diameter of any of these shells was 12 inches (30.48 cm). The test cone was situated inside a very rigid cylinder and hydrostatic pressure applied by oil surrounding the test specimen. A hand pump permitted gradual increments of pressure within the oil. Test data appears in Figure 4.13. Jordan concluded by indicating that the Bijlaard relation indicated a realistic design pressure for elastic buckling. However, it is to be noted that the boundary conditions employed during Jordan's tests were not in good agreement with those assumed by Bijlaard in his analysis.

Another series of tests on complete conical shells was carried out by F.J. Schroeder, E.T. Kirstere and R.A. Hirsch [4.16] in 1958. The models were fabricated from brass sheet 0.010 inches thick (0.254 mm) and had a soldered seam along a generator. The test technique was nearly the same as that employed by Jordan. The authors found that the experimentally determined buckling pressures, shown in Figure 4.13, were in rather close

agreement with the predictions of the von Mises approach for a cylindrical shell having an "equivalent radius" equal to half the radius of the base of the complete cone. Again, the boundary conditions used during testing did not agree with those of the von Mises theory.

In 1954 at the Kazan Aviation Institute, Kh.M. Mushtari and A.V. Sachenkov [4.17] used conical shell equations identical to those proposed by Seide [4.5] but assumed slightly different conditions of end support together with the Galerkin approach to solve the governing equations to obtain a complex expression for the hydrostatic pressure to cause elastic buckling. In that same year P.P. Radkowski [4.18], [4.19] approached the same problem from an energy standpoint, formulated the total potential energy, then applied the Rayleigh-Ritz technique to obtain equilibrium relations between hydrostatic and bucking deflections. This was the same buckled configuration employed earlier by Niordson [4.13]. The results are invalid for a complete (non-truncated) cone.

In 1957 C.E. Taylor [4.20] presented a rigorous application of the Trefftz' theory of elastic stability to the case of hydrostatically loaded conical shells. An energy approach was followed and an approximate solution for the buckling pressure of a complete conical shell was obtained using the Rayleigh-Ritz method. It was found that additional quadratic terms in the energy expression do not significantly affect the value of the buckling pressure. However, Taylor found that these terms in the more accurate strain energy expression are required if large deflection theory is applied to determine buckling of complete or truncated conical shells.

In 1960 P. Seide [4.21] specialized the general equations (2.62) and (2.63) to the case of a conical shell and then determined the bending and extensional energy of the shell from relations (2.66) and (2.69). Thus, the energy was expressed in terms of the three orthogonal displacement components u, v, and w together with the stress function Φ of the shell middle surface forces. The compatibility relation (2.63) was solved exactly in terms of parameters corresponding to the assumed deflection function, and from that information middle surface forces, moments, as well as displacements u and v could be found in series form. This led to a system of homogenous linear equations for the coefficients of the series representing u and v displacements and the stability criterion was obtained by setting the determinant of the coefficients of these equations equal to zero. Seide employed a coordinate transformation due to Mushtari and Sachenkov [4.17], namely

$$e^{z_1} = \frac{x}{x_1} \tag{4.39}$$

where x_1 and x_2 are distances from the vertex to the small and large ends, respectively, as shown in Figure 4.11 to put the compatibility equation in the form of an equation with constant, rather than variable coefficients to obtain a simple representation of the stress function of the middle surface forces. Constants of integration were determined from the four boundary conditions associated with the ends of the truncated conical shell. Seide pointed out that if all boundary conditions on the conical shell are satisfied by the assumed deflection function for w that the method is identical with that employed in [4.17] where the Galerkin method is used to satisfy the equation of equilibrium in the direction normal to the conical surface.

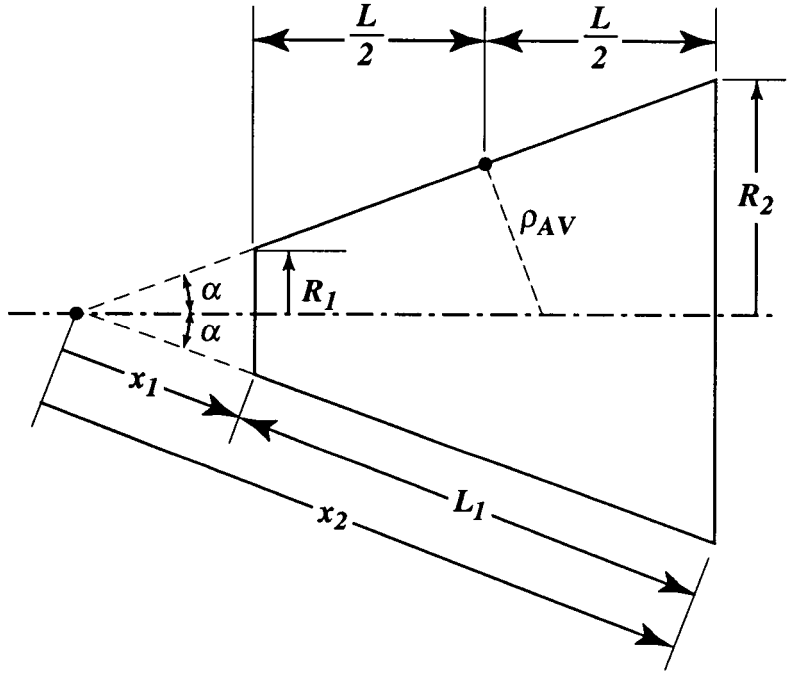

Figure 4.11

For the case of a hydrostatically loaded conical shell Seide [4.21] used the membrane stresses prior to buckling in the form from Equations [4.1] and [4.2] and further assumed that the truncated conical shell is closed by end plates rigid in their own planes, but free to distort out of their planes and which offer no restraint against rotation at the ends of the conical frustum. Employment of the principle of minimum potential energy and dropping of minor terms led Seide to the hydrostatic buckling pressure:

$$p = \frac{\dfrac{\pi\sqrt{6}}{9\left(1-\mu^2\right)^{3/4}} E \tan\alpha}{\left(1-\dfrac{R_1}{R_2}\right)\left(\dfrac{1+\dfrac{R_1}{R_2}}{2}\right)^{3/2}\left(\dfrac{\dfrac{R_2}{\cos\alpha}}{h}\right)^{3/2}} f\left(1-\frac{R_1}{R_2}\right) \tag{4.40}$$

for a truncated cone where R_1 nd R_2 are defined in Figure 4.11. Seide then employed the concept that the hydrostatic buckling pressure of a conical frustum is given approximately by an equation similar to that for an "equivalent" cylindrical shell having a length equal to the slant length of the cone *(L/*cos α*)* together with a radius equal to the average radius of curvature of the cone, i.e.

$$\left[\frac{R}{\cos\alpha}\left(1+\frac{1}{2}\frac{\lambda}{R_1}\tan\alpha\right)\right] \tag{4.41}$$

but with the wave number n replaced by *(n/*cos α*)*. The hydrostatic buckling pressure p_e of this equivalent cylinder was obtained by the Batdorf approach [3.19]. Thus, one can form the pressure ratio p/p_e for a wide variety of conical frustra with semi-vertex angles ranging from 0° to 60°, length/radius ratios ranging from 0.5 to 10.0, and R_1/h ratios ranging from 250 to 2000. The function *f*, based upon this wide range of geometric parameters, is shown in Figure 4.12 as determined by Seide.

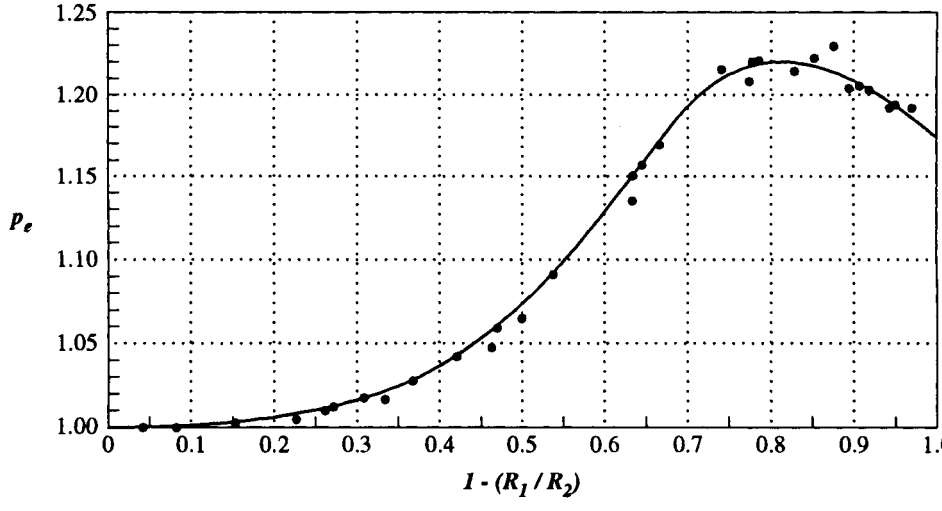

Figure 4.12

Computation in [4.18] apply only to the range

$$0 < \left(1 - \frac{R_1}{R_2}\right) < 0.9719$$

and Equation (4.40) is valid only if $n > 2$. If the cone is relatively thick-walled it will buckle into an oval shape and (4.40) is invalid. The taper ratio for a cylindrical shell is, of course, zero.

For the case of a complete conical shell the taper ratio is unity and Equation (4.40) becomes

$$p \approx 1.175 \frac{\dfrac{4\sqrt{3}\pi}{9\left(1-\mu^2\right)^{3/4}} E \sin\alpha}{\left(\dfrac{R_2}{\dfrac{\cos\alpha}{h}}\right)^{5/2}} \tag{4.42}$$

It is of interest to compare the buckling pressure obtained by Seide with those given by the theories of Niordson [4.13], Bijlaard [4.14], as well as Mushtari and Sachenkov [4.17]. This is presented in Figure 4.13 wherein it it evident that the Niordson solution is a lower bound to the small deflection buckling pressure of a conical shell. Although Niordson employed the Rayleigh-Ritz approach (which should have led to higher values of buckling load) he did introduce modifications to the stability criteria which shifted the usually high values found through use of Rayleigh-Ritz. The very high values indicated in Figure 4.13 when the Mushtari-Sachenkov approach [4.17] is employed indicate that the one-term approximation for the buckled configuration is inadequate for nearly complete conical shells.

Existing experimental data due to Jordan [4.15], as well as F.J. Schroeder, Kirstere, and Hirsch [4.16] and others [4.23] through [4.27] for hydrostatically loaded conical shells are shown in Figure 4.13. There is significant scatter in existing experimental data, more than is usually associated with hydrostatically loaded cylindrical shells. This may possibly be due to initial imperfections being more important for conical shells than for hydrostatically loaded cylindrical shells. Also, the data of Figure 4.13 represent somewhat different boundary conditions for the tests reported.

Another nonlinear analysis of the elastic buckling of truncated conical shells was offered by Hoff and Singer [4.28] in 1960. The linearized terms

in the strain-displacement relations were those derived by Hoff [4.3] and these terms were supplemented by nonlinear terms due to H. Langhaar [4.29]. Energy considerations were developed (see Chapter 2) and the variations in strain energy caused by displacements u, v, and w as well as in the potential of the hydrostatic surface load and the edge forces and moments led to a set of three coupled nonlinear equilibrium equations. Boundary conditions were also obtained through this variational approach and they corresponded (approximately) to simple support end conditions. The u, v, and w displacements during buckling were represented by series of the form

$$w = I_m \sum_{n=1}^{N} C_N x^s \sin n\,\phi \tag{4.43}$$

and similarly for u and v

$$u = I_m \sum_{n=1}^{N} B_N x^s \cos s\,\phi \tag{4.44}$$

$$v = I_m \sum_{n=1}^{N} C_N x^s \sin n\,\phi \tag{4.45}$$

where C_n and w are real (n being the nmber of circumferential waves of the buckled configuration) and s is a complex number defined by

$$s = \gamma + in\,\beta \tag{4.46}$$

where $\beta = \pi/\ln x_2$ (see Figure 4.2) and $\gamma(1-\upsilon/2)$. This leads to a typical term of a series representing radial displacement in the form

$$w_n = C_n x^{\gamma} \sin\,[n\beta\,\ln x] \sin n\,\phi \tag{4.47}$$

The hydrostatic buckling load was determined through satisfaction of the equilibrium equation in the radial direction, leading to an equation involving the physical and geometric parameters of the shell together with the number of waves n into which it buckles in the circumferential direction. The equation was solved by the Galerkin method using the assumed buckled configuration in the radial direction. The buckling pressure p appears in a linear manner in the equations and was determined through enforcing the condition of vanishing of the infinite determinant whose elements are multipliers

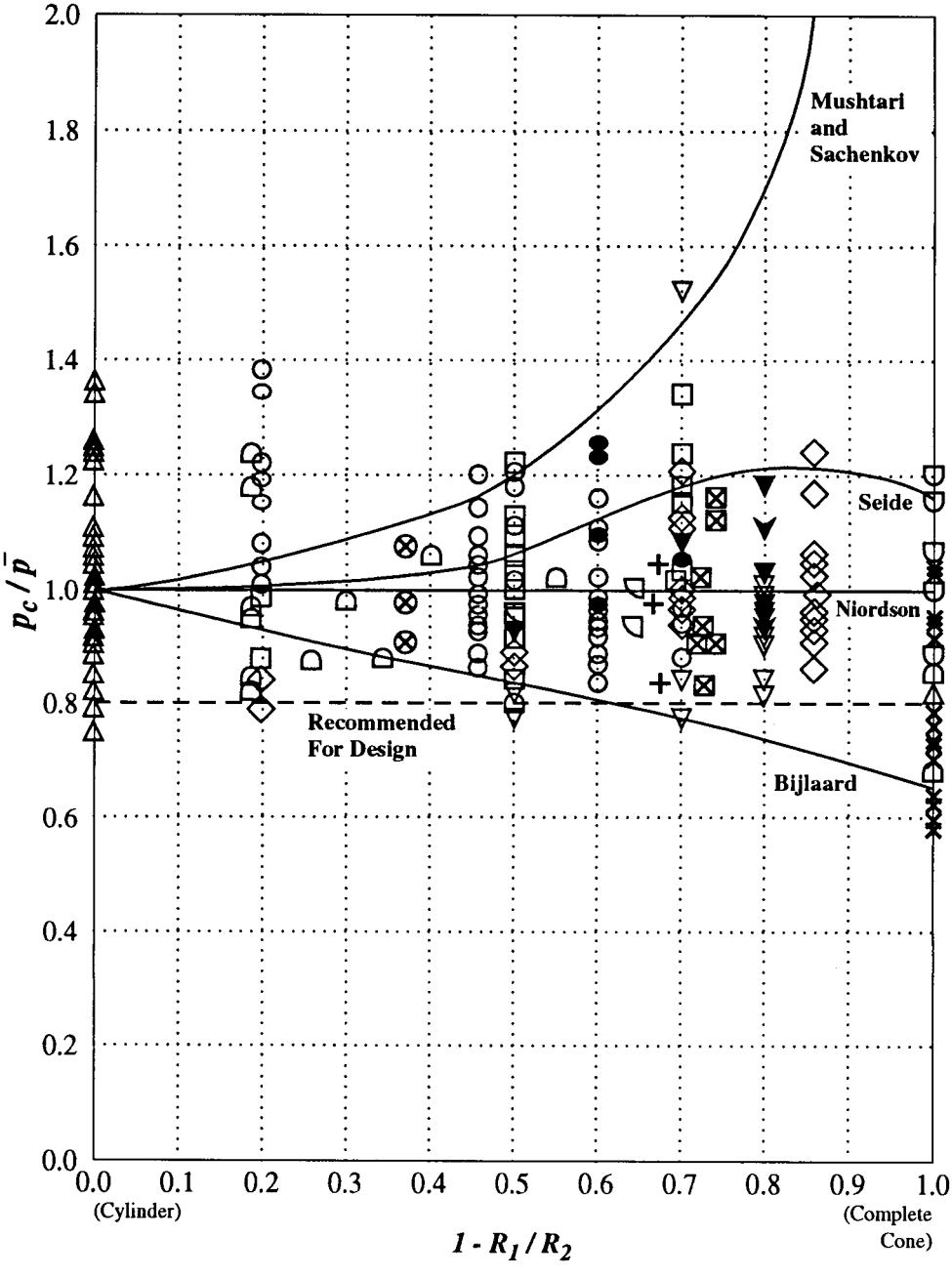
2.0
1.8
1.6
1.4
1.2
1.0
0.8
0.6
0.4
0.2
0.0
$p_c / \bar{p}$
Mushtari and Sachenkov
Seide
Niordson
Recommended For Design
Bijlaard
0.0 (Cylinder)
0.1
0.2
0.3
0.4
0.5
0.6
0.7
0.8
0.9
1.0 (Complete Cone)
$1 - R_1 / R_2$

Figure 4.13

Figure 4.13 Legend

Weingarten, Morgan, and Seide [4.22] Material Cone Angle

Mylar: △ 0°, ○ 10°, □ 20°, ○ 30°, ◇ 45°, ▽ 60°

Steel: ▲ 0°, ● 30°, ▼ 60°, ⮟ 75°

Tokugawa	[4.23]	Brass	⌓
Magula	[4.27]	Steel	+
Westmoreland	[4.24]	Aluminum	⌝
Jordan	[4.15]	Aluminum	×
Homewood	[4.26]	Aluminum	⊗
Schroeder, et al	[4.16]	Brass	⌓
Bowie, et al	[4.25]	Lucite	⊠

of the coefficients of radial displacement during buckling. The hydrostatic buckling pressure for each of a variety of cone geometries was determined using first a one-term expression for radial displacement then a two-term expansion. Results are presented in terms of the dimensionless parameters

$$Z = \left(\sqrt{1-\mu^2}/\sin\alpha\right)\left(a/h\right)\left[(x_2-1)^2/x_2\right] \tag{4.47}$$

$$C_p = \left[12\left(1-\mu^2\right)/\pi^2\right]\left(p_{cr}/E\right)\left(a/h\right)^3(x_2-1)^2 x_2 \sin\alpha \tag{4.48}$$

for a wide range of geometries in Figure 4.14 together with comparable results due to Mushtari and Sachenkov, Niordson, Bijlaard, and Pflüeger. Later J. Singer [4.30] solved the same problem but for the case of a truncated conical shell having clamped ends. It was found that buckling loads for the clamped end case ranged from 30 to 48 per cent greater than for identical geometry shells having simply supported ends.

In 1962 J. Singer and A. Eckstein [4.31] carried out a series of tests to determine hydrostatic buckling pressures of truncated conical shells. The program involved testing of 71 aluminum alloy type 5052 shells having a butt weld along a generator. Argon arc welding was employed for the thick

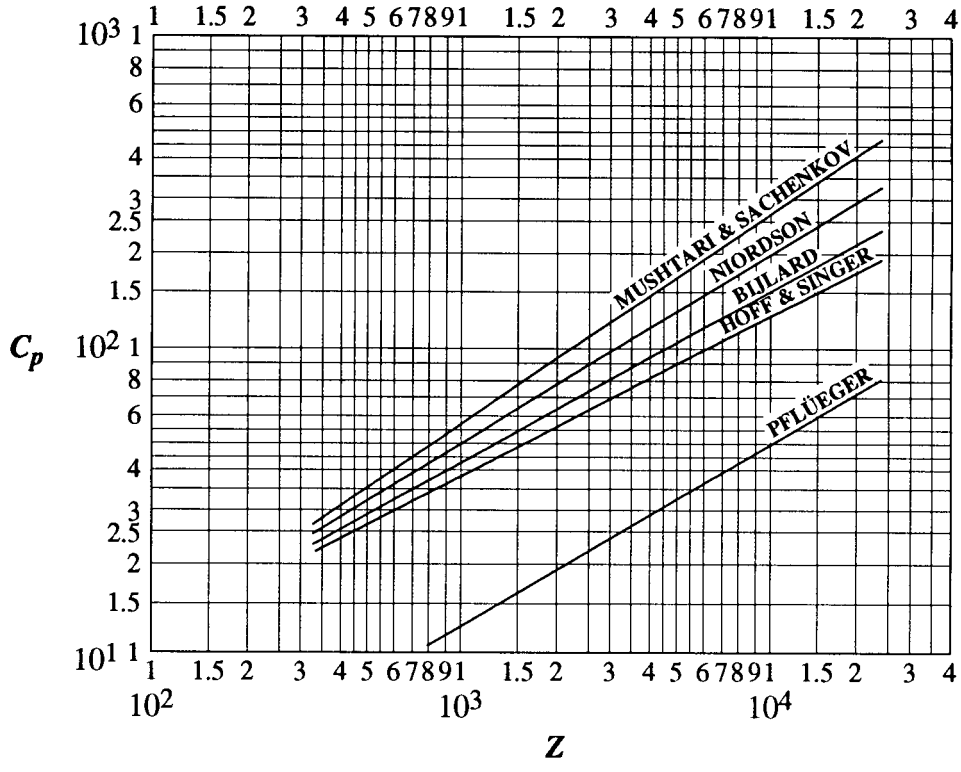

Figure 4.14

er shells and oxyacetylene for the thinner ones. Extreme care was taken during welding to reduce waviness, but some slight distortion always remained near the weld. Adhesive bonding was also employed in an effort to determine deleterious effects of the butt weld. Even in these bonded specimens there was some waviness near the joint which the authors believed more than cancelled the strengthening of the joint. Initial out-of-roundness measurments were made at a number of stations along the length of each specimen and the models embraced a radial out-of-roundness to shell thickness ratio ranging from 0.30 to 2.5.

Test results obtained in [4.30] are plotted in Figure 4.14 where Z and C_p were defined previously. Cones having half-apex angles of 10°, 20°, and 30° were tested to hydrostatic buckling. In general the hydrostatic pressure at the onset of elastic buckling was reasonably well predicted by the theories of both J. Singer [4.32] and P. Seide [4.21]. At least for larger values of Z the expression due to Niordson [4.13] furnished a good lower bound to the experimentally determined pressures. An averaging straight line on this log-log plot leads to the empirical design formula

$$C_p = \frac{p}{E}\left[12\left(1-\mu^2\right)\frac{1}{\pi^2}\right]\left(\frac{L}{h}\right)^2\left(\frac{\rho_{av}}{h}\right)$$

$$\text{or } C_p = 0.83Z^{0.55} \tag{4.50}$$

and a counterpart expression for plastic collapse of the truncated cone led to a plastic buckling coefficient given by

$$\left[\frac{h}{\rho_{av}}\right]C_p = 0.090\,Z^{0.42} \tag{4.51}$$

where $\rho_{av} = \left(\frac{R_1 + R_2}{2}\right)\cos\alpha$ and $Z = \left(1-\mu^2\right)^{1/2}\left(\frac{L}{\rho_{av}}\right)^2$

The effect of initial out-of-roundness was found to be an important factor in the pre-buckling behavior of the shells but not in the determination of the elastic or plastic buckling strength.

A.S. Vol'mir, of the Moscow Aviation Institute, in 1963 [2.2] offered a finite difference solution to the nonlinear equations governing finite deformations of thin, elastic shells for the case of a hydrostatically loaded conical frustum. For the truncated cone having its small diameter clamped and the large diameter simply supported, the Vol'mir hydrostatic buckling pressure is

$$p = C_1 E\left(\frac{h}{x_2}\right)\frac{(\cos\alpha)^{3/2}}{\left(1-\nu^2\right)^{3/4}} \tag{4.52}$$

where x_1 and x_2, and a are defined in Figure 4.11 and C_1 is taken from Figure 4.15. Vol'mir indicated that predictions of Equation (4.52) were within five per cent of experimentally determined buckling pressures due to I.I. Trapezin [4.34] at the same institute.

In 1967 J. Singer and D. Bendavid [4.32] carried out hydrostatic buckling tests on a series of thirteen electroformed truncated conical shells. In this technique for thin shell fabrication a rigid conical mandrel is located in a plating tank with its small end down and its longitudinal axis in a vertical position. It is slowly rotated about this axis at an angular velocity of 1/8 revolution per minute. The mandrel serves as the cathode and a slab of nickel as the anode. The entire system is immersed in the plating fluid, but to achieve uniform thickness of the shell specimen built up in this manner

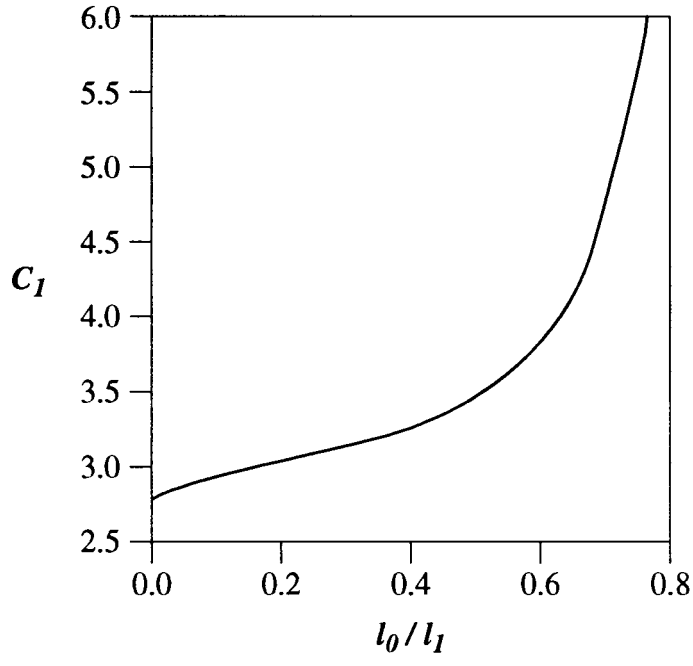

Figure 4.15

not only is the mandrel rotated but in addition portions of the mandrel near the small end were "shaded" to control thickness buildup and thus achieve a shell thickness essentially uniform from one end of the mandrel to the other. After a sufficient length of time has elapsed the mandrel and the film of nickel deposited on it is removed, and the small end of the shell placed on a circular clamping band, so as to obtain essentially a clamped end condition. It was found to be possible to produce an electrodeposited conical shell having less than three per cent thickness variation in the circumferential direction. The minimum thickness that could be plated was about 0.0028 inches (0.071 mm), the thickness being controlled merely by adjusting the plating time. The mandrel was aluminum, since the nickel plated shell does not adhere strongly to it. Out-of-roundess measurements were made at a number of stations along the geometric axis of the shell. External pressure was applied by creating a vacuum within the closed-end conical shell and an inclined water monometer employed to monitor the pressure inside the shell. Ten models having a taper ratio of 0.75 were constructed and three more with a ratio of 0.669. Mean thicknesses ranged from 0.00294 inches (0.061 mm) to 0.00512 inches (0.130 mm). Because of the very small initial geometric imperfections present in the shells, lobes appeared completely around the circumference simultaneously in all models. Thus, the onset of buckling

and complete buckling occurred simultaneously. In all cases buckling pressures were slightly greater than predicted by linearized shell theory. Repeated release and reapplication of pressure led to experimental buckling loads about ten per cent below the initial value.

SUMMARY

To summarize, the scatter of available experimental data, shown in Figure 4.13, makes adoption of any single theory for static design purposes difficult. Also, it is to be remembered that data shown in Figure 4.13 correspond to various degrees of clamping at both ends of the conical frustum. In most tests the ends approximated clamped support conditions, but seldom precisely satisfied any ordinary boundary conditions. From that same Figure one may conclude that Niordson's approach leads to an acceptable mean fit to experimental data, albeit for a variety of not too clearly specified boundary conditions. This pertains to both conical as well as cylindrical shells of a variety of materials for a wide range of taper ratios. Seide [4.21] has recommended that, from Figure 4.13, p_e be determined from the approximation to the earlier work of S. Batdorf [3.19] namely,

$$p_e = \frac{0.92E}{\left(\frac{L_1}{\rho_{AV}}\right)\left(\frac{\rho_{AV}}{h}\right)^{5/2}} \tag{4.53}$$

and that the design buckling load be

$$p = 0.8\, p \tag{4.54}$$

since most of the experimental values indicated in Figure 4.13 fall within 80 per cent of the line $p/p_e = 1$. Also, the results of Hoff and Singer [4.28] can be employed to give a realistic value of conical shell hydrostatic buckling load. These results may readily be computer implemented so that parametric studies of effects of variation of cone parameters can be carried out. Reference [4.28] presents such results for a 10° truncated conical shell.

Dynamically Loaded Conical Shells

Design of submersibles in which the pressure hull consists of conical shell segments must occasionally involve dynamic considerations. These

may arise from water waves moving below the free surface of the sea, collisions with submerged systems, etc.

In 1967, at Kazan University, V.V. Kostylev [4.35] investigated the elastic stability of complete conical shells as well as truncated conical shells subject to dynamically applied hydrostatic pressure. The governing equations employed were obtained from Equations [2.62] and [2.63] specialized to right circular cones. Kostylev used intuition to discard certain first order derivatives of radial displacements and obtained only what he considered significant terms in these two equations. The resulting simplification led to equations that could be solved by simple harmonic series expansions of both the radial displacement as well as the stress function of middle surface forces. These simplified equations were solved in closed form for hydrostatic loadings of (a) pressure increasingly linearly with time, (b) a suddenly applied pressure of constant intensity over the entire exterior surface of the cone, and (c) a harmonically pulsating hydrostatic loading. For these cases cone response as a function of time was determined.

A related investigation of cone dynamics but with consideration of the initial geometric imperfections of the shell was offered by M.S. Shumik [4.35] in 1967. The criteria adopted for loss of stability due to dynamically applied hydrostatic pressure was that a deflection (at any point) equal in magnitude to the shell thickness constituted buckling. The intensity of hydrostatic pressure was assumed to increase as time raised to some power specified by the physical parameters of the experiment. Energy considerations led to dimensionless times to buckling as a function of geometry and loading of the conical shell. In 1973 J. Tani [4.37] at the Institue of High Speed Mechanics in Sendai, Japan examined the dynamics of a truncated conical shell loaded by constant hydrostatic pressure superposed on which was a pulsating component, i. e.:

$$p(t) = p_0 + p_t \cos \omega t \tag{4.55}$$

The nonlinear motion equations were solved, approximately, in series form to obtain dynamic radial response as a function of p_0, p_t, n and time. Stability of motion in terms of these parameters was determined using the criteria due to C.S. Hsu.

REFERENCES

4.1 Kraus, H., *Thin Elastic Shells,* John Wiley & Sons, Inc., 1967, 476 pages.

4.2 Love, A. E. H., *A Treastise of the Mathematical Theory of Elasticity,* Fourth Ed., Dover Publications, New York, 1944, 642 pages.

4.3 Hoff, N. J., "Thin Circular Conical Shells Under Arbitrary Loads," *Journal of Applied Mechanics, Trans. ASME,* Volume 22, 1955, pp. 557-562.

4.4 Pohle, F. V., Discussion of Reference 4.3, *Journal of Applied Mechanics, Trans. ASME,* Volume 23, 1956, pp. 322-323.

4.5 Seide, P., "A Donnell-Type Theory for Asymmetric Bending and Buckling of Thin Conical Shells," *Journal of Applied Mechanics, Trans. ASME,* Volume 24, 1957, pp. 547-551.

4.6 Bowie, O.L., "Design Criterion for Circumferential Ring Stiffeners for a Cone Loaded by External Pressure," Watertown Arsenal Laboratories, Watertown, Massachusets, Report 893/199, 1957.

4.7 Reissner, E., *On the Theory of Thin Elastic Shells,* Reissner Anniversary Volume, J.W. Edwards, Ann Arbor, Michigan, 1949.

4.8 Taylor, C. E., and Wenk, E., Jr., "Analysis of Stress in the Conical Elements of Shell Structures," David Taylor Model Basin, Washington, D.C., Report 981, 1956.

4.9 Raeta, R. V., and Pulos, J. G., "A Procedure for Computing Stresses in a Conical Shell Near Ring Stiffeners or Reinforced Intersections," David Taylor Model Basin, Washington, D.C., Report 1015, 1958.

4.10 Wenk, E., Jr., and Taylor, C. E., "Analysis of Stresses at the Reinforced Intersection of Conical and Cylindrical Shells," David Taylor Model Basin, Washington, D.C., Report 826, 1953.

4.11 Pflüeger, A., "Stabilitat dunner Kegelschalen," *Ingenieur Archiv,* 1937, pp. 151-172.

4.12 Tokugawa, Takesada, "An Approximate Method for Calculating the Collapse Pressure of Thin Cylindrical, Conical, and Spherical Shells Under Uniform External Pressure," presented at the Japanese Zosen Kyokai (Shipbuilding Association) Conference, Tokyo, November, 1940.

4.13 Niordson, F. I. N., "Buckling of Conical Shells, Subjected to Uniform External Lateral Pressure," *Acta Polytechnica Civil Engineering and Building Construction Series,* Vol. 1, No. 3, Stockholm, 1947.

4.14 Bijlaard, P. P., and Wong, R., "Critical External Pressure of Conical Shells That Are Simply Supported at the Edges," Bell Aircraft Corporation, Buffalo, New York, Report No. 02-941-027, 1953.

4.15 Jordan, W. D., "Buckling of Thin Conical Shells Under Uniform External Pressure," Bureau of Engineering Research, University of Alabama, 1955.

4.16 Schroeder, F. J., Kirstere, E. T., and Hirsch, R. A., "An Experimental Determination of the Stability of Conical Shells," Aircraft Armaments Inc., Report ER-1361, May, 1958, Cockeysville, Maryland.

4.17 Mushtari, Kh. M., and Sachenkov, A.V., "Stability of Cylindrical and Conical Shells of Circular Cross-Section with Simultaneous Action of Axial Compression and Extenal Normal Pressure," *Prikladnaia Mathematika i Mekhanika,* Volume 18, No. 6, 1954. Available in English as NACA TM 1433, 1958.

4.18 Radkowski, P.P., "Buckling of Thin Truncated Conical Shells Subjected to Uniform External Pressure," Watertown Arsenal Laboratory, Technical Report 893.3/1, 1958.

4.19 Radkowski, P.P., "Buckling of Thin Single and Multi-Layer Conical and Cylindrical Shells with Rotationally Symmetric Stresses," *Proceedings of the Third U.S. National Congress of Applied Mechanics,* American Society of Mechanical Engineers, New York, 1958, pp. 443-449.

4.20 Taylor, C.E., "Elastic Stability of Conical Shells Loaded by Uniform External Pressure," Proceedings of the Third Midwestern Conference on Solid Mechanics, pp.86-99. Published by University of Michigan Press, 1957.

4.21 Seide, P., "On the Buckling of Truncated Conical Shells under Uniform Hydrostatic Pressure," *Proceedings of the IUTAM Symposium on the Theory of Thin Elastic Shells,* North-Holland Publishing Co., Amsterdam, 1960, pp. 363-388.

4.22 Weingarten, V.I., Morgan, E.J., and Seide, P., "Final Report on Development of Design Criteria for Elastic Stability of Thin Shell Structures," Space Technology Laboratories, Inc., Los Angeles,

CA, 31 Dec. 1960, AFBMD-TR-61-7.

4.23 Tokugawa, T., "Experiments on the Elastic Stability of a Thin-Walled Cone under Uniform Normal Pressure on all Sides, and an Approximate Method for Computing its Collapsing Pressure," Congress of Applied Mechanics League, Shipbuilding Association (Zosen Kyokai) Miscellaneous Publications, No. 125, 1932, pp. 151-169.

4.24 Westmoreland, R.T., "Model Test of Conical Bulkhead, Test No. 1098," North American Aviation Inc., Downey, CA. Report MTL-652, 1955.

4.25 Bowie, O.L. Parker, B.S., Radkowski, P.P., and Bluhm, J.I., "A Study of the IRBM (Jupiter) Bulkheads," Watertown Arsenal Laboratory, Technical Report 880-54, 1956.

4.26 Homewood, R.H., Brine, A.C., and Johnson, A.E., "Bucking Instability of Monocoque Shells," AVCO Technical Report RAD-TR-9-59-20, 1959. Also published in *Experimental Mechanics,* March 1961, pp. 88-96.

4.27 Magula, A.W., "Structural Test-Conical Head Assembly, Test No. 815," North American Aviation Inc., Downey, CA, Report MTL-531, 1954.

4.28 Hoff, N. J., and Singer, J., "Buckling of Circular Conical Shells Under External Pressure," *Proceedings of the IUTAM Symposium on the Theory of Thin Elastic Shells,* North Holland Publishing Co., Amsterdam, 1960, pp. 389-414 (Errata for pages 406-412 distributed by publisher.)

4.29 Langhaar, H. D., "A Strain Energy Expression for Thin Elastic Shells," *Journal of Applied Mechanics,* Trans. ASME, Vol. 16, No. 2, 1949, pp. 138-187.

4.30 Singer, J., "Buckling of Clamped Conical Shells Under External Pressure," Department of Aeronautics and Astronautics, Stanford University, 1964, Report No. 200. Also published in Journal of The A.I.A.A., Volume 4, No. 2, 1966, pp. 328-337.

4.31 Singer, J., and Eckstein, A., "Experimental Investigation of the Instability of Conical Shells Under External Pressure," Bulletin of the Research Council of Israel, Vol. 11c, No. 1, 1962, pp. 97-122.

4.32 Singer, J., "Buckling of Circular Conical Shells Under Axisymmetric External Pressure," Journal of Mechanical Engineering

Science, Vol. 3, No. 4, 1961. Also, Technion Research and Development Foundation, AFOSR TN 60-711, 1960.

4.33 Singer, J., and Bendavid, D., "Experimental Investigation of Buckling of Electroformed Conical Shells Under Hydrostatic Pressure," *Journal of the American Institute of Aeronautics and Astronautics,* Vol. 6, No. 12, 1968, pp. 2332-2338.

4.34 Trapezin, I.I., "Stability of a Thin-Walled Conical Shell of Circular Cross-Section Subject to Loads Axisymmetric About its Axis," *Transaction of the Moscow Aviation Institute,* No. 17, 1952. (In Russian.)

4.35 Kostylev, V.V., "Stability of Circular Conical Shells Subjected to Dynamic External Pressure," *Investigations in the Theory of Plates ans Shells,* No. 5, Kazan, State University Press, 1967, pp. 480-493. (In Russian.)

4.36 Shumik, M.A., "The Behavior of Dynamically Loaded Conical Shells," *Prikladnaya Mekhanika,* Kiev, Volume 5, No. 6, 1969, pp. 15-19. Available in English as *Soviet Applied Mechanics,* Plenum Publishing Corp., New York.

4.37 Tani, J., "Dynamic Stability of Truncated Conical Shells under Periodic External Pressure," *Reports of the Institute of High Speed Mechanics, Tohoku University*, Sendai, Japan, Volume 28, 1973, pp. 135-147.

BIBLIOGRAPHY

Akkas, N., and Bauld, N.R. Jr., "Axisymmetric Dynamic Buckling of Clamped Shallow Spherical and Conical Shells under Step Load," *Journal of the A.I.A.A.,* Volume 8, No. 12, 1970, pp. 2276-2277.

Alumyae, N.A., "On the Determination of the Critical Loading of a Conical Shell Closed at the Apex and Subjected to External Pressure," *Works of the Tallin Polytechnic Institute,* No. 66, 1955. (In Russian.)

Baruch, M., Harabi, O., and Singer, J., "Influence of In-Plane Boundary Conditions on the Stability of Conical Shells Under Hydrostatic Pressure," *Proc. IX Israel Annual Conference on Aviation And Aeronautics,* 1967, pp. 12-24.

Treats simply supported truncated conical shells for various in-plane boundary conditions. Uses Galerkin Procedure.

Baruch, M., and Singer, J., "General Instabilty of Stiffened Circular Conical Shells Under Hydrostatic Pressure," The Technion, Israel, Dept. of Aeronautical Engineering, Report No. 28, 1963.

The influence of ring or stringer stiffeners on buckling characteristics of a conical shell. It is assumed that these ribs are closely spaced.

Fulton, R.E., "Dynamic Axisymmetric Buckling of Shallow Conical Shells Subjected to Impulsive Loads," *Journal of Applied Mechanics,* Transactions of the ASME, Volume 32, No. 2, 1965, pp. 129-134.

Gavrilenko, G.D., "Effect of Shape Flaws and Stiffness Characteristics of Ribs on the Stability of Conical Shells," *Prikladnaya Mekhanika,* Kiev, Volume 22, No. 11, 1986, pp. 59-64. Available in English as *Soviet Applied Mechanics,* Plenum Publishing Corp., New York.

Determines buckling load of a ribbed (or imperfect) conical shell through use of finite differences.

Grigolyuk, E.I., "On the Instability with Large Deflections of a Closed Laminated Conical Shell Subject to Uniform Normal Surface Pressure," *Inzhernernyi Sbornik,* Volume 22, pp. 111-119, Moscow, 1955. Available in English from AVCO Mfgr. Corp. Research and Advanced Development Division, translated by R.M. Haythornthwait of Brown University.

A small deformation treatment of a complete or trancated conical consisting of two layers securely bonded to each other at the entire comon surface.

Karpov, N.I., and Karpova, O.A., "Stability of Conical Shells under Combined Loads," *Problemy Prochnosti,* Kiev, Volume 11, 1981, pp. 40-45. Available in English as *Strength of Materials,* Plenum Publishing Corp.

A successive approximation technique for determining the buckling

load of a conical shell subject to combined radial and axial pressure of different intensities.

Kostylev, V.V., "The Question of Calculating the Dynamic Strength of Thin Conical Shells," *Investigations in the Theory of Plates and Shells,* No. 4, Kazan State University Press, 1966. Available in English as FTD-MT-24-106-72, p. 86-91, 1972.

An approximate solution for response of a conical shell to a normal pressure varying harmonically along a generator of the shell with respect to time.

Kudinov, A.N., "Stability of Shells within and beyond the Elastic Limit when Subjected to a Nonuniform External Pressure", *Works of the VIII All-Union Conference on Theory of Plates and Shells,* Rostov-on-Don, 1973, pp. 139-143. (In Russian.)

Results on tests of aluminum alloy conical shells subject to hydrostatic loading over either the entire or partial external surface.

Leonard, R.W., Anderson, M.S., and Heard, W.L., Jr., "Design of a Mars Entry 'Aeroshell'" *Buckling of Structures,* ed. by B. Budiansky, Springer-Verlag, 1976, pp. 346-364.

Analytical and experimental study of buckling of a truncated conical shell subject to external normal loading of the type occurring in atmospheric reentry vehicles.

Mescall, J.J., "Buckling of Thin Conical Shells under Uniform External Pressure," Watertown Arsenal Laboratories, Watertown, MA. Report 836.32/3, 1961.

A Rayleigh-Ritz approach to determination of hydrostatic buckling loads with dimensionless representations of buckling loads for a wide range of geometries.

Mikhasev, G.I., and Tovstik, P.E., "Stability of Conical Shells acted upon by External Pressure," *Mekhanika Tverdogo Tela,* Volume 25, No. 4, 1990, pp. 99-104. Available in English as *Mechanics of Solids,* Allerton Press.

Lineraized solution to the problem of buckling of a hydrostatically loaded truncated conical shell where the two end bounding planes are not parallel.

Pal'chevskii, A.S., and Sannikov, Yu. A., "Experimental Study of the Stability of Ribbed Conical Shells," *Prikladnaya Mekhanika,* Volume 18, No. 8, pp. 85-89, 1982. Available in English as *Soviet Applied Mechanics,* Plenum Publishing Corp., New York.

Test results on aluminum alloy shells reinforced by rings and/or stringers.

Postnov, V.A., and Korneev, V.S., "Calculating the Stability of Reinforced Shells Using the Method of Finite Elements," *Prikladnaya Mekhanik,* Kiev,

Volume 12, No. 5, 1976, pp. 44-49. Available in English as *Soviet Applied Mechanics,* Plenum Publishing Corp., New York.

A finite element approach to buckling of a ring reinforced truncated conical shell.

Radkowski, P.P., "Elastic Stability of Thin Single-and Multi-Layer Conical and Cylindrical Shells Subjected to External Pressure," AVCO MFGR. Corp., Research and Advanced Development Division, Lawrence, MA, 1957.

A refinement of the 1955 work of E.I. Grigolyuk pertinent to this problem.

Rasskazov, A.O., Semenyuk, N.P., Trach, V.M., and Primak, A.P., "Experimental Examination of Load-Carrying Capacity of Three-Layer Compound Shells of Revolution," *Problemy Prochnosti,* No. 6, 1990, pp. 77-80. Available in English as *Strength of Materials,* Plenum Publishing Corp., New York.

Tests of six filamentary glass reinforced cylindrical shells closed at one end by a truncated conical shell, with the system loaded by hydrostatic pressure. Failure occurred in the conical region for certain values of geometric parameters, and with an audible snap.

Rikards, R.B., Eglais, V.O., and Goldmanis, M.V., "Optimization of a Composite Conical Ring-Reinforced Shell under External Pressure," *Prikladnaya Mekhanik,* Kiev, Vol. 19, No. 12, 1981, pp. 44-51. Available in English as Soviet Applied Mechanics, Plenum Publishing Corp., New York.

The authors examine weight optimization of a hydrostatically loaded truncated conical shell having circumferential internal ring-like ribs. Both shell plating as well as rings are of composite material. Nonlinear programming techniques were employed to determine optimal parameters of the shell as well as ribs. Consideration was given to both (a) local instability of shell plating between rings, and (b) general instability of the shell and rings. An example of a carbon fiber reinforced epoxy system was treated numerically.

Sannikov, Yu. A., "Effect of the Geometric Parameters of the Skin on the Stability of Ribbed Conical Shells," *Prikladnaya Mekhanika,* Volume 21, No. 11, 1986, pp. 54-54. Available in English as *Soviet Applied Mechanics,* Plenum Publishing Corp., New York.

A parametric study of influence of orthogonal rings-stringers on buckling resistance of hydrostatically loaded conical shells.

Savluk, A.R., "Stability of Conical Shells with Meridional and Nonregular Ring Reinforcements," *Prikladnaya Mekhanika,* Volume 26, No. 4, 1990, pp. 56-61. Available in English as *Soviet Applied Mechanics,* Plenum Publishing Corp., New York.

Correlation of theory with experiments for hydrostatically loaded conical shells having an orthogonal ring-stringer system of reinforcing ribs.

Schiffner, K., "Buckling of Conical Shells," *Colloquium on Stability of Plate and Shell Structures,* Ghent University, 1987, Belguim.
Bifurcation points of conical shells are investigated. Numerical results are presented for relative flat conical shells.

Singer, J., Baruch, M., and Reichenthal, J., "Influence of In-Plane Boundary Conditions on the Buckling of Clamped Conical Shells," *Proc. XIII Israel Annual Conference on Aviation and Astronautics,* 1972, pp. 127-139.
Treats buckling of clamped end conical frustrums for various in-plane boundary conditions.

Singer, J., "Buckling of Circular Conical Shells under Axisymmetric External Pressure," Technical Note, No. 1, The Technion, Nov, 1960.
Seides' stability equations were solved by Singer to indicate buckling due to hydrostatic pressure accompanied by lateral pressure varying in the axial direction.

Song, Wei-ping, "Large Deflection of Shallow Conical Shell under Uniform Pressure," *Acta Mechanica, Solida Sinica* (English Edition), Volume 2, 1989, pp. 103-109.

Tani, J., "Influence of Prebuckling Deformation on the Buckling of Truncated Conical Shells under External Pressure," Institute of High Speed Mechanics, Tohoku University, Sendai, Japan, Volume 2, 1973.
Donnell-type equations were employed to determine hydrostatic buckling loads of clamped conical frustra. It was found that neglect of prebuckled deformation will lead to serious errors for the case of short shells.

Trapezin, I.I., "Critical Load and Frequencies of Free Vibration of Orthotropic Conical Shells, Subject to Uniform Hydrostatic Pressure," Moscow Aviation Institute, Pub. No. 130, 1960, pp. 5-18. (In Russian.)

Trapezin, I.I., "Deformation of a Thin Conical Shell Reinforced by Regularly Spaced Longitudian Ribs and Subject to Hydrostatic Pressure," *Raschet na Prochnost (Analysis for Strength),* No. 25, 1984, pp. 232-239. (In Russian.)
Determination of hydrostatic buckling load of a stringer-stiffened conical shell.

Vybornov, V.G., and Tsybul'skiy, I.P., "Experimental Study of the Stability of Closed Conical Shells under the Action of Uniform External Pressure," *Investigations in the Theory of Plates and Shells,* No. 4, Kazan State University Press, 1966, Available in English as FTD-MT-24-106-72, pp. 33-42, 1972.
Reports results on complete conical shells fabricated from aluminum, brass, or steel with total cone angles ranging from 30° to 160°.

Vybornov, V.G., and Velikanova, N.P., "Experimental Research of the Stability of Shallow Conical Panels under External Uniform Pressure," *Investigations in the Theory of Plates and Shells,* No. 9, Kazan State University Press, 1972. Available in English as FTD-HT-32-346-74, pp. 1-10, 1974.

Tests on aluminum as well as steel portions of truncated conical shells, specimens being bounded by two generators as well as two helical lines intersecting the generators at prescribed angles.

Wang, Du, "Nonlinear Buckling of Shallow Conical Shells under Uniformly Distributed Load," *Journal of Harbin University of Technology,* Volume 3, 1958, pp. 135-143. (In Chinese.)

Wang, Xin-zhi, "Nonlinear Stability Problem of Shallow Conical Shell under Uniformly Distributed Load," *Journal of Gansu University of Technology,* Volume 1, 1980, pp. 58-66. (In Chinese.)

Weingarten, V.I., and Seide, P., "Elastic Stability of Thin-Walled Cylindrical and Conical Shells under Combined External Pressure and Axial Compression," *Journal of the American Institute of Aeronautics and Astronautics,* Volume 3, No. 5, 1965, pp. 913-920.

Results of an extensive experimental program on the stability of cylindrical and conical shells subject to hydrostatic loading as well as combined external pressure and axial compression.

Yeh, Kai-yuan, and Song, Wei-ping, "Nonlinear Stability Problem of Shallow Conical Shell under Uniformly Distributed Pressure," *Journal of Lanshou University,* Natural Sciences, Special Number of Mechanics, Volume 19, 1983, pp. 134-145. (In Chinese.)

Zielnica, J., "Critical State of an Elastic-Plastic Shell in the Form of a Truncated Cone," *Rozprawy Inzynierskie (Engineering Transactions),* Polish Academy of Sciences, Volume 28, No. 3, 1980, pp. 401-421. (In Polish.)

Plastic buckling of a conical shell subject to combined hydrostatic pressure and axial compression. Material compressibility as well as strain hardening are considered.

This Page Intentionally Left Blank

CHAPTER 5

STRUCTURAL BEHAVIOR OF SPHERICAL SHELLS

Spherical shells subject to external hydrostatic pressure have been employed as structural components of undersea systems, flight vehicles, vacuum chambers, chambers fixed to the floor of the ocean, and many other applications. For example, complete transparent spherical shells have been employed to house undersea transducers as well as video systems and have been proposed for carriers of humans to significant depths. Incomplete spherical shells have found application as end caps of cylinder–cone–sphere systems as shown in Figure 4.1. Some of these applications have involved transparent partial spheres.

Stress Analysis of Spherical Shells

A complete spherical shell subject to external hydrostatic pressure, assumed to be free of initial (no–load) geometrical imperfections and free of initial stresses, develops a membrane state of stress given by the well-known expression $\sigma = pR/2h$ where σ denotes a membrane stress constant through the shell thickness, p denotes external hydrostatic loading, R the radius to the shell middle surface, and h represents the uniform shell thickness. Because of the point–wise symmetry of loading as well as geometry, this stress exists in all directions at any point in the shell in a plane tangent to the shell middle surface at that point. This simple expression assumes only membrane action in the shell with no bending effects anywhere. Elementary theory [5.1] indicates that the radius of the spherical shell decreases an amount

$$\Delta R = \frac{pR^2}{2Eh}(1-\mu)$$

due to pressure. Here, μ represents Poisson's ratio and E is Young's modulus of the material.

Stress Analysis of Compound Shells

A system consisting of a cylindrical shell closed at one or both ends by hemispherical shells is referred to as a compound shell. Elementary theory [5.1] indicates that the decrease of radius of the cylindrical shell, except close to the end caps, is

$$\frac{pR^2}{Eh}\left(1-\frac{\mu}{2}\right)$$

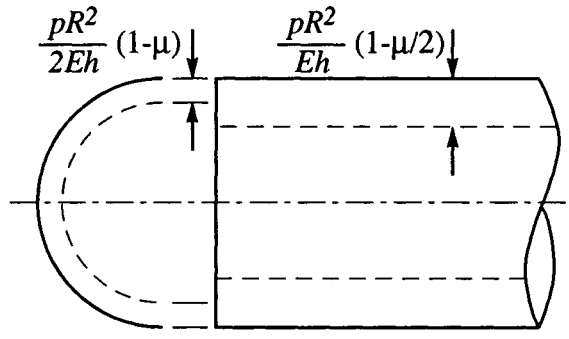

Figure 5.1. Solid lines indicate unloaded configuration of shells, dotted lines deformed configuration due to hydrostatic pressure p.

due to hydrostatic loading p. The corresponding elementary theory of a spherical shell indicates a change of radius of ΔR due to hydrostatic pressure p as shown in Figure 5.1. From this figure it is evident that the radial displacement of the cylindrical shell would be greater than that of the hemispherical shell by a factor of 0.5 pR^2/Eh. If the cylindrical shell is capped at one or both ends by a hemispherical shell, but temporarily for the sake of analysis taken to be cut transversely at the juncture, the original configurations occupied by the shells would appear as shown by solid lines in Figure 5.1 and the deformed positions due to pressure would appear as shown by the dotted lines. Thus, the radial displacement of the cylinder would be greater than that of the sphere by 0.5 pR^2/Eh for Poisson's ratio of 0.3.

In the presence of such a radial gap, the membrane action alone in each of the two component shells is incapable of accounting for the known structural behavior when the shells are joined mechanically into a closed system at the vertical cutting plane. The only way the radial gap can be closed is by

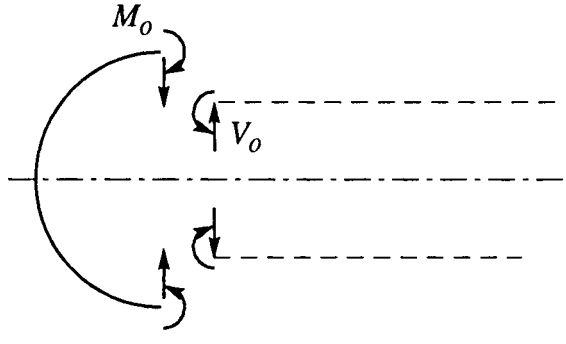

Figure 5.2. Solid lines indicate unloaded configuration of shells, dotted lines deformed configuration due to hydrostatic pressure p.

realizing that axisymmetric radial shearing forces V and bending moments M (per unit length of shell middle surface) act at the juncture as shown in Figure 5.2. The magnitudes of these axisymmetric interactions must be determined so as to enforce continuity of (a) radial displacement, and (b) continuity of slope of a generator of the cylindrical shell where it is joined to a meridian of the spherical shell.

In short, the shearing forces and bending moments acting at this juncture give rise to bending effects near the juncture and proper design of the hemisphere as well as the cylinder requires that localized bending plus membrane stresses near the juncture do not exceed the yield point of the material. Stresses arising from V_o and M_o are termed discontinuity stresses.

The elastic behavior of the relatively long cylindrical shell shown in Figure 5.2 to loadings V_o and M_o acting at the left end of the cylindrical shell has been discussed in Chapter 3. There it was found that the lateral deflection, slope, bending moment, and transverse shear resultant all decay in the form of a negative exponential function with increasing distance (measured along a generator of the cylinder) from the points of application of V_o and M_o. Numerical examples of this have been presented by W. Flugge [5.2], J. R. Vinson [5.3], and H. Kraus [5.4].

It is next necessary to determine structural behavior of the elastic hemispherical shell (shown in Figure 5.2) to V_o and M which are of course equal but oppositely directed to those shown there acting on the cylindrical shell. This problem has been examined in detail by H. Kraus [5.4], P. Seide [5.5], W. Flugge [5.2], S. Timoshenko and S. Woinowsky–Krieger [5.6], and P. Gould [5.7]. In Figure 5.3 the loading due to the edge shearing forces V_o per

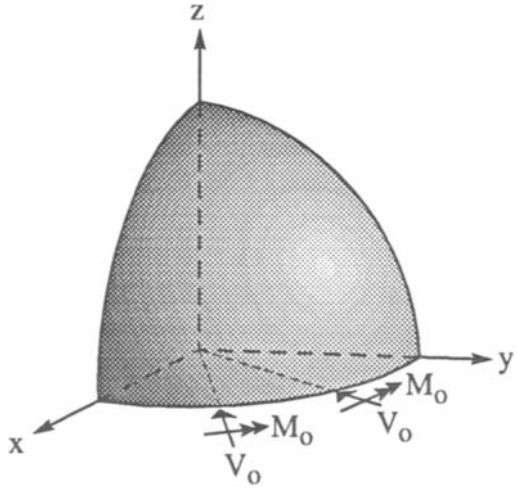

Figure 5.3. Vectors indicate forces and moments per unit length of boundary of hemisphere (only one quarter of hemisphere is shown).

unit length of shell middle surface all lie in the x–y plane and are each directed radially inward toward the center of the hemisphere as shown in Figure 5.2. The bending moments M_o per unit length of shell middle surface have vector representations lying in the x–y plane and at each point of the shell boundary are directed tangentially to the circular boundary of the hemisphere, again see Figure 5.3 quadrant. For simplicity only those vectors in the half of the shell toward the reader are shown. These are the assumed positive directions of V_o and M_o.

Chapter 2 presented equations of an elastic shell in terms of generalized coordinates. If one now specializes these to the case of a thin hemispherical shell loaded only by transverse shearing forces in a diametral plane as shown in Figure 5.3, one is led to a single second–order linear differential equation with variable coefficients. Fortunately, this is the well–known hypergeometric equation that can be solved numerically in power series of rather slow convergence. Alternately, the solution can be obtained by the method of asymptotic integration. This is in certain senses equivalent to employment of the Geckeler approximation discussed in detail by H. Kraus [5.4]. The approximation is valid for shell contours having smoothly varying geometry and leads to approximate expressions for displacements, forces, and moments at any point in the hemispherical shell defined by the co-latitude ϕ shown in Figure 5.4.

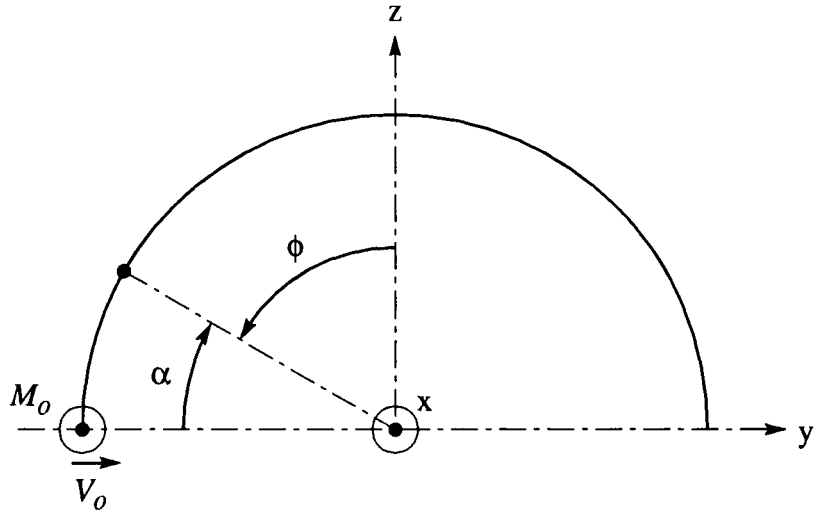

Figure 5.4. Looking toward negative end of x-axis of Figure 5.3

Let us examine forces and displacements in the y–z plane of the hemisphere shown in Figure 5.3. Looking toward the negative end of the x–axis these appear as shown in Figure 5.4. The middle surface displacement at an arbitrary point designated by the angle ϕ (co–latitude) may be expressed either as the vector sum of normal and tangential displacement δ_n and δ_t respectively, or by the displacement δ_R parallel to the y–axis. This latter quantity is better suited to our boundary conditions than the former. We are particularly interested in circumferential and meridional bending moments M_θ and M_ϕ per unit length, and forces constant through the shell thickness in each of these directions denoted by N_θ and N_ϕ. For example, at the arbitrary location ϕ, P. Gould [5.7] has derived the expression for meridional bending moment per unit length in the form

$$M_\phi = \frac{R}{2k} e^{-k\alpha} [(C_1 + C_2) \cos k\alpha - (C_1 - C_2) \sin k\alpha] \tag{5.1}$$

where R denotes shell radius, ϕ denotes the angle (co–latitude) shown in Figure 5.4, and

$$k^4 = \frac{3(1-\mu^2)R^2}{h^2} - \frac{\mu^2}{4}$$

Gould [5.7] also presents explicit expressions for M_θ, N_ϕ, and N_θ as well as δ_R. From such relations it then becomes possible to enforce boundary conditions at the juncture of the hemisphere and the cylindrical shell. At this stage it is probably most efficient to proceed on a numerical basis. Examples are to be found not only in P. L. Gould [5.7], but also W. Flugge [5.2], P. Seide [5.5], and H. Kraus [5.4].

Buckling of Spherical Shells

Hydrostatically loaded complete spherical shells as well as partial spherical shells (caps or domes) may buckle elastically, plastically, or into the elasto–plastic range of action. The earliest published investigations of spherical shell buckling are due to R. Zoelly [5.8] in 1915, L. S. Leibenson [5.9] in 1917, and T. Schwerin [5.10] in 1922. These were all based upon the assumption of axisymmetric buckling in the elastic range. Several years later, A. van der Neut of Delft, The Netherlands, presented a theory based upon asymmetric buckling patterns [5.11]. The Zoelly as well as other approaches were based upon the small elastic deformation of the shell characterized by the linearized versions of the general shell equations (2.62) and (2.63). Solutions of these were obtained in terms of the tabulated Legendre functions leading to the hydrostatic buckling pressure

$$p = \frac{2Eh^2}{R^2\sqrt{3(1-\mu^2)}} \tag{5.2}$$

where E represents Young's modulus, h is the constant shell thickness, μ is Poisson's ratio, and R is the sphere radius to its middle surface. All three authors agreed upon this result. This expression takes no account of initial (no–load) geometric imperfections from a perfect spherical form, nor are fabrication stresses considered. Since for many metals, $\mu = 0.3$, from (5.2) the buckling pressure becomes

$$p = 1.21E\left(\frac{h}{R}\right)^2 \tag{5.3}$$

and the corresponding membrane stress immediately prior to buckling is

$$\sigma = 0.605E\left(\frac{h}{R}\right) \tag{5.4}$$

The buckled configuration corresponding to (5.2) consists of a relatively large number of equally spaced dimples (lobes) located over the entire surface of the closed spherical shell. However, experiments carried out by various investigators, *e.g.*, R. L. Carlson, R. L. Sendenbeck, and N. J. Hoff [5.12] indicate that buckling initiates as a single dimple axisymmetric about a diameter of the sphere, whose size is dependent on shell geometry, and which subtends a relatively small solid angle as shown in Figure 5.5.

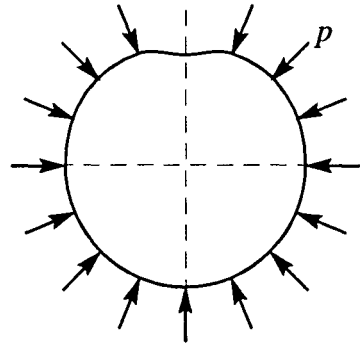

Figure 5.5. Cross-section of a buckled hydrostatically loaded sphere.

With increasing external pressure, the depth of the dimple increases. In fact, the only way in which the investigators [5.12] were able to obtain uniformly distributed dimples over the entire shell surface was to fabricate a

sphere by the electroforming technique described in [4.32]. A wax sphere (mandrel) was employed after being carefully machined to the desired diameter, then nickel plated in a hot bath to form a shell having thickness of approximately 0.0004 inches (0.010 mm). The wax mandrel contracted more upon cooling than did the nickel specimen. When this thin–walled nickel sphere was subject to external uniform pressure a large number of dimples formed, one after the other, each amplitude being limited by the gap existing between the internal surface of the nickel shell and the external surface of the wax form. With this restrained behavior almost the entire surface of the shell could be covered with dimples. However, these conditions do not represent realistic constraints on hydrostatically loaded submersibles. Thus (5.2) is of limited utility to designers of hydrostatically loaded spherical shells.

Contemporary deep submersibles employ either partial or complete spherical shells subject to hydrostatic loading. The partial shells usually cap the ends of cylindrical pressure hulls and are occasionally transparent to permit the viewing of undersea systems. In fact, more effort has been devoted to the buckling analysis of these partial end caps than to investigation of complete, closed spherical shells. The end caps of common interest may have geometries ranging from hemispherical to shallow. A shallow spherical cap, as shown in Figure 5.6, is usually defined as one in which the central altitude H is no more than approximately 1/8 the diameter $2a$.

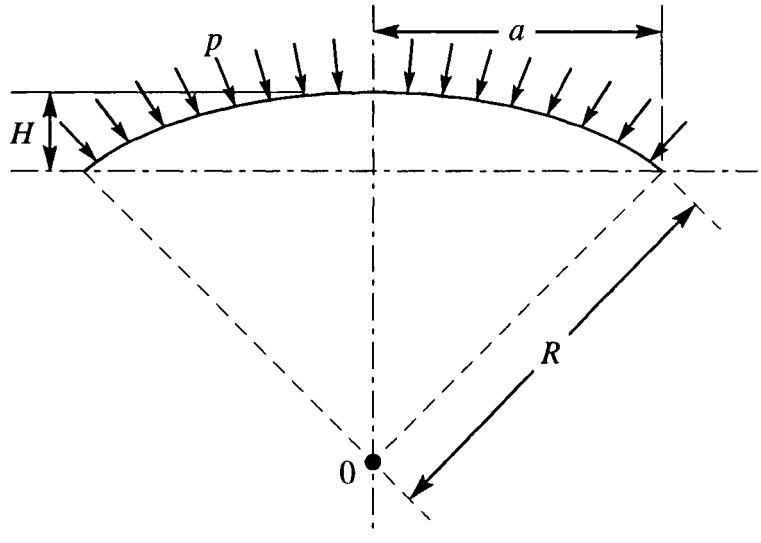

Figure 5.6. Geometry of hydrostatically loaded shallow spherical cap.

The mathematical analysis of such a shallow cap is simpler than for the case of a closed spherical shell, albeit still formidable. Fabrication of test specimens is also simpler for cap investigations than for full spherical shell studies. However, the boundary conditions existing around the circular base of the cap shown in 5.6 usually do not agree with those existing at the junction between a single dimple and the remainder of the complete spherical shell. Hence it is difficult to extrapolate results of spherical cap buckling tests with experiments carried out on complete spherical shells.

Perhaps the earliest experimental investigation of buckling of hemispherical shells is due to E. E. Sechler and W. Bollay at the California Institute of Technology in 1939, the brass models representing the Mt. Palomar Observatory Dome. Loading was accomplished by immersing the hemispheres in mercury. Their unpublished results indicated that buckling occurred at approximately 1/4 the pressure indicated by equations (5.2) and (5.3). Buckling occurred in the form of a single small dimple subtending a solid angle of about 16°. This dimple was directed toward the interior of the dome; according to the analysis corresponding to (5.2) and (5.3) buckling could be either or outward, and extending over the entire spherical surface, obviously at variance with experimental information.

Simultaneously at CalTech in that same year, Th. von Karman and H. S. Tsien [5.13] developed a new and unique approach to shell buckling. This corresponded to nonlinear finite displacements from the prebuckled configuration. In [5.13] the authors considered a shallow spherical cap subject to hydrostatic loading as shown in Figure 5.6 and assumed a buckled configuration in agreement with the experiments mentioned above. Thus, all deformations due to buckling took place in this dimple, with the remainder of the sphere undergoing no bending as shown in Figure 5.7. It was also assumed that there was no bending moment acting at the juncture of the dimple and the remainder of the spherical shell. An energy approach was employed, as outlined in Chapter 2, with bending and membrane energies calculated for the buckled configuration shown in Figure 5.7 and the potential energy corresponding to the work done by the external pressure determined on this same basis. At equilibrium, the total energy must be a minimum, so that they determined the equation of equilibrium by finding a relation between p and a which minimizes the total energy. A plausible buckled configuration suggested by the experiments together with use of the Rayleigh–Ritz approach led to a relation between hydrostatic pressure and central deflection of the form shown in Figure 5.7. Since β is essentially a free parameter of the problem, this was determined by minimization techniques so as to render the buckling stress a minimum. This led to the minimum value of load which would maintain the deflected shape to be

$$p = 0.365E\left(\frac{h}{R}\right)^2 \tag{5.5}$$

in sharp contrast to (5.3) resulting from classical linear analysis. Equation (5.5) is in good agreement with the test results on a brass hemisphere due to Sechler and Bollay which led to

$$p = 0.308E\left(\frac{h}{R}\right)^2 \tag{5.6}$$

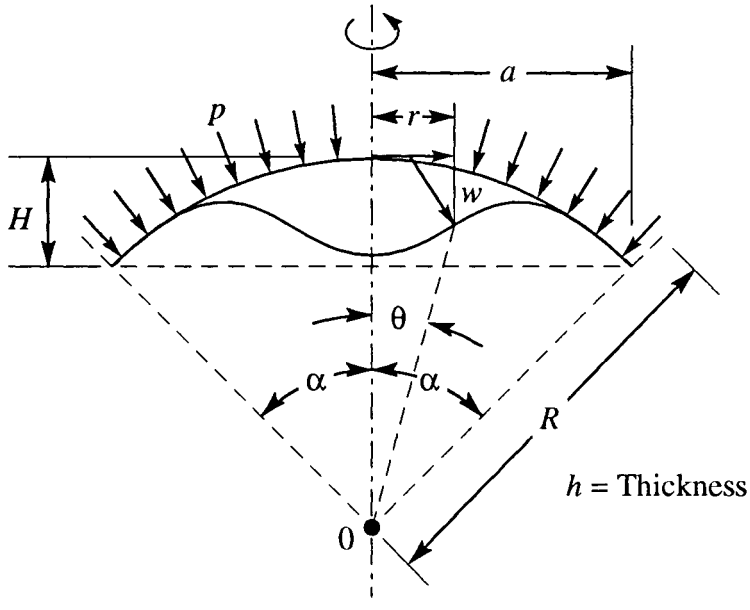

Figure 5.7. Buckled shallow spherical cap.

Buckling of Shallow Spherical Shells

The literature abounds with treatments of behavior of shallow spherical shells (caps) subject to hydrostatic loading. The problem is of interest because it occurs in submersibles as well as flight structures, ground fluid pressure vessels, etc.

One characteristic of this problem is that deformations even at very small amplitudes (less than the shell thickness) depart significantly from predictions of linear analysis. Also, there is a rapid decrease in the equilibrium pressure once a critical value has been reached. The equations governing shallow spherical shell behavior are somewhat simpler than for the case of a complete, closed spherical shell and many investigators have examined the shallow shell behavior with the hope that its solution might shed

light on the behavior of a complete spherical shell subject to hydrostatic pressure.

In 1954 A. Kaplan and Y. C. Fung [5.15] investigated the behavior of a clamped edge shallow spherical shell subject to hydrostatic loading. They cast the governing equations (2.62) and (2.63) in the forms:

$$\frac{d}{dx}\left[\frac{1}{x}\frac{d}{dx}\left(x^2 S_r\right)\right]+\frac{\lambda^2}{k}\left[\frac{dW}{dx}+\frac{1}{2x}\left(\frac{dW}{dx}\right)^2\right]=0 \tag{5.7}$$

and

$$\frac{1}{x}\frac{d}{dx}\left[\frac{1}{x}\frac{d}{dx}\left(x\frac{dW}{dx}\right)\right]-k\lambda^2 S_r+\frac{k^2}{x}\frac{dW}{dx}S_r=6P \tag{5.8}$$

where as shown in Figure 5.7, $x = r/a$ is a dimensionless radial coordinate, $W = w/h$ is dimensionless vertical displacement,

$$P=\left[(1-\mu^2)/E\right]\left(\frac{a}{h}\right)^4 p \tag{5.9}$$

p being true hydrostatic pressure and P is dimensionless hydrostatic pressure, h represents shell thickness, N_r is dimensionless radial membrane force (evaluated over the shell thickness),

$$S_r=\left(\frac{a^2}{Eh^2}\right)N_r$$

is dimensionless radial membrane force,

$$k=\left[12(1-\mu^2)\right]^{1/2} \tag{5.10}$$

where μ is Poisson's ratio, and

$$\lambda=\left[12(1-\mu^2)\right]^{1/4}\left(\frac{R}{h}\right)^{1/2}(\alpha)^{1/2} \tag{5.11}$$

If $\alpha << 1$, then we have, approximately

$$\lambda^2=\frac{ka^2}{Rh} \tag{5.12}$$

Here, S_r and W are the two independent parameters characterizing the problem.

For shallow shells having the semi–opening angle α (see Figure 5.7) small compared to unity, the geometric parameter λ^2 is proportional to the depth/thickness (H/h) of the shell. This is not applicable for deeper shells, such as a hemisphere. The relations (5.7) and (5.8) do not distinguish between vertical and radial displacements of points located on the shallow spherical dome. An alternate formulation employed for mathematical convenience by some investigators is to consider as the two independent variables (a) the rotation in its plane of a meridian at any point and (b) a middle–surface stress function. When $\lambda = 0$, Equations (5.7) and (5.8) reduce to the well–known von Karman equations governing large deformations of an initially flat plate [5.6].

Solution of (5.7) and (5.8) was carried out in [5.15] by a perturbation technique originally applied by W. Z. Chien [5.16] at Tsing Hua University in Beijing in 1947. This involved considering the central deflection of the spherical cap as a parameter W_o and expanding all free variables in powers of W_o. Thus:

$$P = p_1 W_o + p_2 W_o^2 + p_3 W_o^3 + \ldots \tag{5.13}$$

$$W = w_1(x) W_o + w_2(x) W_o^2 + w_3(x) W_o^3 + \ldots \tag{5.14}$$

$$S_R = f_1(x) W_o + f_2(x) W_o^2 + f_3(x) W_o^3 + \ldots \tag{5.15}$$

Substitution of these series in (5.7) and (5.8) and subsequent equating of equal powers of W_o leads to a sequence of pairs of linear simultaneous equations for f_i and w_i. Solution of these equations leads to expressions for f_i in terms of Bessel functions of imaginary arguments. Imposition of boundary conditions at the clamped edge of the shallow spherical shell led to relatively simple expressions for p_i, w_i, and f_i in (5.13), (5.14), and (5.15). This, finally, led to approximate relations between P and λ.

Kaplan and Fung [5.15] also carried out tests on magnesium alloy (type QQ–M–44) shallow shells. These were fabricated by the spinning technique, *i.e.*, hot flat sheets of this material were held against a rotating mandrel (considered to be rigid) and the magnesium alloy plate slowly pressed against the rotating form until the two were in as complete contact as possible. Upon removal from the rotating system there was little spring-back of the

shaped magnesium and, further, a radial cut in the magnesium shell produced only very small separation upon cooling. It was concluded that most of the residual stresses had been removed by this fabrication approach. Pressure tests were then conducted on these specimens. For relatively small values of λ, *i.e.*, relatively shallow shells, oil pressure vs. central deflection (in dimensionless forms) for five models had the form shown in Figure 5.8. Even though more oil was added to the pumping chamber, the pressure decreased as shown in that figure. Deeper shells were loaded by air pressure with an air accumulator in the line so that buckling occurred under very nearly constant pressure. This was in contrast to the oil loading, which came close to constant volume of the surrounding medium transmitting the pressure to the surface of the shell. If equation (5.4) is written in the general form

$$\sigma = KE\left(\frac{h}{R}\right) \tag{5.16}$$

the experimentally determined value of K as found by Kaplan and Fung [5.15] ranged from 0.2 to 0.4. In contrast the classical theory indicates $K = 0.605$. The precise value depends strongly upon geometric deviations from perfectly spherical form, minor deviations from constant thickness, initial fabrication stresses, and method of edge clamping. Detailed test results are shown in Figures 5.8, 5.9, and 5.10.

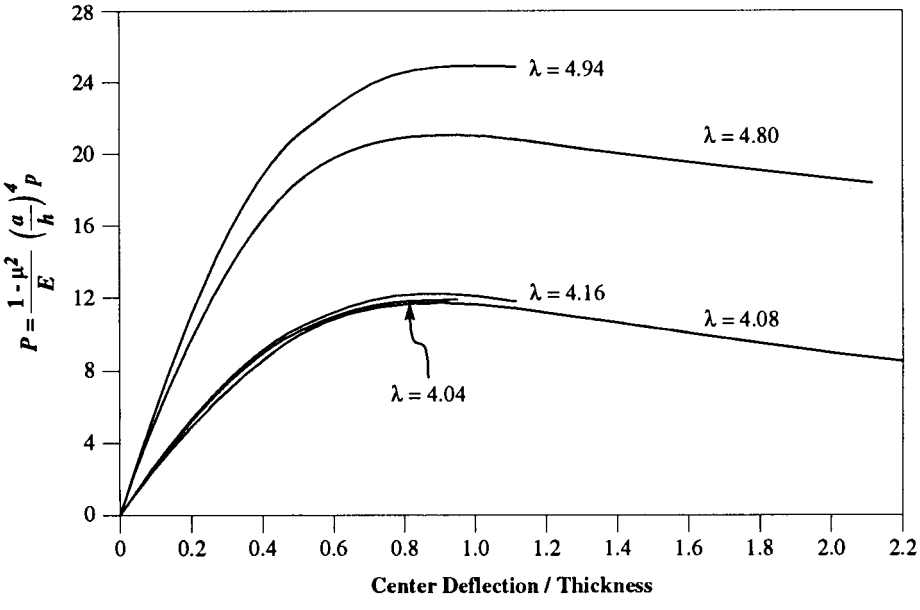

Figure 5.8. Pressure vs. center deflection for shallow spherical shells.*

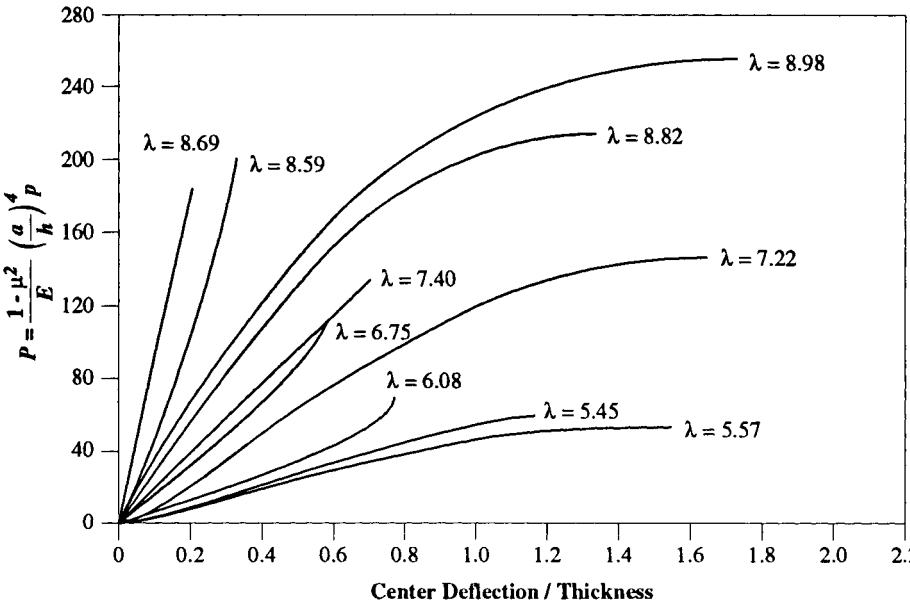

Figure 5.9. Pressure vs. center deflection for shallow spherical shells.*

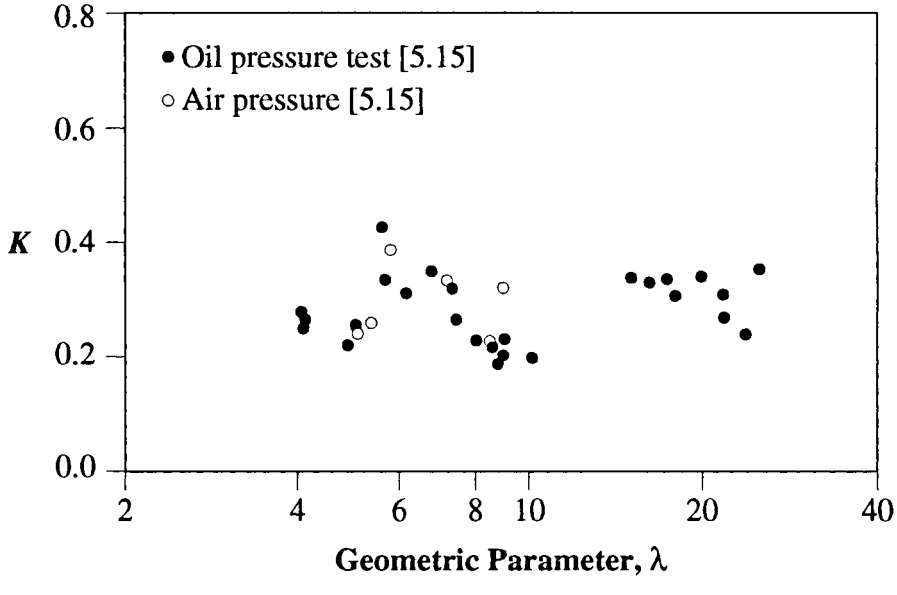

Figure 5.10. Experimental values of K for shallow spherical shell under uniform pressure.*

* Figures 5.8, 5.9, and 5.10 are adapted from "Instability of Thin Elastic Shells," by Y. C. Fung and E. E. Sechler, published in *Structural Mechanics--Proceedings of the First Symposium on Naval Structural Mechanics,* Pergamon Press, 1960, pp. 115–158 [5.17].

A. S. Vol'mir [2.2] adopted the governing equations for a shallow spherical cap as employed by Th. von Karman and H. S. Tsien [5.13] as well as Tsien [5.14] but assumed a slightly different axisymmetric buckled configuration. Using the Bubnov–Galerkin technique for solution, this led to a coefficient $K = 0.31$ in equation (5.14). On the basis of a series of tests on spherical caps carried out by R. G. Surkin and S. G. Stepanov [5.18], Vol'mir suggested modifying this coefficient to 0.155. The test specimens were steel, brass, copper, and aluminum formed into a spherical cap geometry by a deep drawing process.

Additional nonlinear considerations of buckling of hydrostatically loaded shallow spherical shells necessitates a more precise understanding of the buckling phenomena. Figures 5.8 and 5.9 have the generic form shown in Figure 5.11 by the solid line *OABC* for load vs. some significant deflection parameter, say the radial deflection of the apex of the spherical cap. Such results have been found by experiments as well as analytical and computerized finite deflection analyses. If no initial geometric imperfections are present, the load corresponding to point *B* represents the peak load-carrying capacity of the shell, and corresponds to axisymmetric deformations. However, at some lesser load, such as *A*, there exists a possibility of asymmetric deformation and *A* is termed the bifurcation point and *AD* corresponds to increased asymmetric deformations, usually with decreases in hydrostatic pressure. Obviously for any real structure, necessarily having some initial geometric imperfections there is no sharply defined bifurcation load. The behavior of this real system is characterized by the dotted line in Figure 5.11. Failure is usually by "snap–through" as represented by point *E* at the load corresponding to the ordinate of *E*. The postbuckling behavior after passing point *E* will involve asymmetric buckling displacements. In summary, the bifurcation load is usually a good engineering approximation to the actual failure load and mode.

A systematic series of tests of hydrostatically loaded shallow spherical caps was presented by K. Klöppel and O. Jungbluth [5.19] at the Technical University of Darmstadt in 1953. The specimens were manufactured by deep-drawing initially flat steel plates. One series of such spherical caps consisted of ten shells having a radius of curvature of 20.47 inches (52 cm). Another series of twenty shells had a radius of curvature 9.84 inches (25 cm). A relatively rigid heavy steel cylindrical test fixture had a heavy clamping ring to secure the circular edge of the shell and was capable of exhausting the air from inside the sphere and cylinder to create inward snap–through of the test piece. The shells had a base diameter of 15.75 inches (40 cm) for all specimens. Also, all shells were annealed to stress-relieve them from the drawing effects. Although no specific values of residual stress were

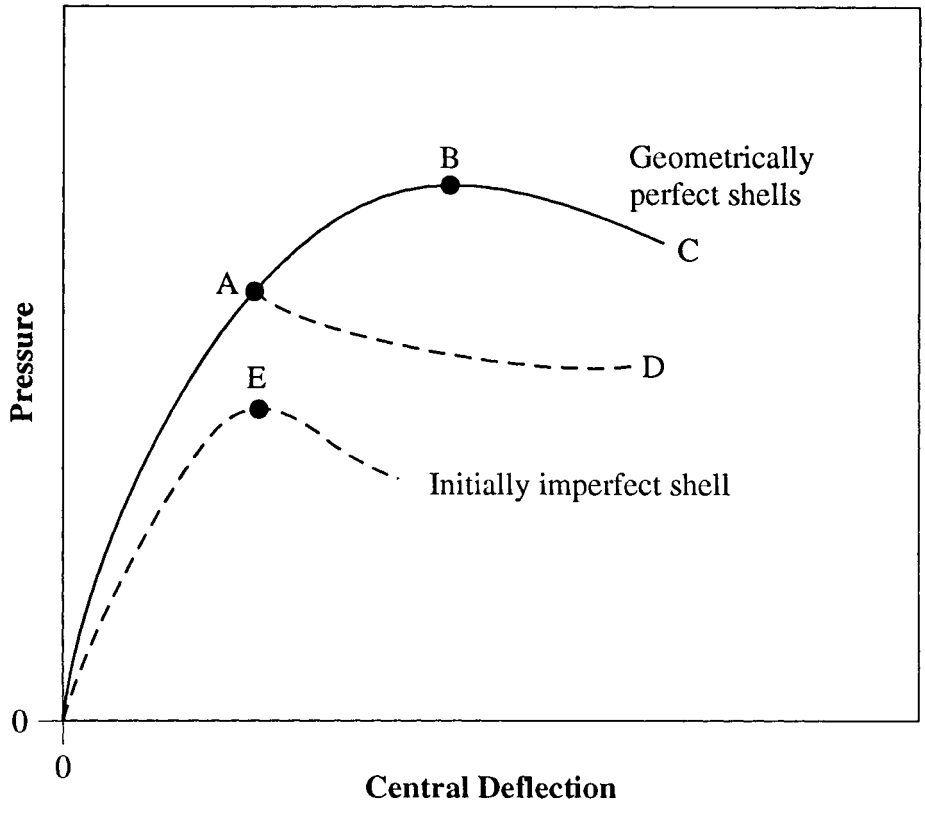

Figure 5.11. General form of pressure - central deflection for a hydrostatically loaded shallow spherical shell.

presented by the authors it was concluded that residual stresses were not heavily responsible for the irregular nature of stress distributions as monitored by electric strain gages. These authors also presented the first high speed photographs of their shallow spherical caps buckling as air was exhausted from the sphere. Pictures were taken at the rate of 1000 images per second and clearly show initiation of a lobe near the clamped edge and subsequent asymmetric growth of that lobe until the entire cap snapped through. In not a single case did the shell buckle axisymmetrically.

Based upon these two series of test results, Klöppel and Jungbluth derived the following empirical expression for hydrostatic buckling pressure:

$$p = \left[1 - 0.175\left(\frac{\alpha - 20^\circ}{20^\circ}\right)\right]\left[1 - 0.07\left(\frac{R}{h}\right)\right]\left[0.3E\frac{h^2}{R^2}\right] \tag{5.17}$$

where α and R are defined in Figure 5.7, h represents shell thickness, and p

the pressure to initiate formation of the first lobe.

One of the earliest studies to ascertain the influence of initial imperfections on buckling of a hydrostatically loaded clamped edge spherical cap is due to *B.* Budiansky [5.20] in 1960. He considered axisymmetric behavior of the cap to be governed by equations (5.7) and (5.8) modified to include consideration of initial geometric imperfections. The pair of equations was cast into integral equation form and solved by computer methods. It was found that the presence of such imperfections lowers the elastic axisymmetric buckling load but not sufficiently to produce agreement with existing experimental data.

The work of W. T. Koiter [5.21–5.23] was the first to provide a rational explanation of the deviation of linearized shell buckling load predictions from experimental results on hydrostatically loaded spherical caps as well as complete spherical shells. The work was based upon detailed analysis of the effect of geometric imperfections present in the shell prior to application of external pressure. This theory indicates the degree of stability of equilibrium at the lowest bifurcation point on the load–deformation diagram (Figure 5.11) as well as determining sensitivity of the maximum load–carrying capacity of the shell to the initial imperfections. Koiter's general postbuckling analysis was presented in the form of an asymptotic expansion of the load in terms of buckled amplitude and led to an asymptotic estimate of the sensitivity of the shell structure to initial imperfections. Both axisymmetric as well as asymmetric initial geometric imperfections were treated for the hydrostatically loaded spherical system. For this case, the postbuckling behavior is found to involve mode interaction.

Asymmetric buckling of hydrostatically loaded shallow spherical caps was treated by N. C. Huang [5.24] who solved the governing nonlinear equations by finite differences. His results indicated that asymmetric buckling would not occur for values of the geometric parameter λ (see equation 5.11) less than approximately 5.5. Comparable results were obtained by R. R. Parmerter and Y. C. Fung [5.25] on the basis of a Galerkin–type solution of the governing nonlinear equations. The shape parameter employed was in agreement with existing experimental evidence. An entirely different approach for establishing buckling pressures was given by J. Famili and R. R. Archer [5.26] in 1965. They carried out a computerized finite difference investigation to determine vibration frequencies of asymmetric modes of the shallow spherical shell subject to known hydrostatic pressure. Then, the buckling pressure was taken to be that value at which the frequency becomes zero. Variation of the assumed number of circumferential waves lead to the critical buckling mode and pressure. Their results indicate highly nonlinear relations between frequency and pressure.

It is of interest to note that G. A. Thurston [5.27] in 1962 employed energy methods to determine the hydrostatic buckling pressure of a shallow spherical cap. He took as the governing nonlinear equations those due to E. Reissner [5.28] and solved them on a computer with the finite difference technique. Load–deflection relations were in relatively good agreement with those obtained experimentally by Kaplan and Fung [5.15]. In 1966 Thurston and F. A. Penning [5.29] carried out tests on aluminum clamped spherical caps subject to hydrostatic loading; initial no–load geometric imperfections were measured on these test specimens. However, since the spherical caps had been formed by an explosive forming process there were probably some unknown magnitude initial stresses present, despite the fact that the caps had been heat–treated to at least partially decrease these stresses.

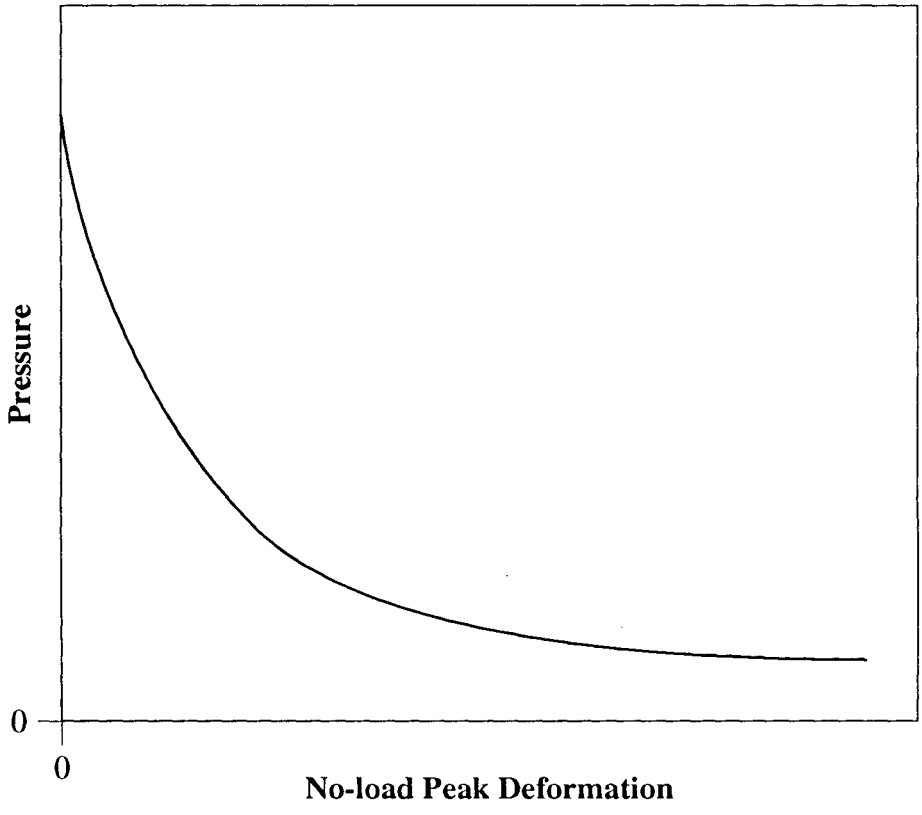

Figure 5.12. Variation of buckling pressure with maximum radial no-load deformation. Reproduced with permission of the David Taylor Model Basin, Department of the Navy, Washington, D.C.

Also, W. A. Nash and J. R. Modeer [5.30] utilized an approximate en-

ergy approach based upon neglect of the second invariant of the middle surface strains, originally applied to finite deflections of elastic plates by H. M. Berger. This technique was applied to the hydrostatically loaded spherical cap with clamped edge, and load–deformation relations in modest agreement with those of Kaplan and Fung [5.15] were found. The neglect of such terms uncouples the governing nonlinear, coupled equations (5.7) and (5.8). The theme of these last few publications is indicated in Figure 5.12 which shows (qualitatively) the variation of (dimensionless) buckling pressure with magnitude of initial, no–load peak geometric imperfection.

During approximately the same period of time, H. J. Weinitschke [5.31–5.33] presented several analysis of buckling of hydrostatically loaded shallow spherical caps. In 1959 he improved convergence characteristics of the power series employed by A. Kaplan and Y. C. Fung [5.15], equations (5.7) and (5.8) were solved by means of the method of analytical continuation employing expansions about the axis of symmetry of the shell and also its outer boundary. He also determined hydrostatic buckling loads for both simply supported as well as freely supported edges. He found that for values of $\lambda > 7$ the circumferential stress near the edge of the shell was about twice the meridional stress, indicating that an asymmetric buckling mode was possible. In particular he obtained buckling loads for asymmetric behavior of the hydrostatically loaded spherical cap in excellent agreement with those offered by N. C. Huang [5.24]. Instability (i.e., imperfection sensitivity) of these asymptotic modes was also found in a 1970 investigation of J. R. Fitch and B. Budiansky [5.34] on the basis of Koiter's nonlinear buckling theory. Also in 1970, S. C. Tillman [5.35] carried out a nonlinear postbuckling analysis on the basis of the Galerkin approach using three symmetric modes in conjunction with two asymmetric modes, the configurations being based upon his experimental evidence. These results indicated that the $n = 1$ mode (n being the number of circumferential lobes) is more unstable than the $n = 2$ mode. Virtually all experimental evidence indicates the final buckled configuration is always a single lobe near the edge, i.e., $n = 1$.

In 1967, J. W. Hutchinson [5.36] examined the imperfection sensitivity of a hydrostatically loaded section of a spherical shell on the basis of the general theory of postbuckling behavior due to W. T. Koiter [5.21]. The approach permitted consideration of axisymmetric and/or asymmetric postbuckling configurations. The predicted mode shapes were found to be in modest agreement with the results of tests conducted by R. L. Carlson, R. D. Sendelbeck, and N. J. Hoff [5.12]. Hutchinson's treatment led to large reduction of buckling pressure from the classical value (5.3) for initial no–load deformations small in comparison with the shell thickness.

In 1963 at the David Taylor Model Basin, Department of the Navy, M.

A. Krenzke and T. J. Kiernan [5.37, 5.38] presented a new approach to the problem of hydrostatic buckling of spherical caps. For the case of shallow, clamped edge spherical caps, seventeen models were machined from type 7075–T6 thick aluminum stock into the configuration indicated in Figure 5.13. Thus each shallow shell model was supported by the very heavy, nearly rigid ring shown and shell and ring were machined as an integral unit.

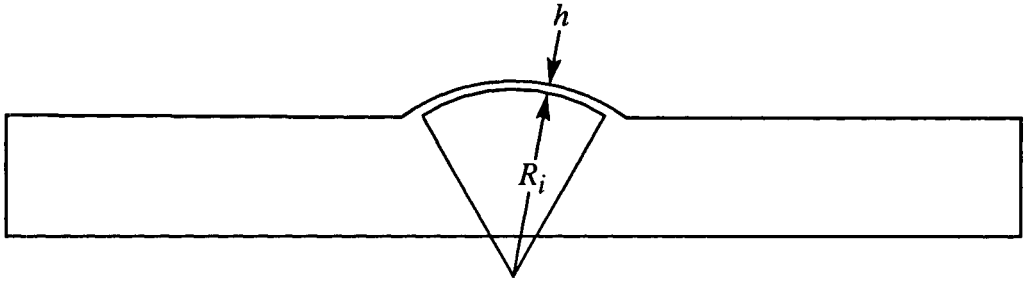

Figure 5.13. Development of a shallow spherical cap from solid aluminum block [5.37]. Reproduced with permission of the David Taylor Model Basin, Department of the Navy, Washington, D.C.

The shell material had a nominal yield strength of 80,000 lb/in^2 (552 MPa) with Young's modulus of 10.8 x 10^6 lb/in^2 (74.4 GPa). These specimens had wall thicknesses ranging from 0.0104 inches (0.264 mm) to 0.0394 inches (1.00 mm) and inside radii of either 2.00 inches (50.8 mm) or 3.00 inches (76.2 mm). Extremely careful machining led to measured variation in local inside radius, usually less than 0.0001 inches (0.00254 mm) with measured variations of shell thickness less than one percent of the shell thickness. Thus, these machined specimens very closely satisfied the assumptions of theories existing at that date than any other series of experiments.

Figure 5.14 illustrates these test results (in terms of dimensionless parameters) together with other test data. Predictions of several types of analytical predictions are also indicated in that figure. The abscissa is a dimensionless geometric parameter θ defined as

$$\theta = \left[\frac{3}{4}\left(1-\mu^2\right)\right]^{\frac{1}{4}} \frac{L_c}{\sqrt{Rh}} \tag{5.18}$$

where R is the middle surface radius of the shell, h is shell thickness, μ is Poisson's ratio and L_c is the unsupported length of the spherical specimen.

From Figure 5.14 one may draw the conclusion that collapse of a spherical cap or shell should be predicted (analytically) on the basis of local geometry over some critical length rather than overall geometry as classical

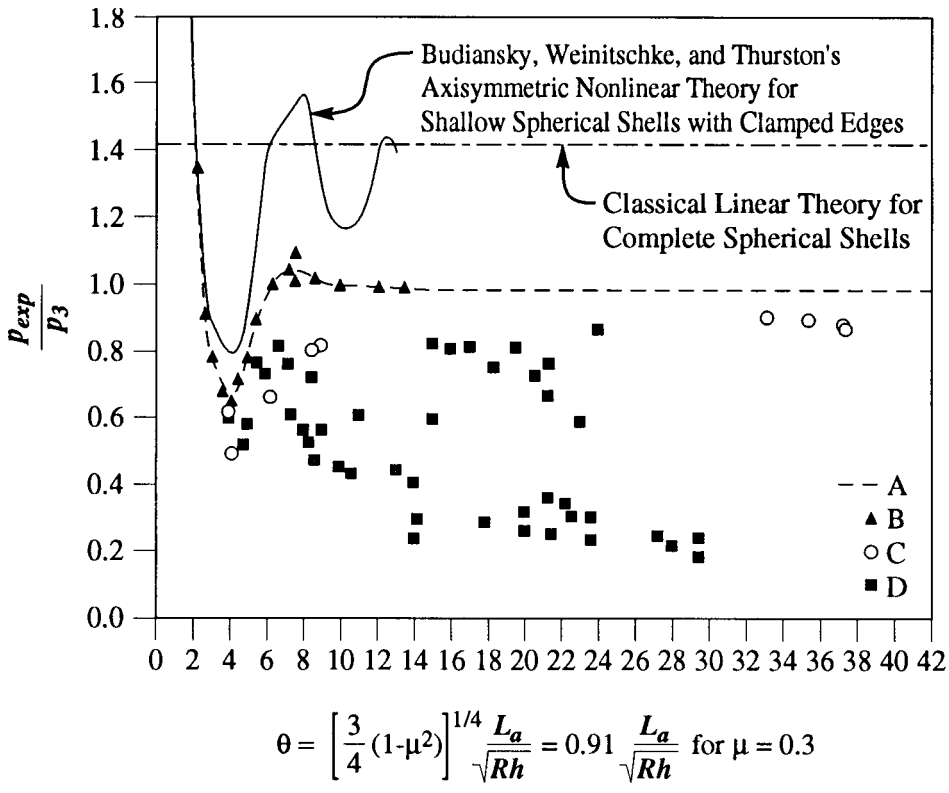

Figure 5.14. Experimental Elastic Buckling Data for Spherical Shells with Clamped Edges. Data are as follows: A: Empirical curve for present tests, B: Present models machined by generating inside contour, C: Present models and models recorded in Reference [5.38] machined by form cutting inside contour, and D: Previous experiments of Tsien, Kaplan, and Fung, von Kloppel and Jungbluth, and Homewood, Brine, and Johnson. Reproduced with permission of the David Taylor Model Basin, Department of the Navy, Washington, D.C. See Equation (5.20) for definition of p_s.

analyses have done. In [5.38] examinations of existing test data indicated that a value θ of 2.2 corresponds to the critical length, then the relationship for L_c becomes

$$L_c = \frac{2.2(R_l h_a)^{1/2}}{\left[\frac{3}{4}\left(1-\mu^2\right)\right]^{1/4}} \tag{5.19}$$

where h_a is mean thickness over the critical length and R_l is the local radius

to the midsurface of the shell over the critical arc length. Pertinent parameters are shown in detail in Figure 5.15.

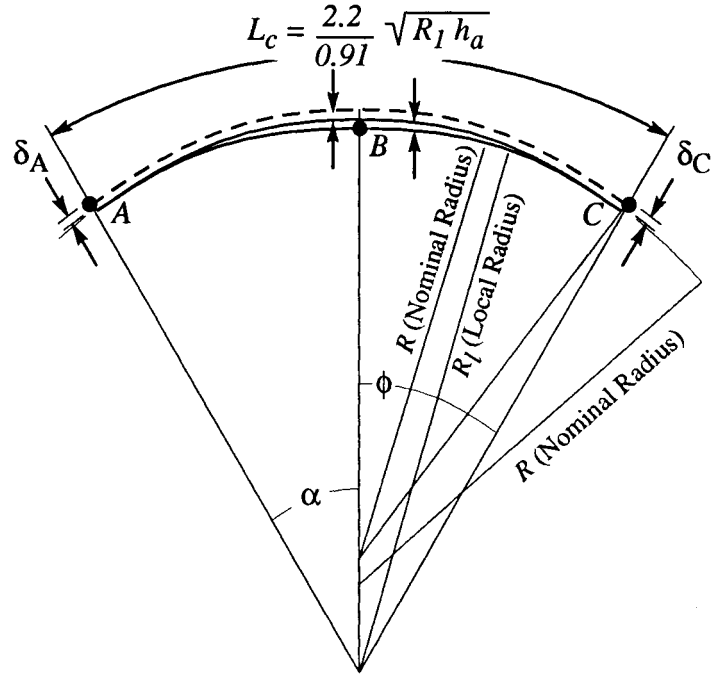

Figure 5.15. Geometric parameters of local geometry of an imperfect spherical shell. Reproduced with permission of the David Taylor Model Basin, Department of the Navy, Washington, D.C.

The experimental data prior to that presented in [5.37] and [5.38] indicated significant scatter. However, the results from [5.37] and [5.38] follow a clear pattern. Because of the near–perfection of the machined test specimens, this demonstrates the detrimental effect on collapse strength of initial no–load geometric imperfections. These results also demonstrate that a short clamped segment can be weaker than a longer clamped segment. For short segments of spherical cap, less than about $\theta = 5.5$, the empirical (dotted) curve of Figure 5.14 through the test data from these machined shells has the same general shape as the curves from the theories for symmetric buckling [5.20], [5.27], [5.29] as well as asymmetric buckling [5.33]. As the shells become longer or deeper, the empirical curve no longer agrees well with the theoretical symmetric buckling curves but instead agrees with the asymmetric theory presented by N. C. Huang [5.24]. The empirical curve lies as much as twenty percent below the theoretical curves for values of θ

approximately 5.5. In 1983 S. Yamada, K. Uchiyama, and M. Yamada [5.39] reported test results on seventy-nine thermovacuum molded polyvinylchloride shallow spherical shells. Prior to loading by hydrostatic pressure very careful measurements of geometric imperfections from perfect sphericity were taken by using a differential transformer. Test results indicated that the buckling of shallow spherical shells depends critically upon initial geometric imperfections.

Buckling of Deep and/or Complete Spherical Shells

The term "deep" usually refers to partial spherical shells in which the central altitude is greater than approximately 1/8 the base diameter. The 1963 work of M. A. Krenzke and T. J. Kiernan [5.38] also included results of tests on eight 300° spherical segments with clamped edges. Again, these were carefully machined from the same material as mentioned previously, i.e., 7075–T6 aluminum. The geometry was as indicated in Figure 5.16. Shell thicknesses of these eight specimens ranged from 0.0248 inches (0.630 mm) to 0.160 inches (4.064 mm). Collapse occurred in the asymmetric mode, in two cases initiating at the juncture of the spherical shell with the heavy end ring (see Figure 5.13), and in the other six cases initiating in areas away from the end ring.

For these eight models values of the parameter θ ranged from 17.20 to 42.73. On the basis of these test results the authors proposed the empirical relation for elastic as well as inelastic collapse pressure of a nearly–perfect deep spherical shell:

$$p_3 = 0.84\sqrt{E_t E_s}\left(\frac{h}{R_o}\right)^2 \text{ for } \mu = 0.3 \tag{5.20}$$

where E_s and E_t denote secant and tangent moduli, respectively, as obtained from coupon compression test of the shell material, h denotes shell thickness, and R_0 is outer radius of the shell. This equation should only be applied if the spherical shell has local variations of radius of less than 2.5 percent of the shell thickness. For greater variations, (5.20) overestimates the collapse strength. The pressure hull of the submersible "Shinkai 6500" mentioned in Chapter 1 was designed on the basis of Equation (5.20).

Krentze and Kiernan [5.38] also reported test results on four models of 7075–T6 aluminum representing, essentially, complete spherical shells. These were fabricated by having a 60° circular opening to permit machining of the inside contour. Metal spherical segments of the same material and curvature were then inserted into this opening, but the area in the vicinity of these segments was machined ten percent thicker than the remainder of the

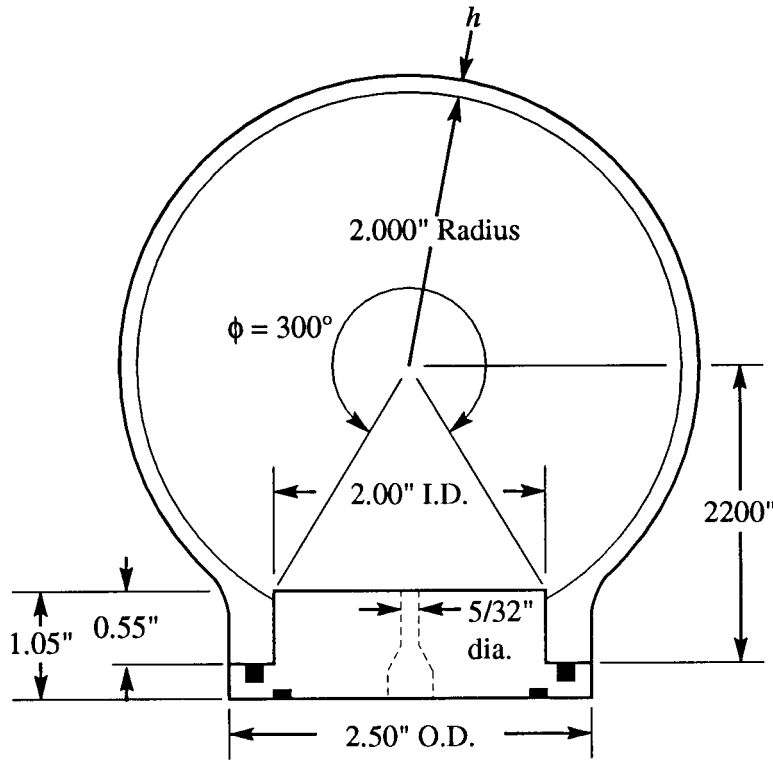

Figure 5.16. Reproduced with permission of the David Taylor Model Basin, Department of the Navy, Washington, D.C.

sphere in an effort to discourage failure in the insert piece. Each of these test pieces ruptured during collapse under hydrostatic loading, with failure initiating in the main body of the sphere, not near the insert. The authors indicated that equation (5.20) again represents inelastic buckling of a complete machined sphere.

Equation (5.20) is in a convenient form for analysis of an existing or proposed shell, but not well–suited for design which usually required thickness determination for a given radius, modulus, and pressure at specified depth of submergence. A tabular approach, well–suited to computer implementation, has been developed by W. E. Heronemus [5.40] for iterative determination of shell thickness with all of the above parameters specified.

Mention should also be made of earlier experiments on the buckling of complete spherical shells. In 1962, J. M. T. Thompson [5.41] at Cambridge University carried out a series of tests on hydrostatically loaded polyvinyl chloride shells of radius 2.1 inches (53.34 mm), and thickness 0.10 inches (2.54 mm). Load–deformation relations of the type shown by dotted lines in Figure 2.17 were found and snapping was traditional in nature. Stable post-

buckling states were characterized by a rotational symmetric dimple for the case of a nearly perfect test specimen. Later, Thompson [5.42] employed the approach of W. T. Koiter to study initial postbuckling behavior of the complete sphere. The work was restricted to axisymmetric deformation. Also, P. G. Hodge [5.43] obtained upper and lower bounds on the plastic collapse load of a geometrically perfect spherical segment. P. P. Bijlaard [5.44], G. Gerard [5.45], and M. E. Lunchick [5.46] considered inelastic buckling of complete spheres. These three investigations each applied a plasticity reduction factor to the buckling pressure predicted by classical linear theory. The solutions are somewhat similar except for the use of different values of Poisson's theory in the plastic range.

Axisymmetric buckling of a complete spherical shell having initial geometric imperfections was examined by T. Koga and N. J. Hoff [5.47] in 1968. In this analysis, the shell is considered to consist of two regions (a) the shallow cap in which the initial imperfection exists, and (b) the remainder of the shell which merely contracts in radius. The rotation of the meridian of the cap was represented by a polynomial function and four boundary conditions were imposed at the juncture of the cap and the remainder of the spherical shell. The total potential energy was minimized following the Rayleigh–Ritz method. Two types of initial imperfections were examined: one is an axisymmetric dimple, and the other is a spherical region whose radius of curvature is greater than that of the corresponding perfect spherical shell. The authors employed the equations developed by E. Reissner [5.28] valid for axisymmetric deformations of shells of revolution undergoing arbitrarily large deformations but small strains. Numerical analysis indicated that for all values of imperfection amplitude the lowest value of buckling pressure is reached when λ (Equation 5.11) is approximately 4. From this it follows that the hydrostatic buckling pressure of a nearly complete spherical shell is approximately one-third of the classical buckling pressure (5.3) when the imperfection amplitude is one-half the thickness of the shell.

In 1973, N. C. Huang and G. Funk [5.48] investigated inelastic buckling of a deep spherical shell subject to hydrostatic loading. The finite deformation shell equations due to J. L. Sanders, Jr. were employed and the possibility of the shell thickness varying along a meridian was considered. The edge of the shell was elastically supported and the material followed the generalized Ramberg–Osgood stress–strain relations together with a power law of creep. Solution was accomplished through solving the finite difference equations by a computerized iterative approach for (a) axisymmetric inelastic buckling and (b) asymmetric bifurcation. Later, R. Kao [5.49] examined elasto-plastic axisymmetric behavior of a shallow spherical cap subject to

hydrostatic loading. Consideration was given to initial imperfections, material nonlinearity, strain hardening on the basis of the Prager–Ziegler kinematic hardening theory, and the Bauschinger effect. Governing equations were solved on a computer by iteration and dimensionless load–deformation results presented for a variety of initial imperfections.

Buckling of Stiffened and/or Orthotropic Spherical Shells

Spherical shells subject to hydrostatic pressure are occasionally reinforced by either (a) radial (meridional) ribs, and/or (b) circumferential ring-like ribs. Such stiffeners may be on either the concave or the convex side of the shell, and may be machined integral with the shell or perhaps joined by brazing, welding, or epoxy after the shell is constructed.

The earliest systematic investigation of the influence of ribs on buckling strength of a spherical cap is due to K. Klöppel and O. Jungbluth [5.19] in 1953. These authors employed the same type of spherical caps as they had for tests on unstiffened shells, but welded radial ribs to some shells, and radial together with ring-like ribs to most of the 73 models tested under hydrostatic pressure. Most of the models snapped–through to the mirror–image of the unloaded configuration, sometimes causing the rib to separate from the shell. For the geometries employed, meridional stiffeners offered greater resistance to snap–through than annular ribs. An approximate orthotropic analysis was developed (assuming closely spaced ribs) and a generalization of equation (5.17) was offered to predict buckling pressure. A comparable analysis was offered by R. F. Crawford and D. B. Schwartz [5.50] in 1965. This study examined optimum design of the grid-stiffened spherical cap and concluded that efficient design of the ribs would lead to total weights of the stiffened shell ranging from thirty to forty percent of the monocoque domes they would replace. In 1973 A. I. Manevich and M. E. Kaganov [5.51] published a closely–related study but with inclusion of the effect of eccentricity from shell middle surface of the ribs.

The 1963 work of M. A. Krenzke and T. J. Kiernan [5.38] also involved tests of seventeen machined hemispherical shells. Of these, nine had only circumferential ribs, four had only meridional ribs, and four had both circumferential as well as meridional stiffeners. All were machined from the same aluminum described earlier in this chapter. In general collapse was by general instability, but visual inspection of the interior of the models indicated that significant local deformation of the shell between ribs occurred during pressure application. In no case was the collapse pressure of the stiffened shell as great as would have been expected for a machined unstiffened shell of the same weight. A 1967 study by F. M. Schwartz [5.52] of a steel hemisphere having both radial as well as circumferential ribs indicated the

collapse pressure was approximately thirty percent greater than that predicted for an unstress-relieved monocoque shell of equivalent weight with the same initial out-of-roundness.

In 1983 M. Yamada [5.53] from Tohoku University in Japan presented a nonlinear analysis of buckling of a spherical shell stiffened by radial as well as circumferential ribs and loaded by hydrostatic pressure. Anisotropic shell theory was employed. Buckling between ribs as well as general instability collapse was examined. In that same year, K. Uchiyama and M. Yamada [5.54] published results of a series of tests on polyvinyl–chloride shallow spherical caps. There was reasonable agreement between test results and the theory [5.53].

REFERENCES

5.1 Nash, W. A., *Theory and Problems of Strength of Materials,* 3rd ed, McGraw–Hill, Inc., New York, 1994, 423 pages.

5.2 Flugge, W., *Stresses in Shells,* Springer–Verlag, Berlin/Gottingen/ Heidelberg, 1960, 499 pages.

5.3 Vinson, J. R., *The Behavior of Thin Walled Structures, Beams, Plates, and Shells,* Kluwer Academic Publishers, Dordrecht, The Netherlands, 1989, 185 pages.

5.4 Kraus, H., *Thin Elastic Shells,* J. Wiley and Sons, New York, 1967, 476 pages.

5.5 Seide, P., *Small Elastic Deformations of Thin Shells,* Noordhoff International Publishing, Leyden, The Netherlands, 1975, 654 pages.

5.6 Timoshenko, S. and Woinowsky-Krieger, S., *Theory of Plates and Shells,* 2nd ed., McGraw-Hill Book Co., Inc., New York, 1959, 580 pages.

5.7 Gould, P.L., *Analysis of Shells and Plates,* Springer-Verlag, New York and Heidelberg, 1988, 491 pages.

5.8 Zoelly, R., *Uber ein Knickproblem an der Kugelschale,* Dissertation, TH Zurich, 1915.

5.9 Leibenson, L. S., "On Application of Harmonic Functions to Problems of Stability of Spherical and Cylindrical Shells," Scientific Notes of Yuryev University, No. 1, 1917, pp. 50–85 (in Russian).

5.10 Schwerin, T., "Zur Stabilitat der Dunnwandigen Hohlkugel unter gleichmaszigem Aussendruck," *A. Zeit. Angewandte Mathematik und Mechanik,* Vol. 2, 1992, pp. 81–91.

5.11 van der Neut, A., *Der Elastische Stabilitet von den Dunwandigen Bol,* Dissertation, TH Delft, The Netherlands, 1932.

5.12 Carlson, R. L., Sendelbeck, R. L., and Hoff, N. J., "Experimental Studies of the Buckling of Complete Spherical Shells," *Experimental Mechanics,* Vol. 7, 1967,pp. 281–288.

5.13 von Karman, Th. and Tsien, H. S., "The Buckling of Spherical Shells by External Pressure," *Journal of the Aeronautical Sciences,* Vol. 7, No. 2, 1939, pp. 43–50.

5.14 Tsien, H.S., "A Theory for the Buckling of Thin Shells," *Journal of the Aeronautical Sciences,* Volume 9, No. 10, 1942, pp. 373-384.

5.15 Kaplan, A. and Fung, Y. C., "A Nonlinear Theory of Bending and Buckling of Thin Elastic Shallow Spherical Shells," NACA Tech. Note 3212, 1954, 58 pages.

5.16 Chien, W. Z., "Large Deflections of a Circular Clamped Phase under Uniform Pressure," *Chinese Journal of Physics,* Vol. VII, No. 2, 1947, pp. 102–113.

5.17 Fung, Y. C. and Sechler, E. E., "Instability of Thin Elastic Shells," published in *Structural Mechanics--Proceedings of the First Symposium on Naval Structural Mechanics,* Pergamon Press, 1960, pp. 115–168.

5.18 Surkin, R. G. and Stepanov, S. G., "Experimental Investigation of the Stability of Spherical Segments Subject to Uniformly Distributed Pressure," *Plates and Shells, Proceedings of the Third All-Union Conference,* Kiev, Publishing House of the Ukranian Academy of Science, 1962, pp. 311 - 313. (In Russian.)

5.19 Klöppel, K. and Jungbluth, O., "Beitrag zum Durchschlags problem dunnwandiger Kugelschalen," *der Stahlbau,* Vol. 22, No. 6, 1953, pp. 121–130.

5.20 Budiansky, B. "Bucking of Clamped Shallow Spherical Shells," *Proceedings of the IUTAM Symposium on the Theory of Thin Elastic Shells,* North Holland Publishing Co., Amsterdam, 1960, pp. 64–85.

5.21 Koiter, W. T., "Concerning the Stability of Elastic Equilibrium," (in Dutch). Published by H. J. Paris, Amsterdam, 1945. Available in English as NASA Report TT F–10, 1967.

5.22 Koiter, W. T., "Elastic Stability and Post-bucking Behavior," *Proceedings of the Symposium on Nonlinear Problems,* edited by R. E. Langer, University of Wisconsin Press, Madison, 1963, pp. 257–275.

5.23 Koiter, W. T., "The Nonlinear Buckling Problem of a Complete Spherical Shell Under Uniform External Pressure," No. I through IV, *Proceedings Koninklike Nederlandische Akademie von Wetenschappen.* Vol. B72, 1969, pp. 40–123.

5.24 Huang, N. C., "Unsymmetrical Buckling of Thin Shallow Spherical Shells," *Journal of Applied Mechanics,* Trans. ASME, Sept.,

1964, pp. 447–457.

5.25 Parmeter, R. R. and Fung, Y. C., "On the Influence of Non-Symmetrical Modes on the Buckling of Shallow Spherical Shells Under Uniform Pressure," in *Collected Papers on Instability of Shell Structures,* NASA D–1510, Washington, D.C., 1962, pp. 491–499.

5.26 Famili, F. and Archer, R. R., "Finite Asymmetric Deformation of Shallow Spherical Shells," *Journal of the American Institute of Aeronautics and Astronautics,* Vol. 3, No. 3, 1965, pp. 506–510.

5.27 Thurston, G. A., "Comparison of Experimental and Theoretical Buckling Pressures for Spherical Caps," *Collected Papers on Instability of Shell Structures,* NASA TN D–1510, 1962, pp. 515–522.

5.28 Reissner, E., "On Axisymmetrical Deformation of Thin Shells of Revolution," *Proceedings of the Symposia in Applied Mathematics,* Vol. 3, McGraw-Hill Book Co., New York, 1950, pp. 27–52.

5.29 Thurston, G. A. and Penning, F. A., "Effect of Axisymmetric Imperfections on the Buckling of Spherical Caps Under Uniform Pressure," *Journal of the American Institute of Aeronautics and Astronautics,* Vol. 4, No. 2, 1966, pp. 319–327.

5.30 Nash, W. A. and Modeer, J. R., "Certain Approximate Analyses of the Nonlinear Behavior of Plates and Shallow Shells," *Proceedings of the IUTAM Symposium on the Theory of Thin Elastic Shells,* North Holland Publishing Co., Amsterdam, 1960, pp. 331–354.

5.31 Weinitschke, H. J., "On the Stability Problem for Shallow Spherical Shells," *Journal of Mathematics and Physics,* Vol. 38, 1959, pp. 209–231.

5.32 Weinitschke, H. J., "The Effect of Asymmetric Deformation on the Buckling of Shallow Spherical Shells," *Journal of the Aerospace Sciences,* Vol. 29, 1962, pp. 1141–1142.

5.33 Weinitschke, H. J., "Asymmetric Buckling of Clamped Spherical Shells," in *Collected Papers on Instability of Shell Structures,* TN D–1510, Washington, D.C., 1962, pp. 481–490.

5.34 Fitch, J. R. and Budiansky, B., "Buckling and Postbuckling Behavior of Spherical Caps Under Axisymmetric Load," *Journal of the American Institute of Aeronautics and Astronautics,* Vol. 8, 1970, pp. 686–693.

5.35 Tillman, S. C., "On the Buckling Behavior of Shallow Spherical Caps Under a Uniform Pressure Load," *International Journal of Solids and Structures,* Vol. 6, 1970, pp. 37–52.

5.36 Hutchinson, J. W., "Imperfection Sensitivity of Externally Pressurized Spherical Shells," *Journal of Applied Mechanics, Transactions of the American Society of Mechanical Engineers,* Vol. 34, No. 1, 1967, pp. 49–55.

5.37 Krenzke, M. A. and Kiernan, T. J., "Elastic Stability of Near-Perfect Shallow Spherical Shells," *Journal of the American Institute of Aeronautics and Astronautics,* Vol. 1, No. 12, 1963, pp. 2800–2857.

5.38 Krenzke, M. A. and Kiernan, T. J., "Tests of Stiffened and Unstiffened Machined Spherical Shells Under External Hydrostatic Pressure," David Taylor Model Basin, Department of the Navy, Washington, D.C., 1963, Report 1741.

5.39 Yamada, S., Uchiyama, K., and Yamada, M., "Experimental Investigation of the Buckling of Shallow Spherical Shells," *International Journal of Non-Linear Mechanics,* Vol. 18, No. 1, 1983, pp. 37–54.

5.40 Heronemus, W. F. (Capt.), unpublished lecture notes, "Practical Spherical Pressure Hulls for Deep Ocean Systems," Civil Engineering #591, University of Massachusetts, Amherst, MA, 1972.

5.41 Thompson, J. M. T., "The Elastic Instability of a Complete Spherical Shell," *The Aeronautical Quarterly,* Vol. 13, May, 1962, pp. 189–201.

5.42 Thompson, J. M. T., "The Rotationally Symmetric Branching Behavior of a Complete Spherical Shell," *Koninklijke Nederland Akademie van Wetenschapen, Proceedings,* Series B, Vol. 67, 1964, pp. 295–311.

5.43 Hodge, P. G., *Plastic Analysis of Structures,* McGraw-Hill Book Co., Inc., New York, 1959.

5.44 Bijlaard, P. P., "Theory and Tests on the Plastic Stability of Plates and Shells," *Journal of the Aeronautical Sciences,* Vol. 16, No. 9, 1949.

5.45 Gerard, G., "Plastic Stability Theory of Thin Shells," *Journal of the Aeronautical Sciences,* Vol. 24, No. 4, 1957.

5.46 Lunchick, M. E., "Plastic Buckling Pressure for Spherical Shells," David Taylor Model Basin, Department of the Navy, Washington, D.C., 1963. Report 1493. Also, Engineering Mechanics Division, American Society of Civil Engineers, EM6, 1962, pp. 13–31.

5.47 Koga, T. and Hoff, N. J., "The Axisymmetric Buckling of Initially Imperfect Complete Spherical Shells," Department of Aeronautics and Astronautics, Stanford University, May, 1968. SUDAAR Report No. 332.

5.48 Huang, N. C. and Funk, G., "Inelastic Buckling of a Deep Spherical Shell Subject to External Pressure," *Journal of the American Institute of Aeronautics and Astronautics,* Vol. 12, 1974, pp. 914–920.

5.49 Kao, R., "Large Deformation Elastic-Plastic Buckling Analysis of Spherical Caps with Initial Imperfections," *International Journal of Computer and Structures,* Vol. 11, 1980, pp. 609–619.

5.50 Crawford, R. F. and Schwartz, D. B., "General Instability and Optimum Design of Grid-Stiffened Spherical Domes," *Journal of the American Institute of Aeronautics and Astronautics,* Vol. 3, No. 3, 1965, pp. 511–515.

5.51 Manevich, A. I. and Kaganov, M. E., "Stability and Weight Optimization of Reinforced Spherical Shells Under External Pressure," *Prikladnaya Mekhanika,* Vol. 9, No. 1, 1973, pp. 20–26. Available in English as *Soviet Applied Mechanics,* Plenum Publishing Corp., New York.

5.52 Schwartz, F. M., "Hydrostatic Tests of a High-Strength Steel Internally Stiffened Hemisphere," David Taylor Model Basin, Department of the Navy, Washington, D.C., 1967. Report 2302.

5.53 Yamada, M., "An Approximation on the Buckling Analysis of Orthogonally Stiffened and Framed Spherical Shells Under External Pressure," in *Shell and Spatial Structures Engineering,* ed. by F. L. L. B. Carneiro, Pentech Press, London, 1983, pp. 177–193.

5.54 Uchiyama, K. and Yamada, M., "Buckling of Orthogonally Stiffened and Framed Spherical Shells Under External Pressure," in *Shell and Spatial Structures Engineering,* ed. by F. L. L. B. Carneiro, Pentech Press, London, 1983, pp. 220–240.

Please note: the David Taylor Model Basin is now (1994) named the Naval Surface Warfare Center.

BIBLIOGRAPHY

Alesso,H.P., "On the Instabilities of an Externally loaded Shallow Spherical Shell," International Journal of Non-Linear Mechanics, Vol. 17, No. 2, 1982, pp. 85 - 103.

One of the earliest efforts to apply Catastrophe Theory to buckling of a hydrostatically loaded elastic spherical cap. The work explores solution regions where a sudden jump in solutions occur while parameters of the governing equations are changing smoothly. Three modes of deflections are identified. One, snap-through behavior, is in agreement with experimental data.

Amiro, I. Ya. and Grachev, O. A., "Stability of Spherical Reinforced Shells–A Review," *Prikladnaya Mekhanika, Kiev*, Vol. 22, No. 11, pp. 3–17, 1986. Available in English as *Soviet Applied Mechanics*, Plenum Publishing Corp., New York.

Axelrad, E. L. and Emmerling, F. A., *Flexible Shells–Theory and Applications*, Springer Verlag, 1984, 282 pages.

A collection of 17 papers presented at the European Mechanics Colloquium Number 165, held in Neubiberg, Germany, in 1983. Of particular interest is a paper by R. Scheidl and H. Troger (Vienna) concerned with axisymmetric buckling of a complete spherical shell with consideration of bifurcation behavior together with Catastrophe Theory.

Babcock, C. D., "Shell Stability," *Journal of Applied Mechanics,* Transactions of the American Society of Mechanical Engineers, December, 1983, Vol. 50, pp. 935–940.

A concise survey of work prior to 1983 in the areas of elastic postbuckling behavior, imperfection sensitivity, plastic flow, dynamic buckling, experiments and computations.

Babenko, V.I., and Ivanova, J.A., "Investigation of Post-Critical Deformation of Thin Anisotropic Shells, III," *Proceedings of the Bulgarian Academy of Sciences, Theoretical and Applied Mechanics,* Vol. 6, No. 2, 1975, pp. 59-65, (in Russian).

The method of A.V. Pogorelev (see Chapter 2) based upon differential geometry of the buckled shape is applied to hydrostatically loaded spherical shels. A buckling coefficient in Equation (5.16) somewhat smaller than that from classical theory is found.

Besseling, J. F. and Heijden, van der (ed)., *Trends in Solid Mechanics, 1979*, Delft University Press, 1979.

A collection of papers on shell buckling, many based upon the initial work of W. T. Koiter.

Budiansky, V., (ed)., *Buckling of Structures*, Springer-Verlag, 1976, 398

pages.

A collection of 28 papers presented at the Symposium on Buckling of Structures held at Harvard University in June 1974. Topics treated include buckling of shells of various geometry, plasticity and creep effects, experiments, and design considerations.

Bushnell, D., "Buckling of Spherical Shells Ring-Supported at the Edges," *Journal of the American Institute of Aeronautics and Astronautics,* Vol. 5, 1967, pp. 2041–2045.

Bushnell, D., "Buckling of Shells–Pitfalls for Designers," *Journal of the American Institute of Aeronautics and Astronautics,* Vol. 19, No. 9, 1981, pp. 1183–1226.

Feodosiev, V. I., "Calculation of Thin Clicking Membranes," *Applied Mathematics and Mechanics,* Vol. X, 1946. (In Russian).

Galletly, G.D., "On the Buckling of Shallow Spherical Caps Subjected to Uniform External Pressure," *Journal of the American Instutute of Aeronautics and Astronautics,* Vol. 14, No. 3, pp. 1331 - 1333, 1976.

Hydrostatic pressure tests on machined spherical caps led to buckling pressure slightly higher than those predicted theoretically but were not as great as those reported by Sunakawa and Ichida in 1974. It is evident that more work is required to account for the very high values obtained by these two researchers.

Galletly, G.D., Blachut, J., and Kruzelcki, J., "Plastic Buckling of Imperfect Hemispherical Shells Subjected to External Pressure," *Proceedings of the Institution of Mechanical Engineers,* Vol. 201, No. C3, 1987, pp. 154-171.

Plastic buckling presures for externally pressurized imperfect hemispherical shells were determined through use of the BOSOR5 computer program. Parameters considered were the yield point, the radius/thickness ratio, and the amplitude of initial imperfection at the pole. These values were compared with predictions of several design codes.

Gjelsvik, A. and Bodner, S. R., "Non-symmetrical Snap Buckling of Spherical Caps," Journal of the Engineering Mechanics Division, American Society of Mechanical Engineers, Proc. ASCE, EM5, 1962, pp. 135–165.

Grachev, O. A., "Effect of Rib Eccentricity on the Stability of Spherical Shells Under External Pressure," *Prikladnaya Mekhanika, Kiev,* Vol. 21, No. 2, pp. 53–60, 1985. Available in English as *Soviet Applied Mechanics*, Plenum Publishing Corp., New York.

An analytical investigation based upon linearized theory to determine influence of distance of centroid of each rib from the shell middle surface. The author concludes that this parameter should be employed in determination of strength of a deep spherical shell.

Grachev, O. A. and Pal'chevskii, A. S., "Experimental Study of the Stability of Ribbed Spherical Shells Under External Pressure," *Prikladnaya Mekhanika, Kiev*, Vol. 19, No. 2, pp. 52–57, 1983. Available in English as *Soviet Applied Mechanics*, Plenum Publishing Corp., New York.

Results of hydrostatic tests of 29 deep shells formed by deep drawing of either titanium or steel sheets. Shells were reinforced by a system of meridional/circumferential ribs either welded or riveted to the shell.

Grigolyuk, E. I., "On the Unsymmetrical Snapping of Shells of Revolution," *Proceedings of the IUTAM Symposium on the Theory of Thin Elastic Shells*, North Holland Publishing Co., Amsterdam, 1960, pp. 112–121.

A discussion of the effect of asymmetric imperfections on the basis of a two-term potential approach in the Galerkin solution.

Hutchinson, J. W. and Koiter, W. T., "Postbuckling Theory," *Applied Mechanics Reviews*, Vol. 23, 1970, pp. 1353–1366.

A comprehensive review of postbuckling behavior of spherical shells until about 1970.

Hutchinson, J. W., "Plastic Buckling," *Advances in Applied Mechanics*, Vol. 14, Academic Press, New York, 1974, pp. 67–144.

Jones, N. and Ich, N. T., "The Load-Carrying Capacities of Symmetrically Loaded Shallow Shells," *International Journal of Solids and Structures*, Vol. 8, No. 12, pp. 1339–1351, 1972.

Limit analysis of a rigid-perfectly plastic shallow spherical shell subject to hydrostatic loading. Limit loads are determined for three approximate yield surfaces.

Kao, R. and Perrone, N., "Asymmetric Buckling of Spherical Caps with Asymmetric Imperfections," *Journal of Applied Mechanics, Transactions of the American Society of Mechanical Engineers*, Vol. 38, 1971, pp. 172–178.

Illustrates use of a relaxation method combined with Newton's method to obtain load-deflation for a spherical cap subject to hydrostatic pressure.

Kaplan, A., "Buckling of Spherical Shells," in *Thin-Shell Structures–Theory, Experiment, and Design*, edited by Y. C. Fung and E. E. Sechler, Prentice Hall, New Jersey, 1974, pp. 247–288.

Keller, H. B. and Reiss, E. L., "Spherical Cap Snapping," *Journal of the Aero/Space Sciences*, October, 1959, Vol. 26, pp. 643–652.

The nonlinear equations governing the finite deformation of a clamped spherical cap subject to hydrostatic pressure are solved by finite differences. Upper as well as lower bounds are given for the buckling load. Shell boundary layers are also investigated.

Khairullin, S. Kh., "Stability of a Spherical Shell with Large Deflections," *Investigations in the Theory of Plates and Shells*, Vol. 5, 1967, pp. 363–367. (In Russian).

The influence of axisymmetric initial imperfections on buckling load is treated by nonlinear shell theory. Load-deflection relations are determined numerically for very thin shells.

Kiernan, T. J., "Predictions of the Collapse Strength of Three HY–100 Steel Spherical Hulls Fabricated for the Oceanographic Research Vehicle ALVIN," David Taylor Model Basin, Department of the Navy, Washington, D.C., 1964. Report 1792.

Initial, no-load out-of-roundness measurements were taken on three spherical pressure hulls fabricated for the research vessel ALVIN. Over a critical arc length the maximum ratio of local radius to nominal radius was measured to be 1.05. Collapse strength was evaluated by means of the analysis due to M. A. Krenzke [5.38].

Knightly, G. H. and Sather, D., "Buckled States of a Spherical Shell Under Uniform External Pressure," *Archive for Rational Mechanics and Analysis,* Vol. 72, 1980, pp. 315–380.

The equations due to F. John together with asymptotic methods plus Newton's method are employed to obtain and relate preferred buckling configurations to those found in experiments carried out by R. L. Carlson, R. L. Sendelbeck, and N. J. Hoff [5.12].

Knightly, G. H. and Sather, D., "Nonlinear Axisymmetric Buckled States of Shallow Spherical Caps," *Society for Industrial and Applied Mathematics, Journal of Mathematical Analysis,* Vol. 6, No. 6, 1975, pp. 913–924.

The title problem is approached via the Lyapunov-Schmidt method and solution indicates that buckled states exist very near every eigenvalue of the linearized problem.

Krenzke, M.A., "The Elastic Buckling Strength of Near-Perfect Deep Spherical Shells with Ideal Boundaries," David Taylor Model Basin, Department of the Navy, Washington, D.C., 1963, Report 1713.

Krenzke, M. A. and Charles, R. M., "The Elastic Buckling Strength of Spherical Glass Shells," David Taylor Model Basin, Department of the Navy, Washington, D.C., 1963. Report 1759.

Twenty hemispheres of annealed Pyrex glass were subjected to hydrostatic loadings as great as 43,250 lb/in^2 (298 MPa). An empirical design equation for elastic bucking strength with consideration of initial imperfections was presented.

Krenzke, M., Jones, R., and Kiernan, T., "Design of Pressure Hulls for Small Submersibles," American Society of Mechanical Engineers, Paper No. WA/UNT-7, 1967.

A documentation of state-of-the-art for design of single, unstiffened shells loaded by hydrostatic pressure. The case of two or even three nearly complete spherical shells connected to one another along a longitudinal axis of symmetry as a pressure hull is discussed in detail.

Krenzke, M.A., and Kiernan, T.J., "The Effect of Initial Impefections on the Collapse Strength of Deep Spherical Shells," David Taylor Model Basin, Department of the Navy, Washington, D.C. 1965, Report 1757.

Sixty-two deep spherical shells were machined with local thin spots or flat spots and loaded by hydrostatic pressure. A relatively simple empirical relation was developed to indicate effects of initial departure from sphericity and thickness vatiations on elastic as well as inelastic collapse strengths.

Kruger, D. S. and Glockner, P. G., "Experiments on the Stability of Spherical and Paraboloidal Shells," *Experimental Mechanics,* Vol. 11, 1971, pp. 252–262.

Kollar, L., "Buckling of Complete Spherical Shells and Spherical Caps," published in *Buckling of Shells*, ed. by E. Ramm, Springer-Verlag, Berlin, 1982, pp. 401–425.

A comprehensive survey of elastic buckling of spherical shells and caps up to approximately 1973. Theory and experiments and their correlations are presented.

Liu, R. H. and Li, D., "On the Non-Linear Stability of a Truncated Shallow Spherical Shell Under a Uniformly Distributed Load," *Applied Mathematics and Mechanics,* Vol. 9, Number 3, 1988, pp. 205-217. (In Chinese, with English summary.)

The finite deformations of a spherical dome having a central cutout (or stiffened at the apex by a rigid disc) is investigated.

Mescall, J. F., "Large Nonsymmetric Deflections of Thin Shells of Revolution," *Proceedings of the Army Symposium on Solid Mechanics*, Army Mechanics and Materials Research Center, –MS 68–09, pp. 143–157.

Postbuckling analysis based upon a finite difference approach to solve the governing nonlinear equations. Computer time was minimized through matrix partitioning.

Nishida, K., "Tests of Machined Multi-Layer Spherical Shells with Clamped Boundaries under External Hydrostatic Pressure," David Taylor Model Basin, Department of the Navy, Washington, D.C., 1965. Report 2012.

Description of an experimental program to determine the feasibility of utilizing either two or four layered spherical caps to withstand hydrostatic loading. Three of the models were bonded at the interface with epoxy resin, and the remaining three were unbonded. Four monolithic shells were also tested to form a basis of comparison. The bonded

shells collapsed at pressure approximately equal to that of the monolithic model. The unbonded shells showed considerable reduction in pressure carrying capability.

Perrone, N. and Kao, R., "Large Deflection Response and Buckling of Partially and Fully Loaded Spherical Caps," *Journal of the American Institute of Aeronautics and Astronautics,* Vol. 8, 1970, pp. 2130–2136.

A finite difference approach to determine nonlinear large deformations of a shallow spherical cap subject to uniform normal pressure or nonuniform axisymmetric normal pressure.

Simitses, G. J. and Cole, R. T., "General Instability of Eccentrically Stiffened Thin Spherical Shells Under Pressure," *Journal of Applied Mechanics, Transactions of the American Society of Mechanical Engineers,* Vol. E-37, No. 4, pp. 1165–1168, 1970.

Stiffeners are assumed to be identical and equally spaced. Sanders' thin shell theory (linearized) is employed to set up an eigenvalue problem.

Srubshchik, L. S., "Flexibility of a Deep Spherical Dome," *Applied Mathematics and Mechanics,* Vol. 32, No. 3, 1968, pp. 435–444. (In Russian). Available in English, Pergamon Press.

Application of asymptotic methods to integrate the E. Reissner equations for large deformations of shells of revolution.

Srubshchik, L. S., "Use of an Iterative Method for Analyzing the Asymmetric Buckling and Postbuckling Behavior of Elastic, Spherical Shells," Monograph, Rostov-on-Don State University, 1982, 48 pages. (In Russian).

Use is made of the Donnell-Mushtari large deformation equations for a shallow spherical cap subject to hydrostatic loading. The equations are solved by a computerized iteration procedure to indicate load-central deformation relations.

Sunakawa, M. and Ichida, K., "A High Precision Experiment on the Buckling of Spherical Caps Subjected to External Pressure," *Institute of Space and Aeronautical Science,* University of Tokyo, Report No. 508, Vol. 29, No. 5, 1975.

Test results on eleven shallow spherical caps formed from poly-methylmethacrylate plate and subject to uniform pressure on the convex surface.

Thompson, J. M. T., "Making of Thin Metal Shells for Model Stress Analysis," *Journal of Mechanical Engineering Science,* Vol. 2, No. 2, 1960, pp. 105–108.

Reports of the first successful attempt to fabricate thin shells by electroplating copper on a wax mandrel. The wax was subsequently removed by draining the heated wax through a very small hole in the copper. The technique has subsequently been applied to fabricate nickel specimens.

Thompson, J. M. T., "Elastic Buckling of Thin Spherical Shells," *Proceedings of the Symposium on Nuclear Reactor Containment Buildings and Pressure Vessels*, Glasgow, May, 1960, Butterworth Publishers Ltd., pp. 257–285.

The work of von Karman and Tsien (5.13) is reexamined on the basis of a non-zero Poisson ratio together with elimination of the assumption that shell displacement must be parallel to the axis of rotation. A Galerkin approach was employed for a simple, but realistic deflected configuration.

Thompson, J. M. T. and Hunt, G. W., *A General Theory of Elastic Stability*, John Wiley and Sons, London, 1973, 322 pages.

Tvergaard, V., "Buckling Behavior of Plate and Shell Structures," *Proceedings of the Fourteenth International Congress of Theoretical and Applied Mechanics*, North-Holland Publishing Co., 1976, pp. 233–247.

Wan, F.Y.M., "Polar Dimpling of Complete Spherical Shells." *Theory of Shells*, ed. by W.T. Koiter and G.K. Mikhailov, North-Holland Publishing Co., Amsterdam, 1980, pp. 589-605.

A relatively simple method for obtaining a simple approximate characterization of the dimple mode deformation for dome-type thin elastic shells of revolution. Applicable to nonshallow shells.

Wang, L. R. L., Rodriquez-Agrait, L., and Litle, W. A., "Effect of Boundary Conditions on Shell Buckling," *Journal of the Engineering Mechanics Division, Proceedings of the American Society of Civil Engineers*, EM6, 1966, pp. 101–116.

Reports buckling test results of 84 polyvinyl chloride shallow spherical caps subject to hydrostatic load.

Wang, L. R. L., "Effects of Edge Restraint on the Stability of Spherical Caps," *Journal of the American Institute of Aeronautics and Astronautics*, Vol. 4, 1966, pp. 718–719.

Wang, L. R. L., "Discrepancy of Experimental Buckling Pressure of Spherical Shells," *Journal of the American Institute of Aeronautics and Astronautics*, Vol. 5, 1967, pp. 357–359.

Wedellsborg, B. W., "Critical Buckling Load on Large Spherical Shells," *Journal of the Structural Division, Proceedings of the American Society of Civil Engineers*, Vol. 88, No. ST1, 1962.

One of the first treatments of localized buckling of a spherical shell, with the approach of determination of peak radial deviation over an average chord of the flattened region.

Yeh, K. Y., Song Wei, W. P., and Cleghorn, W. L., "Axisymmetric Buckling of Thin Shallow Circular Spherical Shells Under Uniform Pressure for Large Values of the Geometric Parameter λ," Scheduled for publication in the *International Journal of Non-Linear Mechanics,* Vol. 29, 1994.

The Newton spline function technique is employed to solve the governing non-linear equations. Numerical results for load-central deflections are presented for values of the geometric parameter λ as great as 50.

Yoshimire, Y. and Uemura, M., "The Buckling of Spherical Shells Due to External Pressure," Tokyo University Physical-Engineering Institute Report, Vol. 3, No. 11–12, 1949, pp. 316–322. (In Japanese).

The approach of von Karman and H. S. Tsien [5.13] is applied to buckling of a shallow spherical cap, but with a different buckled configuration. Postbuckling behavior is investigated in detail.

This Page Intentionally Left Blank

CHAPTER 6

OTHER SHELL AND PLATE GEOMETRIES

Spheroidal Shells

Recent developments in the structure of submersibles have led to consideration of pressure hull geometries other than spherical. Let us examine the equation

$$\frac{x^2}{a^2}+\frac{y^2}{b^2}+\frac{z^2}{c^2}=1 \tag{6.1}$$

where a, b, and c are positive real numbers. This is the equivalent of a surface called an ellipsoid, appearing as in Figure 6.1. If $a > c$ this ellipsoid is the result of a revolution of an ellipse about its minor axis and is termed an *oblate spheroid.* If $a < c$ the ellipsoid is the result of a revolution about its major axis and is termed a *prolate spheroid.* If $a = c$ the ellipsoid of revolution is a sphere [6.1]. The terms *oblate ellipsoid* and *prolate ellipsoid* are occasionally employed by some authors.

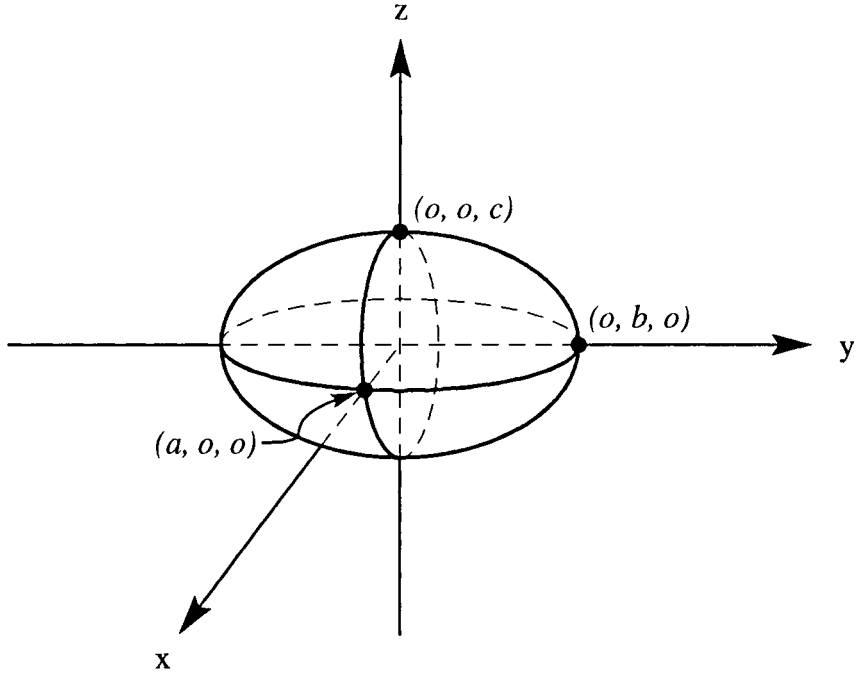

Figure 6.1

The prolate spheroid offers, in certain circumstances, some advantages over the sphere, in particular ease of arrangement of interior systems, improved hydrodynamic characteristics, and reduced susceptibility to initial geometric imperfections. The only buckling analysis based upon linear shell theory is due to Kh. M. Mushtari and K. V. Galimov [6.2] and indicates the buckling pressure

$$p = \frac{2Eh^2}{\left[3\left(1-\mu^2\right)^{\frac{1}{2}}\left(2a^2-b^2\right)\right]} \tag{6.2}$$

which for the special case of a spherical shell reduces to the result due to Zolley (Chapter 5, Equation (5.1). Unfortunately, as *a/b* becomes very large, which corresponds to a very long cylindrical shell, the above relation indicates a zero pressure. There is, consequently, considerable doubt about the validity of Equation (6.2). The first nonlinear analysis of buckling of a prolate spheroidal shell is due to R. G. Surkin [6.3] but this too is not completely satisfactory because he introduced only one free parameter for each of the displacements and took for the other parameters the values found from analysis of a perfectly spherical shell.

The most rational analysis of instability of a prolate spheroidal shell was given by B. Hyman in 1964 and 1965 [6.4] and [6.5]. He employed the coordinate system for the shell shown in Figure 6.2 and considered the buckling mode to consist of a single isolated indentation whose boundary lies in a plane parallel to the *x*-*z* plane and lying perpendicular to the *y*-axis. Thus, the equation of the boundary of the lobe is given as the intersection of the surface defined by Equation (6.1) with the plane $y = c$ and is shown by the curved line in Figure 6.2.

By defining a new parameter ϕ by the relations:

$$\begin{aligned} x &= b\left(1-c^2/b^2\right)^{\frac{1}{2}}\cos\phi \\ z &= a\left(1-c^2/b^2\right)^{\frac{1}{2}}\sin\phi \end{aligned} \tag{6.3}$$

any point in the middle surface of the shell may be located by assigning appropriate values to the parameter c and ϕ.

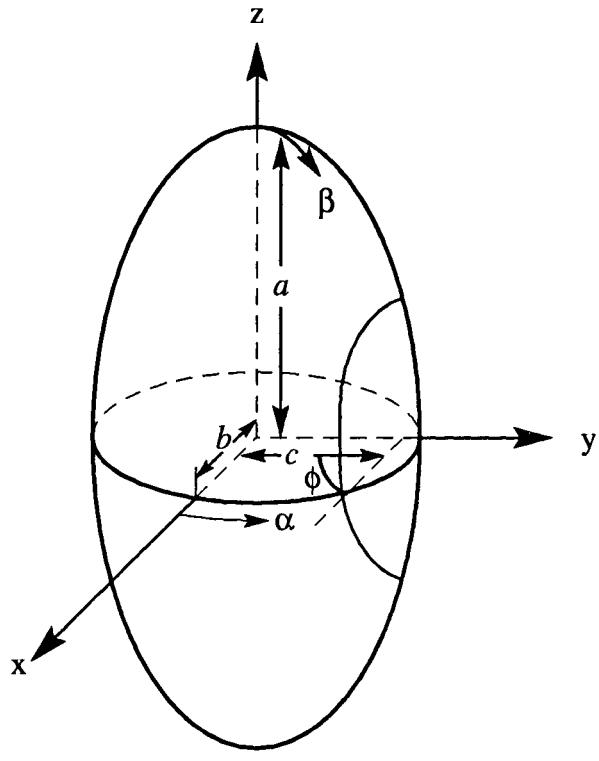

Figure 6.2

The differential geometry of the prolate spheroidal surface may be expressed in terms of a, b, c, α and β shown in Figure 6.2 and from these relations the three orthogonal displacements components are formulated. Now, the total potential energy of the system subject to hydrostatic loading may be formulated in terms of three free parameters. The Rayleigh-Ritz procedure is then invoked to obtain three coupled nonlinear equations governing the postbuckling of the prolate spheroidal shell. These equations are best suited to computer solution using an iterative procedure. Hyman presented computer results for load-deformation relations for a prolate spheroidal shell having a thickness/minimum principal axis length of 1/40 and loaded by hydrostatic pressure. Complete load-deformation relations were presented for several modes. Results were compared with those obtained by R. G. Surkin [6.3] but there was no way to identify the mode corresponding to the Surkin solutions. The effect of varying the eccentricity of the generating ellipse on buckling pressure was presented graphically in [6.4].

Also in 1965 J. J. Healey [6.6] published results of hydrostatic tests on a series of 25 unstiffened, epoxy resin prolate spheroidal shells. These had

length-diameter ratios ranging from 1.25 to 4.00 and thickness-radius ratios from 0.02 to 0.10. Empirical elastic buckling equations were presented from these test data. The relatively small scatter of experimental results supports the contention that prolate spheroidal shells are less sensitive to initial imperfections than spherical shells. Two ring-stiffened prolate spheroidal shells were loaded by hydrostatic pressure and a semi-empirical method developed for prediction of the elastic buckling resistance of such shells. Also, the use of a plasticity reduction factor provides a method for estimation of inelastic buckling strength of the hydrostatically loaded spheroidal shell.

A 1977 publication by A. Z. Bakirova [6.7] from Kazan State University was concerned with effect of no-load geometric deviations from a perfect prolate spheroidal shell configuration subject to hydrostatic loading. It was assumed that the final buckled shape was geometrically similar to the no-load configuration and nonlinear shell analysis was employed to determine load-deformation relations. It was demonstrated that the effect of the initial irregularities is more serious for spheroids having a geometry close to that of a perfect sphere.

Toroidal Shells

Toroidal shells may serve to store compressed gas within a submersible. The toroidal configuration can, in certain circumstances, offer an attractive utilization of space not found for more conventional shapes such as cylindrical or spherical. Toroidal shells may be of circular or non-circular cross-section, constant or variable wall thickness.

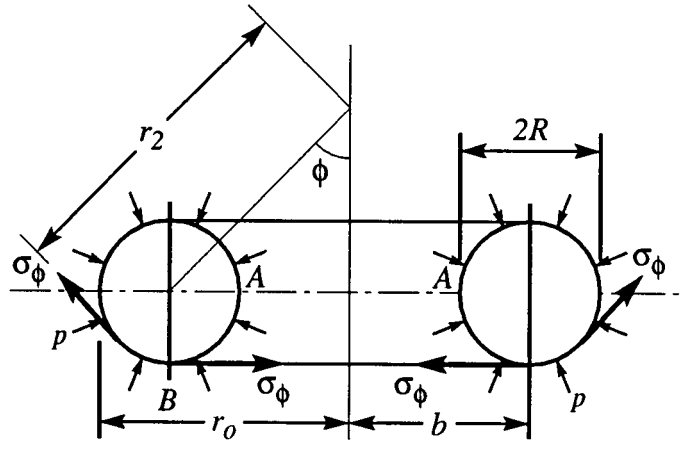

Figure 6.3

The membrane stress analysis of an internally pressurized toroidal shell is a problem from elementary strength of materials [5.1]. A convenient coordinate system wherein any point in the shell middle surface is described by the coordinate ϕ together with the longitude θ is shown in Figure 6.3. Elementary theory indicates the principal stresses in the middle plane of the shell wall to be

$$\sigma_\phi = \frac{pR(r_o + b)}{2\pi r_o h} \tag{6.4}$$

$$\sigma_\phi = \frac{pR}{2h} \tag{6.5}$$

where h denotes constant wall thickness, p represents pressure and R is "tube radius." For the same shell subject to external hydrostatic pressure the algebraic signs of Equations (6.4) and (6.5) would be negative to indicate compressive stresses prior to buckling. The problem of stresses in a circular cross-section toroidal shell whose thickness varies linearly along a generator from A to B in Figure 6.3 has been considered by V. A. Sukharev [6.8] using asymptotic integration techniques as well as computerized numerical integration.

One of the earliest analytical investigations of the stability of hydrostatically loaded toroidal shells is due to O. Machnig [6.9] in 1956. He considered both axially symmetric as well as asymmetric buckling modes through the use of power series expansions of the orthogonal displacement components. Buckling loads as well as modes were presented in dimensionless form. However, in recent years some questions have arisen concerning the validity of the power series expansion for small values of b/R (see Figure 6.3). In 1966, P. F. Jordan [6.10] published the results of asymptotic solution of the governing equations for axisymmetric buckling of the torus and obtained lower buckling loads than found in [6.9].

In 1965 L. H. Sobel [6.11] and later Sobel and W. Flügge [6.12] specialized the stability equations for shells of revolution to the case of the torus and solved these equations in terms of harmonic functions. A detailed numerical study was made of the number of terms in the series required to obtain a numerically acceptable value of the hydrostatic buckling load. For engineering purposes it was shown that rarely are more than 20 terms required in the harmonic expansions of the buckling displacement components. These authors also carried out experiments on toroidal shells pressed from type 17-7PH steel as well as type 6A1-4V titanium. Test buckling loads were approximately ten per cent above or below the analytically predicted values. The models had a b/R ratio of either 8.04 or 6.32 but the authors

pointed out that agreement of test with theory might not be so good for smaller values of *b/R*.

In 1970, E. Fishlowitz [6.13] presented results of a series of hydrostatic tests on eight plastic toroidal shells of circular cross-section. The models were cast in aluminum molds in the shape of half of a full circular cross-section of a torus. The model material consisted of a mixture of two epoxies heated and poured into the warmed molds into which was forced a solid, machined, wood toroidal form to simulate the interior of the desired torus and placed to that the cured epoxy would fill the space between the aluminum mold and the wood core. The wood form was then removed and the inside surface of the cured epoxy then machined to create a smooth interior surface to the the torus. Then, two such epoxy models were joined along a diametral plane by the same mixture of epoxies employed in casting the shell. Models were tested either by (a) submerging the toroidal shell in a pressure tank, or (b) removing some of the air in the model to create a differential pressure with the atmospheric pressure on the shell providing the loading. Shell thicknesses were monitored and electric resistance strain gages mounted to monitor strains during the loading procedure.

Buckling pressures found experimentally were then compared with two analyses. The first is due to L. H. Sobel and W. Flügge [6.12] and the second is due to D. Bushnell [6.14]. The latter was developed for any shell of revolution but here specialized to the case of a circular cross-section toroidal shell. It was found that the Bushnell analysis agreed rather well with test results. The Sobel-Flugge theory agreed well with about half of the experimental results but over-estimated the buckling load for models having *b/R* ratios ranging from 2.3 to 3.6. In general, the Bushnell analysis is somewhat more conservative in its predictions. Lastly, test results showed that hydrostatically loaded toroidal shells are insensitive to imperfections.

Another instance where toroidal shells may be found in submersibles is as a component of an end cap for a cylindrical shell containing compressed gas for various on-board uses. The diametral cross-section of the internally pressurized vessel is of the form shown in Figure 6.4, where the pressure vessel consists of a circular cylindrical shell, a relatively shallow spherical cap, with a portion of a toroidal shell serving as a transition element between the sphere and the cylinder. The toroidal region is usually termed a knuckle, and the entire system is axisymmetric about the vertical axis of revolution, and subject to uniform internal gas pressure.

In 1959 G.D. Galletly [6.15] was the first to point out that the dominating stress in the knuckle is a relatively large compressive hoop stress. Consequently, for relatively thin knuckles buckling of the knuckle is one possible mode of failure. The buckling is elastic if the material of the

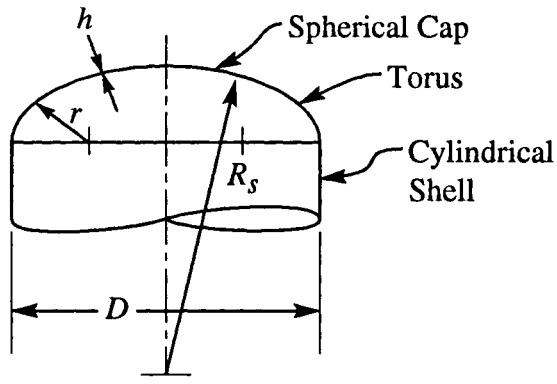

Figure 6.4

knuckle has a relatively high value of the ratio of yield stress to elastic modulus. If the knuckle is sufficiently think, failure will usually be by plastic collapse. This was investigated by D.C. Drucker and R.T. Shield [6.16] on the basis of limit analysis. Tests carried out by J. Mescall [6.17] on internally pressurized shells of the configuration shown in Figure 6.4 indicated that the elastic buckling failure occured with formation of a relatively large number of essentially equally spaced lobes (dents) along a meridian extending over the entire toroidal region, i.e. from the juncture of the toroidal segment to the cylindrical shell, and also to its juncture with the shallow spherical cap. The models tested were polyvinyl chloride.

In summary, this relatively common configuration of an *internally pressurized* gas or liquid storage container may *buckle* elastically or into the elasto-plastic range of action. This unusual situation is in contrast to other geometries discussed in this book. Galletly [6.15] has given a warning to designers that this rather unusual (and startling) possibility must be remembered. Further, he has found that it is necessary to utilize finite deformation shell theory for both stress analysis as well as buckling analyses in the elastic as well as elasto-plastic ranges in order to obtain satisfactory agreement between theory and experiment [6.19]. To achieve this he employed the shell computer program BOSOR-5 due to D. Bushnell [2.5], [6.18] which permits finite deformations into the elasto-plastic range and takes account of isotropic strain-hardening. Either flow or deformation theory may be used in this program. His work indicated that buckling of internally pressurized torispherical shells is relatively insensitive to small geometric imperfections of no-load geometry. The numerical investigations covered the dimensionless parameters $R_s/D = 1$, $r/D = 0.06$ to 0.20 and $D/h = 750$, 1000, and 1250 where these parameters are defined in Figure 6.4. Curve fitting applied to these numerical results led to the relation

$$\frac{p}{\sigma_{yp}} \approx \frac{285[1-125\sigma_{yp}](r/D)^{0.84}}{(D/t)^{1.53}(R_s/D)^{1.1}} \tag{6.6}$$

for $500<D/h<1500$ where σ_{yp} denotes yield point of the material and p represents internal pressure that will cause buckling of the torisphere and knuckle. In 1981 Galletly [6.19] and in 1985 Galletly and J. Blachut [6.20] carried out further numerical studies to include D/h ratios as low as 250 and employed additional values of yield stress. These results led to the approximate equation

$$\frac{p}{\sigma_{yp}} \approx \frac{120(r/D)^{0.81}}{(D/t)^{1.46}(R_s/D)^{1.18}} \tag{6.7}$$

for buckling pressure based upon deformation theory of plasticity.

Circular Plates

Circular plates, usually with a concentric circular hole, are often found in submersibles. They serve to strengthen a cylindrical pressure hull as well as offering a point of attachment for various optical or electronic or electric sub-systems carried inside the vehicle.

The hydrostatic loading on the cylindrical hull is transmitted to the circular plate (diaphragm) by means of (a) compressive radial forces acting at the outer boundary of the plate and directed toward the longitudinal axis of the cylinder, and (b) bending moments acting on the outer circular edge of the plate representing interaction between the flat plate and the cylindrical shell.

The stress analysis based upon linearized small deformation theory of elasticity for a thin, hollow circular plate subject to radial compressive forces, as shown in Figure 6.5 is found in many sources treating elasticity and will not be repeated here. Buckling of the circular plate is a somewhat more difficult problem. The classical analysis based upon small lateral deflections is to be found in [6.21]. In it, the governing equation has the form

$$D\nabla^4 w + p\nabla^2 w = 0 \tag{6.8}$$

where w denoted lateral deflection, D is flexural rigidity, and p denotes radial pressure. Also ∇^4 represents the biharmonic operator and ∇^2 the Laplacian in polar coordinates. In [6.21] Equation (6.8) is solved to find the critical load necessary to hold a clamped edge plate having no central hole in a deflected axisymmetric configuration to be

$$(N_r)_{cr} = \frac{14.68D}{R_o^2} \tag{6.9}$$

where N_r is the radially-oriented edge load per unit length of plate circumference and R_o represents the outer radius of the plate. Reference [6.21] also gives buckling loads for the circular plate having a concentric circular cutout of radius R_i in terms of the ratio R_o/R_i.

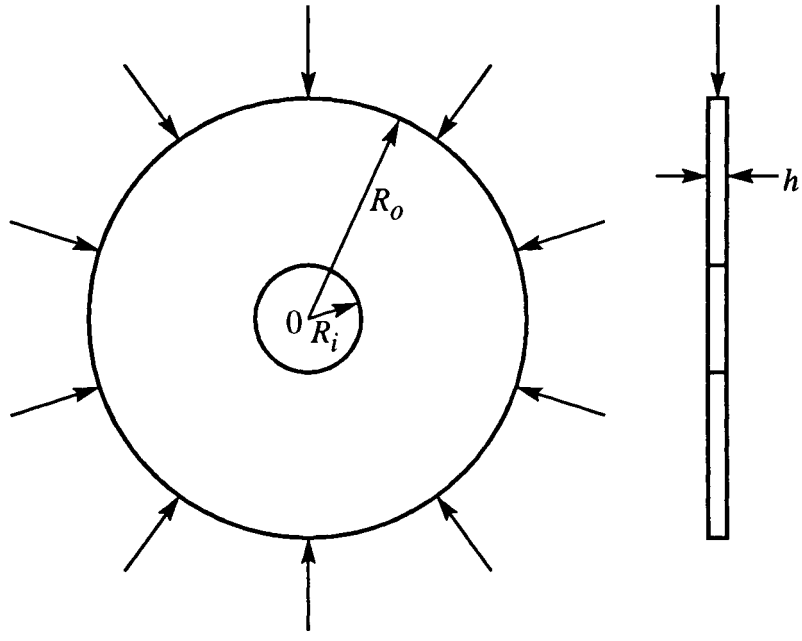

Figure 6.5

Large lateral deflections of buckled circular plates are governed by the polar coordinate form of (2.62) and (2.63). Axisymmetric buckling of the edge-compressed circular plate has been studied by G. A. Wempner and R. Schmidt [6.22] through a rapidly converging series solution of each of the two governing deformation parameters. The same problem was investigated by I. J. Weinberg [6.23] using the governing equations due to E. Reissner [6.24]. Buckling loads were determined for (a) clamped outer edge, and (b) simply supported outer edge conditions.

Perhaps the most comprehensive information available to designers of in-plane loaded circular plates was offered by G. M. Hong, C. M. Wang, and T. J. Tan [6.25] in 1993. It pertains to a thick circular plate subject to radial loading around its outer boundary and allows for no-load initial imperfections of the plate. Since the plate was taken to be thick shear effects were

included and shown to be as important as the initial deformations. The finite deformation plate equations [2.62] and [2.63] were extended to include the shear deformations. An analytical solution for load-central deflection relations was obtained for the case of (a) clamped, and (b) simply supported boundaries under uniform radial in-plane loadings.

Viewing Windows

Many of the submersibles mentioned in Chapter 1 have viewports, usually of contemporary acrylic. DENISE employed by J. Y. Cousteau in 1960 had two two-inch (50.8 mm) diameter windows facing forward. The initial configuration of ALVIN with a steel pressure hull having a depth capability of 6000 feet (1,830 meters) had five plexiglas windows designed by J. W. Mavor, Jr.[6.26] based upon the work of August Piccard [6.27] related to TREISTE II. ALUMINAUT had four four-inch (101.6mm) windows facing forward. The DEEP OCEAN WORK BOAT had two windows, one facing forward, the other facing directly underneath the vehicle. All more recent submersibles had comparable viewing systems. In most cases the windows were clear acrylic (plexiglas or lucite) having a lower index of refraction and higher light transmission than optical quality glass. Further, at high pressure such as found at the floor of the sea, acrylic exhibits cold flow, thus distributing internal stresses. Also, acrylic becomes translucent prior to failure, thus giving warning of impending disaster. Glass, when reaching critical stress, behaves in a brittle manner prior to bursting.

In the late 1960's, J. D. Stachiw [6.28], [6.29] and [6.30] carried out tests on determination of critical hydrostatic pressure on (a) flat acrylic windows, (b) conical acrylic windows, and (c) spherical windows each subject to short-term loading. For short-term the loading rate was taken to be 650

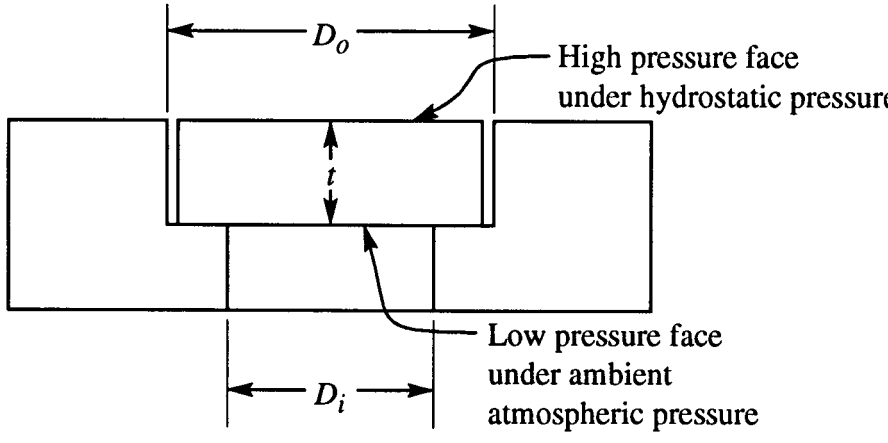

Figure 6.6

pounds/in^2 (4.48 MPa) per minute from zero to the moment of failure of the window. For flat acrylic windows, specimens were machined to have the thickness/diameter ratio less than unity, and with unsupported openings in the flange of the test apparatus (Figure 6.6) of 1.5, 3.3, and 4 inches (38.1, 83.8, and 101.6 mm). Peak pressure as great as 28,000 pounds/ inch^2 (193 MPa) were required to fracture the specimens.

For conical windows, tests were carried out using a machined conical opening in a massive steel block for various cone angles as shown in Figure 6.7.

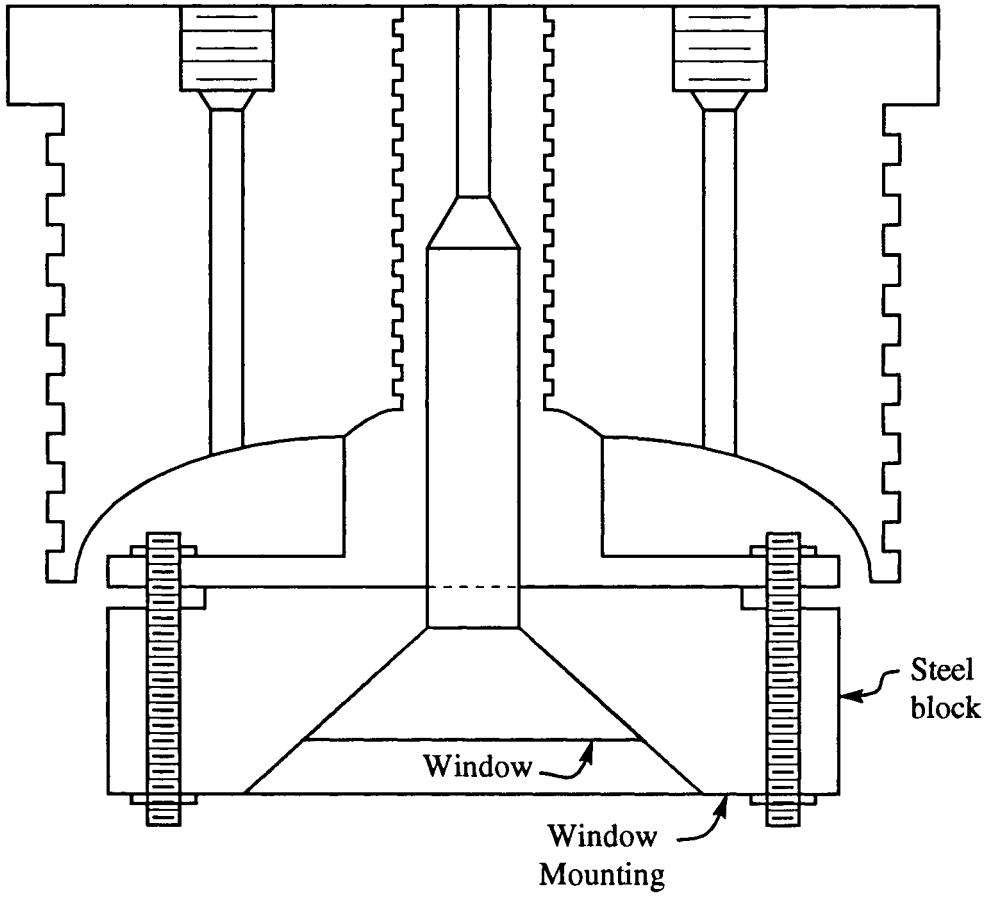

Figure 6.7 Reprinted from Reference [6.29] with permission of the American Society of Mechanical Engineers

The investigation included 30, 60, 90, 120, and 150° cone angles. Another parameter employed was the ratio of window thickness to the minor diameter, D_i, i.e., the diameter of the low pressure surface of the conical window. All window specimens had a one inch (25.4 mm) minor diameter.

Extra support was given the edges of the acrylic conical window so to prevent premature failure near the flat surfaces of the window. This support was introduced by the wall of the cylindrical cavity shown in Figure 6.7 so that when the window extrudes through the opening in the steel block the acrylic is restrained radially. Windows were sealed in the machined opening by means of silicone grease. Pressurization was at the rate of 659 pounds per square inch (4.54 MPa) per minute. Three types of window failure resulted, depending upon window geometry. Extrusion of the model through the opening shown in Figure 6.7 occurred for windows having a 30° cone angle, and to some extent in the 90° windows. Combined cold flow-crater flexure failure occurred primarily in the 60° windows and to some extent in the 90° models. Fracture cones, analagous to a conch shell, developed on the low pressure faces, and a cold flow crater on the high pressure face. Combined shear cone-flexure occurred in most of the 120° and 150° conical windows. It was concluded that the cone angle is an important factor in resistance of such windows to short-term hydrostatic loading, an increase in the angle usually leading to an increase in the critical pressure of the window. The 90° cone angle was thought to lead to optimum resistance under short-term loading, while needing only a modest size mounting.

Another investigation of acrylic, conical viewports was carried out by F. M. Schwartz [6.31] at the Naval Ship Research and Development Center, Washington, D. C. in 1968. Windows with inside diameter-to-thickness ratios of 1.0, 1.5, and 2.0 were tested under hydrostatic pressure with significant strains being monitored by electric resistance strain gages. The conical viewport was also studied by means of a finite element analysis for hydrostatic loading. Good agreement was found between measured strains and the finite element predictions. Cyclic loading was also investigated experimentally, as well as dynamically applied hydrostatic loading. Loading rates varied over the range of 100 pounds/in^2 (0.690 MPa) to 15,000 pounds/in^2 (103.4 MPa) per minute. For these acrylic specimens Young's modulus in compression was found to 4.6 x 10^5 pounds/in^2 (3171 MPa) in compression and slightly less than this value in tension. The modulus was temperature dependent, increasing as temperature decreased. Strength was found to be dependent upon loading rate. An ultimate compressive strength of approximately 14,300 pounds/in^2 (98.6 MPa) was measured at 74°F (23.3°C) and a strength of 19,500 pounds/in^2 (134.4 MPa) existed at 36°F (2.2°C). Tensile strengths ranged from 7200 to 4800 pounds/in^2 (49.6 to 33.1 MPa). Creep was measured under uniaxial compression and was noticeable at relatively low stress levels. Normal strains increased approximately 20 percent at a stress level of 6000 pounds/in^2 (41.4 MPa) over 72 hours at 36°F (2.2°C). Very rapid creep was observed at 15,000 pounds/

in^2 (103.4 MPa) and creep became uncontrollable at 18,000 pounds/in^2 (124.1 MPa). Results were presented in the form of a plot of submergence depth as a function of the dimensionless ratio of window inside diameter to thickness for (a) satisfactory cyclic performance, (b) initiation of permanent deformation at window center at 72 hours, and (c) short-term collapse while descending at a rate to 500 ft/minute (152.5 m/minute).

J. D. Stachiw continued his earlier work at the Naval Civil Engineering Laboratory to include long-term hydrostatic pressure of 20,000 pounds/in^2 (137.9 MPa) in 1970 acting on a conical acrylic window with cone angles varying from 30° to 150° [6.32]. This peak pressure was maintained for times up to 1000 hours duration He tested 1200 specimens having thickness to minor diameter ratios of 0.750 to 2.000. Tests indicated that only windows with thicknesses to minor diameter (t/D) greater than unity with cone angles to 60° or more will not fail in less than 1000 hours of sustained hydrostatic loading despite the fact that some cracking in the interior of the window will take place. For optically acceptable service of 1000 hours duration under 20,000 pounds/in^2 (137.9 MPa) the window must have t/D greater than two with a cone angle of at least 90°.

For spherical windows, [6.33] model as well as full scale acrylic specimens in the form of spherical shell lenses with parallel convex and concave surfaces were subjected to hydrostatic loading on their convex surfaces at the rate of 650 pounds/in^2 (4.48 MPa) per minute while at the same time the concave surface was at atmospheric pressure. Thirty-six models were tested, as shown in Figure 6.8 with model window thicknesses ranging from 0.250 to 1.200 inches (6.35 to 30.48 mm) and of the full scale windows from 0.564 to 4.000 inches (14.3 to 101.6mm), while the included spherical sector angle of the window varied from 30° to 180° in 30° increments. The face of the window exposed to hydrostatic pressure had a diameter ranging from 6.200 to 35.868 inches (157.5 to 911.0 mm) while the face exposed to atmospheric pressure had diameters ranging from 1.423 to 5.500 inches (36.14 to 139.7 mm). Experimental results indicated that the critical pressure of the spherical acrylic windows was always greater than for the conical or flat disc acrylic window of the same thickness low pressure face diameter subjected to this short-term hydrostatic loading. The spherical windows also provided a larger field of view to the observer.

At the Naval Undersea Research and Development Center, San Diego, California, J. D. Stachiw and colleagues [6.34] have examined the feasibility of utilizing complete spherical acrylic pressure hulls for undersea exploration. It was demonstrated experimentally that such acrylic pressure hulls are reliable if the viscoelastic temperature-dependent properties of the acrylic are taken into account during the design stage. Such pressure hulls with

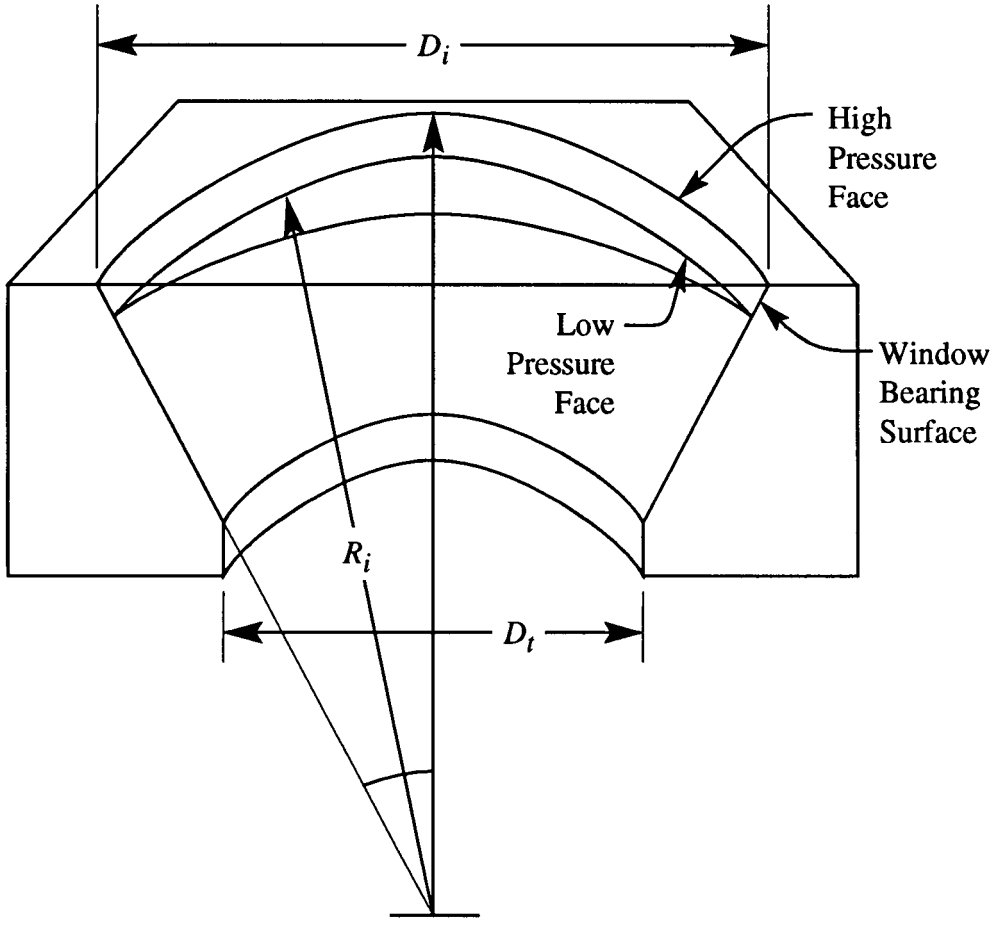

Figure 6.8 Reprinted from Reference [6.30] with permission of the American Society of Mechanical Engineers

panoramic visibility are highly desirable for many undersea activities. This study led to construction of the NEMO Model 2000 spherical pressure hull suitable for manned submersibles with 3000 foot (915 m) operational depth capability. The 66 inch (1.68 m) outside diameter acrylic spherical shell with aluminum hatches successfully withstood 24 hour external pressurizations of as much as 1800 pounds/in^2 (12.4 MPa). Crackfree fatigue life of 1000 pressure cycles to 1500 pounds/in^2 (10.3 MPa) was determined experimentally. In summary, the NEMO model 2000 spherical acrylic pressure hull was considered to be acceptable for 3000 feet (915 meter) operational depth capability.

It has become customary to rate such submersibles in terms of "ft.hr" where, as an example, if the system has been subjected to 1,000 cycles (dives) each to a 3000 foot depth, with each dive having a duty time of four

hours, then that is calculated as (1000 cycles) (3000 foot)(4 hours), amounting to 12 x 10^6 ft.hr. When the sum of feet.hours comes to 12 x 10^6, gaskets, nozzles, etc., should be removed and the pressure hull subjected to a detailed visual examination. The NEMO Model 2000 tests indicated a cyclic fatigue life of at least 12,000,000 ft.hr.

In summary, adequate experimental data exist to permit rational design of acrylic windows suitable for almost any ocean depth under static as well as load-cycling conditions.

REFERENCES

6.1 Albert, A.A., *Solid Analytical Geometry,* McGraw-Hill Book Co., 1949.

6.2 Mushtari, Kh.M. and Galimov, K.V., *Nonlinear Theory of Thin Elastic Shells,* (in Russian, 1957) See pp. 308 - 314. Available in English as NASA-TT-F-62, also, U.S. Department of Commerce, Publication 61-31227, 1961.

6.3 Surkin, R.G., "On the Theory of Stability of a Prolate Spheroidal Shell under Uniform External Pressure," Series in Physical-Mathematical and Engineering Science, Kazan Branch of the Soviet Academy of Sciences, Engineering Sciences, No., 7, 1955 (In Russian). Available in English as David Taylor Model Basin Translation 317, Washington, D.C. 1964.

6.4 Hyman, B.I., "Buckling and Postbuckling Behavior of Prolate Spheroidal Shells under Uniform External Pressure," Ph.D. Dissertation, Virginia Polytechnic Institute, 1964.

6.5 Hyman, B.I., "Elastic Instability of Prolate Spheroidal Shells under Uniform External Pressure," David Taylor Model Basin, Department of the Navy, Washington, D.C. 1965, Report 2105. Also published in the *Proceedings of the 9th Midwestern Mechanics Conference,* Madison, Wisconsin, 1965.

6.6 Healey, J.J., "Parametric Study of Unstiffened and Stiffened Prolate Spheroidal Shells Under External Hydrostatic Pressure," David Taylor Model Basin, Department of the Navy, Washington, D.C., Report 2018, 1965.

6.7 Bakirova, A.Z., "Stability of Elongated Spheroidal Shells with Initial Irregularities of the Form," *Strength and Stability of Shells, Work of the Seminar,* Kazan, Vol. 9, 1977, pp. 76 - 79. (In Russian.)

6.8 Sukharev, V.A., "Axisymmetric Deformation of a Toroidal Shell with Variable Wall Thickness," *Transaction of the Higher Schools, Series in Machine Design,* No. 6, 1966, pp. 16 - 20. (In Russian.)

6.9 Machnig, O., "Uber Stabilitatsprobleme von Torusformingen Schal-

en," *Wissenschaften Zeitschriften der Verkehrswesen Hochschule,* Dresden, Vol. 4, 1956, pp. 179 - 204.

6.10 Jordan, P.F., "Vibration and Buckling of Pressurized Torus Shells," American Institute of Aeronautics and Astronautics, Paper 66 - 445, 1966.

6.11 Sobel, L.H., "Stability of Shells of Revolution: General Theory and Application to the Torus," Ph.D. Dissertation, Stanford University, 1965.

6.12 Sobel, L.H., and Flügge, W., "Stability of Toroidal Shells under Uniform External Pressure," *Journal of the American Institute of Aeronautics and Astronautics,* Volume 5, No. 3, 1967, pp. 425 - 431.

6.13 Fishlowitz, E.G., "Investigation of Elastic Stability of Circular Toroidal Shells under Uniform External Pressure," Naval Ship Research and Development Center, Washington, D.C., Report 3338, 1970. Also: M.S. Thesis, George Washington University, Washington, D.C., 1970.

6.14 Bushnell, D., "Buckling and Vibration of Ring-Stiffened Segmented Shells of Revolution," Lockheed Missiles and Space Co., Report 6-78-68-37, August, 1968.

6.15 Galletly, G.D., "Torispherical Shells - A Caution to Designers," *Journal of Engineering for Industry, Transactions of the American Society of Mechanical Engineer,* Series B, Vol. 81, 1959, pp. 51-62.

6.16 Drucker, D.C., and Shield, R.T., "Limit Analysis of Symmertically Loaded Shells of Revolution," *Journal of Applied Mechanics, Transactions of the American Society of Mechanical Engineers,* Vol. 81, 1959, pp. 61-68.

6.17 Mescall, J., "Stability of Thin Torispherical Shels under Uniform Internal Pressure," Technical Report AMRA-TR-63-06, U.S. Army Materials Research Agency, Watertown, MA, 1963.

6.18 Bushnell, D., "BOSOR-5 -- Program for Buckling of Elastic-Plastic Complex Shells of Revolution Including Large Deflections and

Creep," *Computers and Structures,* Vol. 6, 1976, pp. 221-239.

6.19 Galletly, G.D., "Plastic Buckling of Torispherical and Ellipsoidal Shells Subjected to Internal Pressure," *Proceedings of the Institution Mechanical Engineers,* Part C, Vol. 195, No. 26, 1981, pp. 329-345.

6.20 Galletly, G.D., and Blachut, J., "Torispherical Shells under Internal Pressure - Failure due to Asymmetric Plastic Buckling or Axisymmetric Yielding," *Proceedings of the Institution of Mechanical Engineers,* Part C, 1985, Vol. 199, pp. 225-238.

6.21 Yamaki, N., "Buckling of a Thin Annular Plate Under Uniform Compression," presented at the Annual Meeting of the American Society of Mechanical Engineers, New York, 1957, Paper No. 57-A-11.

6.22 Wempner, G.A., and Schmidt, R., "Large Symmetric Deflections of Annular Plates," *Journal of Applied Mechanics, Transactions of the American Society of Mechanical Engineers,* Vol. 25, No. 4, 1958, pp. 449 - 450.

6.23 Weinberg, I.J., "Symmetric Finite Deflections of Circular Plates Subjected to Compressive Edge Forces," *Journal of Mathematics and Physics,* Vol. XLI, No. 2, 1962. pp. 104 - 115.

6.24 Reissner, E., "Finite Deflections of Circular Plates," *Proceedings of the Symposia in Applied Mathematics,* Volume 41, 1949, pp. 213 - 219, McGraw-Hill Publishing Co.

6.25 Hong, G.M., Wang, C.M., and Tan, T.J., "Analytical Buckling Solutions for Circular Mindlin Plates: Inclusion of In-Plane Prebuckling Deformation," *Archive of Applied Mechanics,* Vol. 63, 1993, pp. 534 - 542.

6.26 Mavor, J.W., Jr., "Observation Windows of the Deep Submersible ALVIN," *Journal of Ocean Technology,* Volume 1, No 1, 1966, pp. 2 - 16.

6.27 Piccard, A., "Au Fond des Mers en Bathyscape," *ARTHAUD,* 1954.

6.28 Stachiw, J.D., "Critical Pressure of Flat Acrylic Windows Under Short-Term Hydrostatic Loading," Paper No. 67-WA/UNT-1, The American Society of Mechanical Engineers, 1967.

6.29 Stachiw, J.D., "Critical Pressure of Conical Acylic Windows Under Short-Term Hydrostatic Loading," *Transaction of the American Society of Mechanical Engineers, Journal of Engineering for Industry,* Series B, August, 1967, pp. 427 - 426.

6.30 Stachiw, J.D., "Critical Pressure of Spherical Shell Acrylic Windows Under Short-Term Pressure Loading," *Transaction of the American Society of Mechanical Engineers, Journal of Engineering for Industry,* Series B, August, 1968, pp. 573 - 584.

6.31 Schwartz, F.M., "The Structural Performance of Acrylic Viewports for Deep Submersibles," Naval Ship Research and Development Center, Washington, D.C., Report 3167, August, 1969.

6.32 Stachiw, J.D., "Conical Acrylic Windows Under Long Term Hydrostatic Pressure of 20,000 Psi.," *Transactions of the American Society of Mechanical Engineers, Journal of Enginering for Industry,* Series B, February, 1970, pp. 237 - 256.

6.33 Stachiw, J.D., "Spherical Acrylic Pressure Hulls for Undersea Exploration," *Transactions of the American Society of Mechanical Engineers, Journal of Engineering for Industry,* Series B, Vol. 93, No. 2, 1971, pp. 731 - 750.

6.34 Stachiw, J.D., "NEMO Type Acrylic Plastic Spherical Hull for Manned Operation to 3000 Feet Depth," *Transactions of the American Society of Mechanical Engineers, Journal of Engineering for Industry,* Series B, Vol. 98, No. 2, May, 1976, pp. 537 - 549.

BIBLIOGRAPHY

D'yachkov, I.I., Kvitka, A.L., Komyagin, Yu. V., and Morganyuk, V.S., "Construction of an Optical Porthole. Communication 1. State of Stress and Strain of the Flat Glass Element," *Problemy Prochnosti,* No. 9, 1986, pp. 114-119. Available in English as *Strength of Materials,* Plenum Publishing Corp., New York, 1987, pp. 1278-1283.

D'yachkov, I.I., Kvitka, A.L., Komyagin, Yu. V., and Gnuchii, Yu.B., "Construction of an Optical Porthole. Communication 2. State Of Stress and Strain of the Disk-Shaped Glass Element in the Assembled Unit," *Problemy Prochnosti,* No. 9, 1986, pp. 119-123. Available in English as *Strength of Materials,* Plenum Publishing, Corp., New York, 1987, pp. 1284-1288.

D'yachkov, I.I., Kvitka, A.L., Komyagin, Yu.V., and Gnuchii, Yu.B., "Construction of an Optical Porthole, Communication 3. The State of Stress and Strain and the Strength of a Flat Glass Element," *Problemy Prochnosti,* No. 11, 1986, pp. 97 - 101. Available in English as *Strength of Materials,* Plenum Publishing Corporation.

Hydrostatic pressure tests were carried out on eight flat optical glass discs, types K8 and KV glass. Experimentally determined strains were in modest agreement with those given by a finite element analysis.

Lankes, L.R., "Viewing Systems for Submersibles," *Optical Spectra,* May, 1970, pp. 61 - 67.

Nordell, W.J., and Crawford, J.E., "Analysis of Behavior of Unstiffened Toroidal Shells," *Proceedings of the Pacific Symposium on Hydrodynamically Loaded Shells,* International Association of Shell Structures, Honolulu, Hawaii, 1971, pp. 304-313.

Seven epoxy toroidal shells were subjected to hydrostatic pressure and strains as well as buckling pressures determined. Results compared well with predictions of a finite element program developed by the authors, utilizing 240 elements.

Speir, E.E., Wilson, P.E., and Slick, E.M., "Nonlinear Analysis of Thin Toroidal Shells of Circular Cross-Section," *American Institute of Aeronautics and Astronautics,* Paper 65 - 144, 1965.

Stachiw, J.D., and Burnside, O.H., "Acrylic Plastic Spherical Shell Windows Under Point Impact Loading," Paper No. 75-WA/OcE-6, Winter Annual Meeting of the American Society of Mechanical Engineers, Dec. 1975.

An experimental investigation of point impact against the convex surface of a hydrostatically loaded spherical viewport. Such considerations may arise in practice because of the vehicle striking a submerged peak, or of being impacted by a moving shark (as in the case of ALVIN.)

Stachiw, J.D., and Sletten, R., "Spherical Shell Sector Acrylic Windows with

12,000 ft. Operational Depth for Submersible ALVIN," *Transactions of the American Society of Mechanical Engineers, Journal of Engineering for Industry,* Series B. Vol. 98, No. 2, 1976, pp. 523 - 536.

Stachiw, J.D., and Smith, N.E., and Burns, O.H., "Structural Performance of Acrylic Plastic Plane Disk Windows with Twin Conical Bearing Surfaces," *Transactions of the American Society of Mechanical Engineers, Journal of Engineering for Industry,* Series B, Vol. 100, No. 2, 1978, pp. 273 - 286.

An experimental investigation of behavior of a flat circular acrylic window locked in position by rigid conical discs on both sides of the plane disc, with the acrylic having much the appearance of a pulley. The design was found to be satisfactory.

Thurston, G.A., and Holston, A.A. Jr., "Buckling of Cylindrical Shell and Closures by Internal Pressure", NASA CR-540, July, 1966, 22 pages.

An analytical study that establishes the fact that elliptical end domes of internally pressurized cylindrical shells cannot buckle if the cross-section has a geometry shallower than $\sqrt{2}$:1. Finite deformation theory was used to determine the prebuckling stress distribution. This approach leads to bifurcation pressures that are greater than found from linear theory.

Vol'mir, A.S., and Khairnasov, K.Z., "Stability of Toroidal Composite Shells," *Mekhankia Kompozitnykh Materialov,* No. 3, 1982, pp. 545-459. Available in English as *Mechanics of Composite Materials,* Plenum Publishing Corp., New York.

A finite element analysis of a composite material toroidal shell subject to hydrostatic loading. The shell is characterized as orthotropic.

This Page Intentionally Left Blank

AUTHOR INDEX

SUBJECT INDEX

This Page Intentionally Left Blank